UNIVERSIDADE FEDERAL DO CEARÁ
CENTRO DE TECNOLOGIA
DEPARTAMENTO DE ENGENHARIA HIDRÁULICA E AMBIENTAL
PROGRAMA DE PÓS-GRADUAÇÃO EM ENGENHARIA CIVIL

MARIA DE JESUS DELMIRO ROCHA

ASSESSMENT AND MODELING OF THE PHOSPHORUS DYNAMICS IN THE WET AND DRY PERIODS IN TROPICAL SEMIARID RESERVOIRS

FORTALEZA
2022

MARIA DE JESUS DELMIRO ROCHA

ASSESSMENT OF THE PHOSPHORUS DYNAMICS IN THE WET AND DRY PERIODS OF TROPICAL SEMIARID RESERVOIRS

Dissertação apresentada ao Programa de Pós-Graduação em Engenharia Civil da Universidade Federal do Ceará, como requisito parcial para obtenção do grau de mestre em engenharia civil. Área de concentração: Recursos Hídricos.

Orientador: Prof. Dr. Iran Eduardo Lima Neto.

FORTALEZA

2022

Dados Internacionais de Catalogação na Publicação
Universidade Federal do Ceará
Biblioteca Universitária
Gerada automaticamente pelo módulo Catalog, mediante os dados fornecidos pelo(a) autor(a)

D418a Delmiro Rocha, Maria de Jesus.
Assessment of the phosphorus dynamics in the wet and dry periods of tropical semiarid reservoirs /Maria de Jesus Delmiro Rocha. – 2021.
143 f.

Dissertação (mestrado) – Universidade Federal do Ceará, Centro de Tecnologia, Programa de Pós-Graduação em Engenharia Civil: Recursos Hídricos, Fortaleza, 2021.
Orientação: Prof. Dr. Iran Eduardo Lima Neto.

1. phosphorus balance. 2. land use. 3. sediment release. 4. internal and external loads. 5. water quality modeling. I. Título.

CDD 627

MARIA DE JESUS DELMIRO ROCHA

ASSESSMENT OF THE PHOSPHORUS DYNAMICS IN THE WET AND DRY PERIODS OF TROPICAL SEMIARID RESERVOIRS

Dissertação apresentada ao Programa de Pós-Graduação em Engenharia Civil da Universidade Federal do Ceará, como requisito parcial para obtenção do grau de mestre em engenharia civil. Área de concentração: Recursos Hídricos.

Aprovada em: 04/02/2022

BANCA EXAMINADORA

_____

Prof. Dr. Iran Eduardo Lima Neto (Orientador)
Universidade Federal do Ceará (UFC)

_____

Prof. Dr. Michael Mannich
Universidade Federal do Paraná (UFPR)

_____

Profª. Drª. Vanessa Becker
Universidade Federal do Rio Grande do Norte (UFRN)

ACKNOWLEDGEMENTS

I acknowledge my master's degree scholarship funded by the Coordination for the Improvement of Higher Education Personnel Foundation (CAPES).

I am very grateful to my supervisor Dr. Iran Eduardo Lima Neto for his dedicated guidance. His ideas and encouragement made this an inspiring experience for me.

I am thankful to the Water Resources Management Company of the State of Ceará (COGERH) for providing the data necessary to accomplish this work.

RESUMO

Esta dissertação apresenta uma avaliação da dinâmica do fósforo total (PT) em reservatórios semiáridos estratégicos, desde a escala de bacia hidrográfica até o reservatório. Foram avaliadas a produção e chegada do fósforo da bacia a esses corpos hídricos, dependendo do período climático, e a compreensão das causas para a liberação e ressuspensão de fósforo do sedimento dos reservatórios. O objetivo da primeira avaliação foi desenvolver uma nova metodologia para estimar a carga de fósforo total que chega aos reservatórios nos períodos úmido e seco e encontrar evidências de produção de carga interna. O objetivo da segunda avaliação foi descrever a importância das fontes pontuais e difusas de poluição, quantificar a carga de fósforo produzida na bacia hidrográfica, obter a carga média afluente aos reservatórios e desenvolver relações fluxo-concentração de fósforo total para a entrada nos reservatórios. A terceira avaliação focou na produção de carga interna de fósforo no reservatório. Os fluxos diários brutos e as taxas de liberação médias sazonais líquidas foram estimados para melhorar a compreensão da liberação de fósforo do sedimento. Importantes resultados obtidos nesta dissertação relacionam-se i) à adaptação de modelos clássicos de balanço de massa para estimar a produção de carga de fósforo impactando reservatórios semiáridos, independentemente do período do ano, ii) ao detalhamento do comportamento da relação fluxo-concentração de fósforo dependendo do uso do solo da bacia, iii) à combinação de métodos para avaliar e quantificar taxas de liberação de fósforo do sedimento e iv) a proposição de modelos e novos indicadores para estimar a carga de fósforo. Os resultados deste trabalho são inovadores, visto que a quantificação das cargas externas e internas de fósforo foi aproximada pela estimativa das cargas produzidas durante os períodos úmido e seco, respectivamente. Ademais, este estudo não apenas avançou o conhecimento da dinâmica do fósforo em reservatórios tropicais do semiárido, mas também forneceu evidências da produção de cargas internas significativas nesses ecossistemas. Espera-se que as metodologias simples apresentadas nesta dissertação auxiliem no entendimento das questões relativas ao fósforo total em regiões áridas/semiáridas e auxiliem em ações de gestão integrada da qualidade da água em reservatórios estratégicos de abastecimento humano.

Palavras-chave: Balanço de fósforo; Uso do solo; Liberação do sedimento; Cargas interna e externa; Modelagem da qualidade da água.

ABSTRACT

This dissertation presents an assessment of the dynamics of total phosphorus (TP) in strategic semiarid reservoirs, from a catchment to an in-lake scale. The catchment phosphorus production and delivery to these water bodies depending on the climate period and the understanding of the drivers to sedimentary phosphorus release and resuspension were evaluated. The purpose of the first assessment was to develop a novel methodology to estimate the total phosphorus load arriving to the reservoirs in the wet and dry periods and find evidence of internal loading production. The purpose of the second assessment was to quantify the phosphorus load produced in the catchment, describe the importance of point and non-point sources of pollution, and obtain mean input load and inlet concentration-flow relationships. The third assessment focused on the internal phosphorus regeneration into the reservoir. Gross daily fluxes and net seasonal average release rates were estimated to improve the understanding of sedimentary TP fluxes. Important fundamental results obtained in this dissertation were i) the adaptation of classical mass balance models to estimate phosphorus load production impacting semiarid reservoirs regardless of the rainfall-related period, ii) the detailing of the flow-concentration relationship behavior depending on catchment landuse, iii) the combination of methods to assess and quantify sedimentary fluxes under sediment-data constraints, and iv) the proposition of models and new indicators to estimate TP load. The findings of this work are novel as the quantification of external and internal P loads was approximated by the estimation of the loads produced during the wet and dry periods, respectively. Furthermore, this study not only advanced the knowledge of P dynamics in tropical semiarid reservoirs, but also provided evidences of significant internal loading to these ecosystems. It is expected that the simple methodologies presented in this dissertation help to understand the phosphorus issue in arid/semiarid regions and assist integrated water quality management actions in strategic water supply reservoirs.

Keywords: Phosphorus balance; Land use; Sediment release; Internal and external loads; Water quality modeling.

LIST OF FIGURES

LIST OF TABLES

SUMMARY

CHAPTER 1

General Introduction

1.1 Total phosphorus dynamics and water quality

Phosphorus is an essential nutrient for all living organisms and its cycle influences phytoplankton ecology and productivity in both marine and freshwater ecosystems as well as those of natural and agriculture vegetation systems on land (Mackey et al., 2019). From a catchment perspective, the major source of phosphorus to aquatic environments is the weathering of minerals on land that are introduced into water bodies by fluvial and eolian sources. Furthermore, human activities such as farmland production and soil enrichment by fertilizers enhances the phosphorus availability to be carried out through runoff.

Once into the lake or reservoir, these water bodies may act as final destination for this nutrient depending on their retention capability. The phosphorus accumulation in the bottom sediment of the reservoirs is generally a long-term process. In the sediments, it may exist in many different physical and chemical states and may also shift from associations with minerals such as calcium, magnesium, iron and aluminum. Then, the phosphorus cycle into the reservoir and the net result from sink, release or resuspension results from the action of several physical and biogeochemical mechanisms.

Researches world-wide largely pointed out the key role of phosphorus pollution in the water quality issue. Eutrophication is one of the most common causes of water quality degradation of inland waters. It is triggered by changes in the quantity, relative proportions or chemical forms of nitrogen and phosphorus entering the lake/reservoir. Then, it generates major disruptions to the aquatic ecosystem and impacts goods, services, economic activities, and human health of the regions where it occurs (Moal et al., 2019).

1.2 Water quality management in semiarid regions

To deal with water quality issues and manage to prevent future degradation events in semiarid reservoirs is very challenging. However, it is particularly important considering human supply as the main use of water for these reservoirs. Although water resource protection policies need to be based on robust science, some uncertainties still remain over the main drivers of eutrophication, the nutrient coupling and processing across the air‐land‐freshwater‐estuarine continuum, the influence of watershed-scale processes and the impact of the internal sources (Jarvie et al., 2013).

Considering phosphorus one of the main drivers to water quality degradation, controlling measures to reduce phosphorus input to the water bodies may be taken on a catchment or reservoir basis. Each approach, however, requires different efforts and has a distinct cost, time response and duration. From a catchment scale, actions may be taken regarding the soil, agriculture, and the rural population contributions. While some measures might be impractical to be taken, others may be possible, although reaching a government level. From a reservoir scale, measures to control internal phosphorus regeneration are more challenging. For instance, literature suggests the water level variation control to minimize its negative impact on water quality deterioration. However, semiarid regions are exposed to high evaporation rates (Brazil, 2021) and recurrent drought events what makes unrealistic this controlling, so the waterbodies respond freely to the environmental drivers. From a broader perspective encompassing the entire water supply network with strategic water supply reservoirs, support the water management agencies and decision-makers with knowledge on this matter intends to help the development of optimized pollution management strategies.

1.3 Dissertation organization

This dissertation is composed of three contributions on total phosphorus modeling, including: i) an overall assessment of the total phosphorus load production in the different rainfall-related periods of the semiarid climate, ii) an evaluation of the catchment production and delivery of the total phosphorus load to downstream reservoirs and iii) an assessment of the internal load production and driving mechanisms inducing phosphorus release from bottom sediments into the reservoirs. Each contribution is presented in a separate chapter. Following is a brief introduction to each chapter.

Chapter 2 describes the dynamics of total phosphorus in eighteen strategic reservoirs of the high-density reservoir network of the Brazilian semiarid during the wet and dry periods over the past 12 years. The objective of this study was to develop a novel methodology based on a transient complete-mix mass balance model to estimate the wet and dry period TP loads to strategic water supply reservoirs in the Brazilian semiarid region. Specifically, the goals were: (i) to evaluate the dynamics of seasonal and interannual epilimnion and average water column TP concentration under the influence of the wet and dry periods, (ii) to model and assess circumstantial evidences for the large likelihood of internal loading, (iii) to compare estimated internal loads in the context of external loading, and (iv) to analyze and propose general correlations between TP loads and reservoir/catchment characteristics. The results from this

study intends to improve the knowledge of the limnology of tropical semiarid reservoirs and propose potential tools to promote sustainable integrated water management in dry lands.

Chapter 3 presents the development of a new approach designed to investigate the issue of phosphorus pollution in semiarid regions with intermittent rivers. The methodology was applied for twenty reservoirs in the State of Ceará, Brazilian semiarid. Hydrological data and total phosphorus concentration at reservoirs' outlet were combined in a transient complete-mix model to obtain mean input loads and inlet concentration-flow relationships. The objectives of this study were (i) to provide a methodology to estimate and evaluate average TP load and concentration at reservoirs' inlet through a mass-balance approach, (ii) to extend the application of TP-discharge relations to regions of intermittent rivers, (iii) to improve the understanding of flow conditions on TP concentration at reservoirs' inlet, and (iv) to provide a tool to address the TP issue in water bodies in data scarce regions. This study presents a simple way to deal with the phosphorus pollution issue and the challenging lack of monitored data in semiarid environments.

Chapter 4 presents the improvements in the understanding of sedimentary total phosphorus fluxes in thirty reservoirs of dryland regions. Net and gross average seasonal sediment fluxes were estimated and its relationships between physical, limnological and climatic drivers were investigated. The seasonal estimates and long-term variability were statistically connected with single factors (P external fluxes, physical and environmental drivers, trophic state index) and coupling factors (mean lake level fluctuation and wind speed/volume ratio). Additionally, models were proposed to predict release rates from a new practical surrogate indicator (the wind speed/volume ratio). This study innovated in evaluating the internal P loading potential of semiarid reservoirs under data constraints while elucidating particular relevant driving factors affecting P release in dryland regions. Finally, Chapter 5 presents some general conclusions.

CHAPTER 2

Phosphorus mass balance and input load estimation from the wet and dry periods in tropical semiarid reservoirs[1]

2.1 Introduction

The reduction of phosphorus (P) loading has been the major effort to deal with the eutrophication issue in lakes (Le Moal et al., 2019). Total P in water consists of a variety of organic and inorganic forms (Doan et al., 2018), in which the processes within the lake are also an important source of contribution (Nürnberg 2009). Additionally, lake's morphometry, climatic conditions, oxygen concentration and macrophyte presence play an important role on P dynamics (Kowalczewska-Madura et al., 2019; Seitz et al., 2020; Wiegand et al., 2021), especially on its spatial and temporal variability (North et al., 2015).

A broader distinction regarding P origins is widely accepted: phosphorus carried through rivers to downstream lakes or reservoirs is called external P loading (Song et al., 2017), which may be further divided into point and non-point sources (Bowes et al., 2008). In contrast, P released from sediments within the waterbody is known as internal loading (Nikolai and Dzialowski 2014). P enriched sediments are a result of a long-term accumulation process from P entering the lake. Then, at some extent, there is a relation between these two sources once the external one origins internal nutrient recycling. The formidable challenge, though, is to track lake water P and distinguish its origin from internal or external sources (Nürnberg et al., 2013).

Commonly, external load represents a higher percentage in an annual P budget and its relevance have formed the basis for classic predictive models such as the one of Vollenweider (1968) (Lepori and Roberts 2017). The majority of P that comes to a lake ecosystem, however, is usually stored in the bottom sediment (Kiani et al., 2020), which in appropriate conditions returns to the water column (Moura et al., 2020b). P releasing from sediments results from physical and/or biogeochemical mechanisms that operate on different temporal and spatial scales in a complex process (Orihel et al., 2017; Søndergaard et al., 2003; Araújo et al., 2019). Therefore, internal loading might pose a high risk of becoming an additional P source, contribute to the total in-lake P bioavailability and to the deterioration of the trophic state and water quality (Doan et al., 2018).

---

[1] The content of this chapter has been published in Environmental Science and Pollution Research (https://doi.org/10.1007/s11356-021-16251-w)

For tropical semiarid regions, such as the Brazilian Northeast, most water supply reservoirs are already eutrophic or hypereutrophic, which turns the P pollution issue a great concern for water resources management (Lopes et al., 2014; Pacheco and Lima Neto, 2017; Lacerda et al., 2018; Lira et al., 2020; Rocha and Lima Neto, 2021b). Additionally, the reservoirs are under two periods marked by a clear seasonality: the dry and wet one. The dry period extends to almost the entire second semester of the year and has an inflow virtually nil (Costa et al., 2020). In this region, the internal load production is expected to be stronger in the dry season, as hypolimnetic dissolved oxygen usually falls below 1.0 mg L^{-1} (Souza Filho et al., 2006), the water volume decreases and the wind speed intensifies (Mesquita et al., 2020). Under these effects, anoxia-induced P release and wind-induced resuspension are highly likely (Moura et al., 2020b). Additionally, only a few regions (mostly arid or semiarid environments) present intermittent rivers in which is possible to have a controlled period with the minimal interference of external inputs on P modeling. Hence, an analysis focusing on these two distinct periods (wet and dry seasons) might contribute to the understanding of TP dynamics and the role of internal and external TP load in waterbodies of dryland areas.

Despite the importance of internal loading for lake modeling, its quantification and/or comparison to external loading is seldom performed, mainly in semiarid aquatic ecosystems. External loading is normally evaluated from the product of flow rate with measured or modeled P concentration at the lake inlet (Bowes et al., 2008). As for internal load quantification, there are several ways to determine it depending on data availability (Nürnberg et al., 2012), such as: determination from hypolimnetic P increases, regression analysis, time-dynamic modeling, estimates from anoxic active area and mass balance approaches (Nürnberg 2009). Widely applied, mainly when calculating multiyear averages (Nürnberg et al., 2012), is the P load estimation by constructing a whole-lake mass balance accounting for a global sedimentation rate (Orihel et al., 2017). The issue of P budget from measured concentration, however, is the difficulty to distinguish between different sources (Nürnberg et al., 2012). Meantime, a mass balance analysis in a controlled period when the inflow is nil, such as the dry period of the Brazilian semiarid, may allow the quantification of the internal load as the main TP input. The climatic conditions imposed upon the waterbodies in this region, such as a diurnal mixing cycle (Lira et al., 2020; Mesquita et al., 2020), weak stratification patterns (about 1-5ºC) (Lacerda et al., 2018) and low depths due to drought events (Wiegand et al., 2020), support the application of parsimonious models to quantify TP load production.

Thus, the objective of this work was to develop a novel methodology based on a transient complete-mix mass balance model to estimate the wet and dry period TP loads to

strategic water supply reservoirs in the Brazilian semiarid region. Specifically, the goals were: (i) to evaluate the dynamics of seasonal and interannual epilimnion and average water column TP concentration under the influence of the wet and dry periods, (ii) to model and assess circumstantial evidences for the large likelihood of internal loading, (iii) to compare estimated internal loads in the context of external loading, and (iv) to analyze and propose general correlations between TP loads and reservoir/catchment characteristics. The results from this study will improve the knowledge of the limnology of tropical semiarid reservoirs and the proposed model/correlations will be potential tools to promote sustainable integrated water management in dry lands.

2.2 Methodology

2.2.1. Study area

The study area covers eighteen monitored water supply reservoirs in the State of Ceará, Brazil, presented in Figure 2.1. Table 2.1 details their specific location and general characteristics. These reservoirs are scattered in the twelve hydrologic regions in which the State of Ceará is divided for water resources management. The combined area of their catchments represents about 59% of the state's area and their volume reach a total accumulated capacity of 10.19 km³. The shallowest reservoir is Colina (maximum depth of 12 m), while the deepest is Castanhão (maximum depth of 71 m deep). These water bodies support the network that supplies water for human, industrial and agricultural uses. On average, the reservoirs have a depth of 23.85 m. However, due to the six-year drought event within the study period (Moura et al., 2020a), this average dropped to 13.35 m.

Landuse in the catchments is dominated by managed grasslands with a spread anthropogenic presence in which a variety of animal husbandry is carried out, including fish farming in some reservoirs. Agricultural land with irrigated crop production can be found in Jaguaribe river basin, whilst dispersed rural population practices primarily subsistence agriculture and plant extraction. With regards to climate, rainfall vary from 605.07 mm yr^{-1}, in the Colina reservoir catchment to 1378.62 mm yr^{-1} in the Itauna catchment. The rivers which supply these reservoirs are intermittent, with inflow occurring only during the rainy season (January to July). From 2012, almost the entire State of Ceará has faced a prolonged drought period that led to a continuous reduction in the reservoirs' volume (Wiegand et al., 2020). A more detailed description of the geology, geomorphology and land use of the studied catchments can be found in Ceará (2020).

Figure 2.1 - Location of the eighteen studied sites in the State of Ceará - Brazil, whose description is presented in Table 2.1

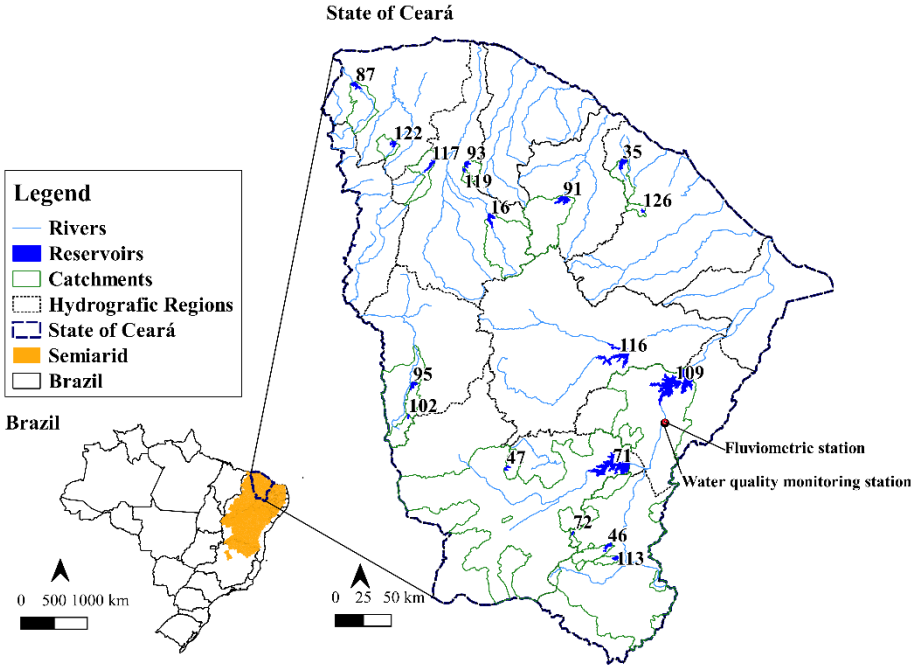

Table 2.1 - Physical characteristics of the studied reservoirs, their catchments and the period of available water quality data

ID	Reservoir	Main river	Catchment area (km²)[a]	Mean surface area (km²)[a]	Mean depth (m)[a]	Data period	Inventory date [b]
16	Edson Queiroz	Groaíras	1778	7.90	17.32	2008-2019	2011
35	Sítios Novos	São Gonçalo	446	4.35	10.96	2008-2019	2008
46	Rosário	Rosário	337	3.83	10.40	2010-2019	2011
47	Rivaldo de Carvalho	Rivaldo de Carvalho	318	0.68	9.12	2008-2019	2011
71	Orós	Jaguaribe	24538	61.34	6.51	2008-2019	2011
72	Olho D'água	Machado	72	1.18	12.52	2008-2019	2008
87	Itauna	Timonha	781	11.48	7.30	2011-2019	2011
91	General Sampaio	Curu	1582	10.10	17.54	2008-2019	2011
93	Forquilha	Oficina	191	3.05	7.71	2008-2019	2008
95	Flor do campo	Poti	663	3.82	10.96	2010-2019	2011
102	Colina	Poti	363	1.31	6.00	2008-2019	2009
109	Castanhão	Jaguaribe	44800	123.14	35.50	2008-2019	2011
113	Cachoeira	Caiçara	143	1.92	12.00	2008-2019	2011
116	Banabuiú	Banabuiú	14243	18.86	28.44	2008-2019	2011
117	Ayres de Souza	Jaibaras	1102	6.94	14.45	2010-2019	2009
119	Arrebita	Sabonete	79	1.50	9.10	2008-2019	2011
122	Angicos	Juazeiro	286	5.98	9.45	2008-2019	2011
126	Acarape do Meio	Pacoti	210	1.50	15.04	2008-2019	2008

[a] Ceará (2021)
[b] Ceará (2020)

2.2.2 TP load estimation

Considering the available data for this study, the method used for the internal P loading estimation was a complete P budget. The basic assumption for the load estimation process considered that during the wet season (high inflow) prevails external loads, while the internal load is dominant during the dry season (absence of inflow). However, it is acknowledged the possible existence of the internal load, even in small percentage during the wet season or possible external load contribution through point source, such as eventual animal's access to the waterbody, during the dry season. Then, to avoid a generalization, the loads estimated in the rainy season will be referred as the wet period load and those estimated for the dry season as dry period load, while they intend to represent the external and internal loads, respectively. This assumption is considered adequate since during the wet season the well-mixed behavior in the reservoirs is favored by the inflow as well as a reduction in any stratification pattern (Lima Neto, 2019). Moreover, as the reservoirs have rural catchments, significant external P input is expected from runoff during the wet period. On the contrary, during the dry season the inflow is negligible, the water level is lower and the wind velocity higher (Wiegand et. al, 2021), which enhances physical processes such as P resuspension in addition to biogeochemical ones. Furthermore, it is widely reported the prevailing of external load during the rainy period and the internal loading during the dry period in the study region and other semiarid environments (Freire et. al, 2009; Coppens et. al, 2016; Cavalcante et al., 2018; Barbosa et al., 2019).

2.2.2.1. Total phosphorus model

The transient complete-mix model presented in Equation (2.1) was designed to predict the average TP concentration in hypothetically well mixed waterbodies (Vollenweider 1968; Chapra 2008). The model involves parameters related with the lake morphometry, water balance and nutrient dynamics. It was applied as a calibration process of the load for time intervals of, at most, four months, in which the initial and final TP concentrations were available. The remaining parameters were calculated as an average over the period between the TP measurements. TP concentration, morphometric and water withdrawal data were provided by the Water Resources Management Company of the State of Ceará (COGERH), for the eighteen studied reservoirs (Ceará, 2021). Regarding the water quality, TP measurements are usually collected four times a year, twice per semester, generally at the beginning and at the end of the wet and dry periods. Thus, in this study, the data collected from January to July were

considered representing the wet season, while the data from August to December were considered as representative of the dry one.

$$TP(t) = TP_o e^{-\left(\frac{Q}{V}+k\right)t} + \frac{W}{Q + kV}\left[1 - e^{-\left(\frac{Q}{V}+k\right)t}\right] \quad (2.1)$$

In which TP(t): Total phosphorus concentration at a specific time (kg m^{-3}); TP_o: Total phosphorus concentration at the initial time (kg m^{-3}); t: Elapsed time (yr); V: Reservoir volume averaged over the elapsed time (m^3); W: TP load (kg yr^{-1}); Q: Released flow (m^3 yr^{-1}); k: TP settling loss rate (yr^{-1}).

The application of Equation 2.1 consisted of taking paired measurements of surface TP concentration [TP_o and TP(t)], the elapsed time between these measurements (t) and the mean parameters of the reservoir for this time interval (V, Q and k) to estimate the average TP load (W). For the paired TP concentration measured during the wet season, the fitted W refers to the load of the wet period. Similarly, from TP concentrations measured during the dry season, W refers to the load of the dry period. This process was applied whenever there was available data for both periods (wet and dry) among the years presented in Table 2.1. The results, then, were converted to a monthly average. The areal phosphorus load was also obtained from the division of each estimated load by the mean lake surface area of the same time interval. The surface area was obtained through level-area-volume curves available in Ceará (2021).

The TP load estimation was performed to identify and differentiate the roles of the wet and dry seasons in the input loading production. However, in larger reservoirs such as Castanhão, periods of low hypolimnetic dissolved oxygen (< 2 mg L^{-1}) are observed during the rainy season (Santos et al., 2017). This suggests the occurrence of P release during the rainy period. Meantime, since in this period most of the total load is external due to high inflow, the internal load contribution to the budget during the rainy season is expected to be small (Freire et. al, 2009). Furthermore, although internal load is typically ortho-phosphate release, its estimation from TP concentration was originally proposed by Nurnberg and LaZerte (2001), accounting primarily for the unavailability of P speciation data. It was also highlighted that P speciation, such as the analysis of ortho-phosphate as DRP, does not necessarily lead to a reliable quantification of internal load. Only in anoxic hypolimnia with elevated TP concentrations DRP determination may be used to accurately quantify internal load (Nürnberg, 2009). Additionally, the internal load quantification as a mass of total phosphorus has been widely applied (Nürnberg 2009, 2012, 213; North et. al, 2015; Horpilla et. al, 2017).

2.2.2.2 Settling loss rate (k) and retention time (RT)

The TP model applied in this study integrate the processes of P removal from the water in the parameter k, a global decay coefficient which accounts for the average P settling. The empirical relationship that correlates k with the theoretical hydraulic residence time (RT) presented in Equation (2.2) was a workaround to the difficulty of estimating k experimentally. Moreover, it was adjusted and validated by Toné and Lima Neto (2020) for a wide range of Brazilian semiarid reservoirs and also validated by Lima (2016) and Araújo et al., (2019) for reservoirs located specifically in the State of Ceará. It is noteworthy that similar empirical relations with k varying with the inverse of $RT^{1/2}$ were also developed for temperate and tropical lakes (Vollenweider, 1976; Salas and Martino, 1991). However, this correlation (Equation 2) intended to consider the effect of the higher water temperature of the Brazilian semiarid reservoirs (~30ºC), as compared to those for temperate (~10ºC) and tropical (~20ºC) lakes. Higher water temperature leads to a combined effect of increasing P consumption by algae and decreasing water viscosity, then favoring higher phosphorus sedimentation rates (Toné and Lima Neto 2020). Equation (2) can also be obtained by applying the equations accounting for algae consumption and water viscosity (see Castagnino 1982) to convert the values of k from temperate or tropical lakes to semiarid ones. Therefore, it was assumed to be reliable for the purposes of the present study.

$$k = \frac{4}{RT^{1/2}} \tag{2.2}$$

The real residence time, depending on reservoir morphometry and hydrodynamics (Castellano et al., 2010), was replaced by the theoretical hydraulic residence time (RT). It was considered a consistent assumption since it is in accordance with the complete-mix hydraulic behavior adopted and has demonstrated to have good accuracy for relatively well-mixed lakes (Pilotti et al., 2014). The RT was calculated as presented in Equations (2.3) and (2.4) for the wet and dry periods, respectively. The common definition of residence time (Equation 2.3) accounts for continuous river flow. However, as the rivers in the study area are intermittent, the replacement of the inflow (I) by the sum of the rates of released (Q) and evaporated (E) flow was performed when modelling a time interval during the dry conditions.

$$RT = \frac{V}{I} \tag{2.3}$$

$$RT = \frac{V}{Q + E} \quad (2.4)$$

2.2.3. Water quality and water balance data

Epilimnion TP concentration and chlorophyll-a measurements consisted in the most complete dataset available. Samples were collected about four times a year close to the reservoir dam or the floating pumping station, and then analyzed according to APHA (2005). The measurements of TP in the hypolimnion, however, represented a shorter dataset and were used to perform statistical analysis and evaluate the mixing hypothesis adopted as well to support the use of TP concentration in the upper layers as a reference to estimate the input load. With regards to TP load data, COGERH has also elaborated an environmental inventory covering the catchment of each studied reservoir for the year shown in Table 2.1. Since they are highly costing and time demanding, they were elaborated only once. The methodology applied estimated the annual TP load produced by each catchment based on the Export Coefficient Modelling (ECM) approach (Johnes 1996). Details on the calculation process of this reference load is available in Ceará (2020).

COGERH also provided the water level measurements and level-volume curves, used to obtain the morphometric data and the water balance data (inflow and released flow) on a monthly basis. Particularly for the inflow, since it is obtained from water balance, it accounts the water coming from all sources to the water body. Then, possible P-rich groundwater occurring during the wet period are incorporated in the model as external P sources, according to Orihel et al., (2017). Lastly, the evaporated height was quantified from the climatological normals of the closest climatological station to each reservoir (Brazil, 2021).

2.2.4 Comparison of different P modeling approaches and model validation

The validation of the estimated loads was performed through a correlation analysis between the mean modeled annual TP load and the reference load available by Ceará (2020). Moreover, as the Castanhão reservoir features two additional measured water quality and quantity datasets, the validation specifically of the wet TP load estimated for this reservoir was performed. An active fluviometric station is located in its main river allied with a water quality monitoring point in which riverine TP concentration is measured (see Figure 2.1). The proximity between the fluviometric station and the water quality sampling point (less than 50 meters) and of those two the reservoir (less than 24 km) allows the estimation of the wet TP load from a flow-concentration approach (Bowes et al., 2008). This load was estimated by

multiplying the measured riverine TP concentration (kg m^3) and the daily average flow (m^3 s^{-1}) observed in the fluviometric station for the same day of TP sample. Then, these loads were correlated with the ones obtained according to Equation (2.1), for the same time period.

2.2.5. Statistics and uncertainty analysis

The load estimation process might arise uncertainties from the hydrological parameters and water quality data (Hollaway et al., 2018). Initially, an outlier analysis of the TP concentration and chlorophyll-a data was performed. For the TP data it was considered the limiting value of 4000 µg L^{-1} for TP concentration in wastewater (Sperling, 2007), in which values over this limit were excluded. Additionally, the coefficient of variation of the estimated loads was calculated for each reservoir, as well as the bias existing between the modeled loads and the reference load. A further quality analysis of this statistical parameters in comparison the available literature for TP load estimation was performed. Finally, a research was carried out to gather mean error values for the TP load estimated by the ECM methodology. The value of 31% was the maximum reported in the searched literature (Johnes 1996; Ding et al., 2010; Matias and Johnes 2012; Delkash and Al-faraj 2014; Greene et al., 2015; Tsakiris and Alexakis, 2015). Then, it was used to discuss and evaluate the variations of the reference load in comparison with the variation of the estimated loads.

The variation in the epilimnion TP concentrations and the chlorophyll-a between the two studied periods (dry and wet) was statistically analyzed with the Kruskal-Wallis and Mann-Whitney tests. These non-parametric tests were suitable due to the unequal length of observations within each period. They were also performed to evaluate differences between surface TP concentrations and those measured in other depths. The results allowed to reinforce the representativeness of the epilimnion concentration for the water column at the sampling point. Statistical packages in Python programming were used for pairwise comparisons.

Additionally, a sensitivity analysis was carried out to identify the most influencing parameters in the modeling and support the understanding of the variability or the estimated loads. The reservoir inflow and volume were chosen to evaluate since they were explanatory variables of the proposed predictive models for the wet and dry periods, respectively. The other evaluated variables were the elapsed time between the TP measurements and the ratio of the final TP concentration by the initial concentration (TP(t)/TP0). One variable was taken at a time to test a range of variation while the others were kept unchanged. As a preliminary result these four variables were listed as the highest influencing ones. Then, considering the maximum mean error of the reference load of 31% (which will be further addressed in detail), one

parameter was tested at a time varying by ±30% as the others remained unchanged. The mean deviation in the estimated loads were discussed.

2.2.6. Correlation analysis

The TP load presents some well-known characteristics and strong correlations with parameters related to the catchment or the reservoir. Firstly, larger catchments have the potential to produce more TP load (Marques et al., 2019). Additionally, there is a relation between nonpoint sources P pollution with flow conditions (Greene et al., 2011). Some particular correlations even between internal and external load were also reported in literature (Nürnberg et al., 2012). In contrast, the complex behavior of the internal load brings more undefined correlations with these parameters. Aiming to explore the existence of similar relationships in the studied area, a correlation analysis was carried out between: TP load and catchment area, load of wet period and reservoir inflow, load of dry period and reservoir volume, and loads of the wet and dry periods. The goodness of fit was evaluated trough the Pearson's correlation coefficient.

2.3. Results and discussion

2.3.1. Catchment and reservoir hydrology

The variation of the volume and the inflow regime of each reservoir for the studied period are presented in Figure 2.2. The interannual variability of the reservoirs' volume can be observed in the large range of variation of the boxes. The reservoirs Orós, Castanhão and Banabuiú differed from the others with the highest stored volumes in the period. Their median volume was roughly 1,363 hm^3 while the maximum median volume after them was 79.95 hm^3 for the Edson Queiroz. The reservoirs Colina, Flor do Campo and Rivaldo de Carvalho achieved critical storage in the studied period with minimum volumes ranging from 0.01 to 0.04 hm^3. These reservoirs are the smallest ones and become nearly empty on a yearly basis, which makes them "annual reservoirs". Contrastingly, the larger and more resilient ones (Orós and Castanhão) are considered "interannual reservoirs" (Lopes et al., 2014; Campos et al., 2016; Lacerda et al., 2018).

Figure 2.2 - Main hydrologic variables of each reservoir for the studied period

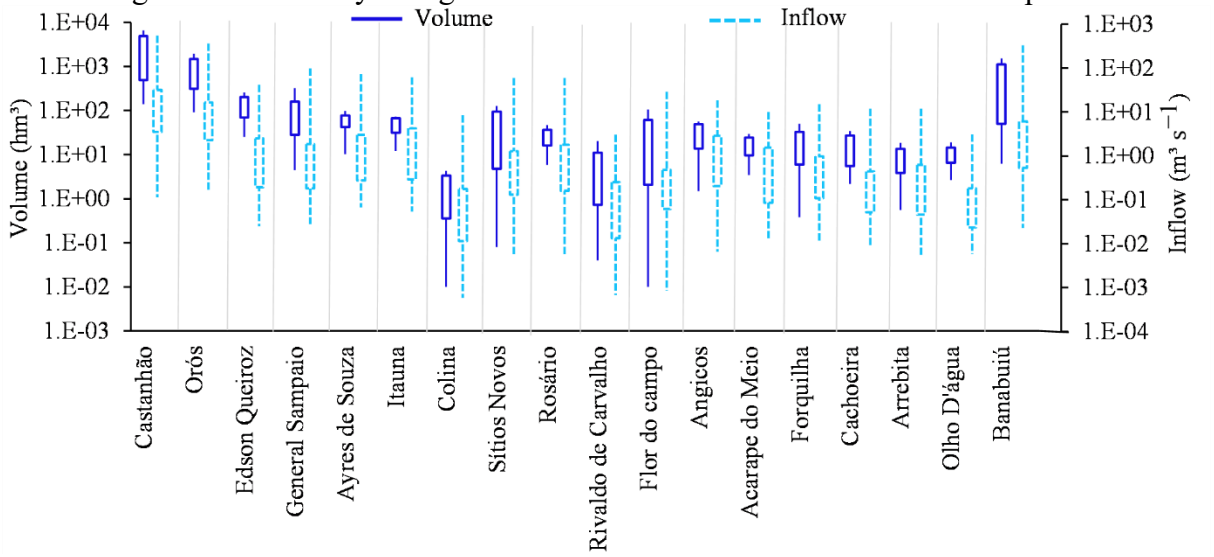

Regarding the mean inflow, the sum of the mean streamflow from the rivers and tributaries flowing to the reservoir, a great variation of flow regime was observed. The reservoir Olho D'água presented the lowest values, from 0.003 to 3.07 $m^3\ s^{-1}$, while the Castanhão catchment produced the highest ones, from 0.11 to 549.13 $m^3\ s^{-1}$. Additionally, some catchments could be grouped by similar characteristics in the period. The reservoirs Cachoeira, Arrebita and Forquilha, with the smallest catchments and an average precipitation on record of 916, 1,063 and 679 mm yr^{-1}, respectively, presented similar inflow patterns in the period, from 0.008 to 14.97 $m^3\ s^{-1}$ in average.

Similarly, the reservoirs Angicos and Acarape do Meio presented similar patterns, from 0.007 to 14.44 $m^3\ s^{-1}$ in average, with median inflows of 0.63 and 0.69 $m^3\ s^{-1}$ and catchment areas of 285.62 and 210.01 km^2, respectively. In contrast, the catchment of the reservoirs Rosário, Rivaldo de Carvalho, Colina and Flor do Campo, tough, have shown a more anomalous behavior compared with the others. Rosário presented a small variability while the remaining presented low values of inflow. It is noteworthy that the catchments of Flor do Campo and Colina share similar climatic characteristics due to their proximity (about 40 km between reservoirs). They had average precipitations of 577.10 and 615.40 mm yr^{-1}, respectively, which are very low and, as a consequence, contribute with low inflow rates.

Changing in precipitation levels throughout years is the main driver for interannual variability in reservoir volume and inflow in the State of Ceará (Broad et al., 2007), as a decline in the mean inflow is expected mostly during low precipitation periods (Zhang et al., 2015). Besides, the reservoirs have experienced a dramatic reduction on their volume due to the prolonged drought during the studied period (Lacerda et al., 2018, Wiegand et al., 2020).

Mamede et al., (2018) also highlight the reservoirs' density in the watersheds of Ceará as a contributing characteristic to the inflow variabilities since the reduction of the contributing area to downstream and strategic reservoirs reduces the inflow consequently.

2.3.2 Characterization of the water column TP concentration

The variation of the TP concentration in the hypolimnion and epilimnion was evaluated for the reservoirs from measurements at the sampling points near the dams. The dataset collected encompasses the entire studied period. Figure 2.3 summarizes this result for four reservoirs. They were selected because their depth ranged from the shallowest to the deepest reservoir. The vertical profile of the seasonal mean TP concentration for each depth in the studied period is presented along with the standard errors. In the wet period, the mean TP concentration in the water column, considering the measurements in all depths, varied from 37.39 to 533.86 μg L^{-1}, with a median of 67.87 μg L^{-1}. In the dry period, the ranges were from 27.73 to 227.35 μg L^{-1} with a median of 61.93 μg L^{-1}. The statistical analysis was performed between the two datasets encompassing all measurements in the wet and dry periods. The results indicated no significant p-value to support differences in the average TP concentration in the water column between these periods ($p>0.05$) for seventeen reservoirs, except Colina, which is the shallowest reservoir. Shallow water bodies are more susceptible to wind-induced water column mixing which leads to increasing nutrient concentration driven by resuspension (Nürnberg et al., 2012).

Overall, it was observed that the mean concentration for the two seasons is very similar for more than 90% of the reservoirs. This was attributed to a trade-off between the hydrological and limnological processes occurring in the two seasons, following the dynamics described by Equation (2.1). While in the wet period the total load, reservoir volume and flushing rate are expected to be higher, in the dry period, all these parameters are expected to be lower. On the other hand, while in the wet period the retention time is expected to be lower and, consequently, the settling loss rate higher, the contrary is expected to occur in the dry period (see Equations. 2.2, 2.3 and 2.4).

Figure 2.3 - TP concentration in the water column for the sampling point near the dam of the reservoir (a) Itaúna, (b) Sítios Novos, (c) Acarape do Meio e (d) Castanhão. Arithmetic averages from 2008 to 2019 and standard errors (bars) are presented.

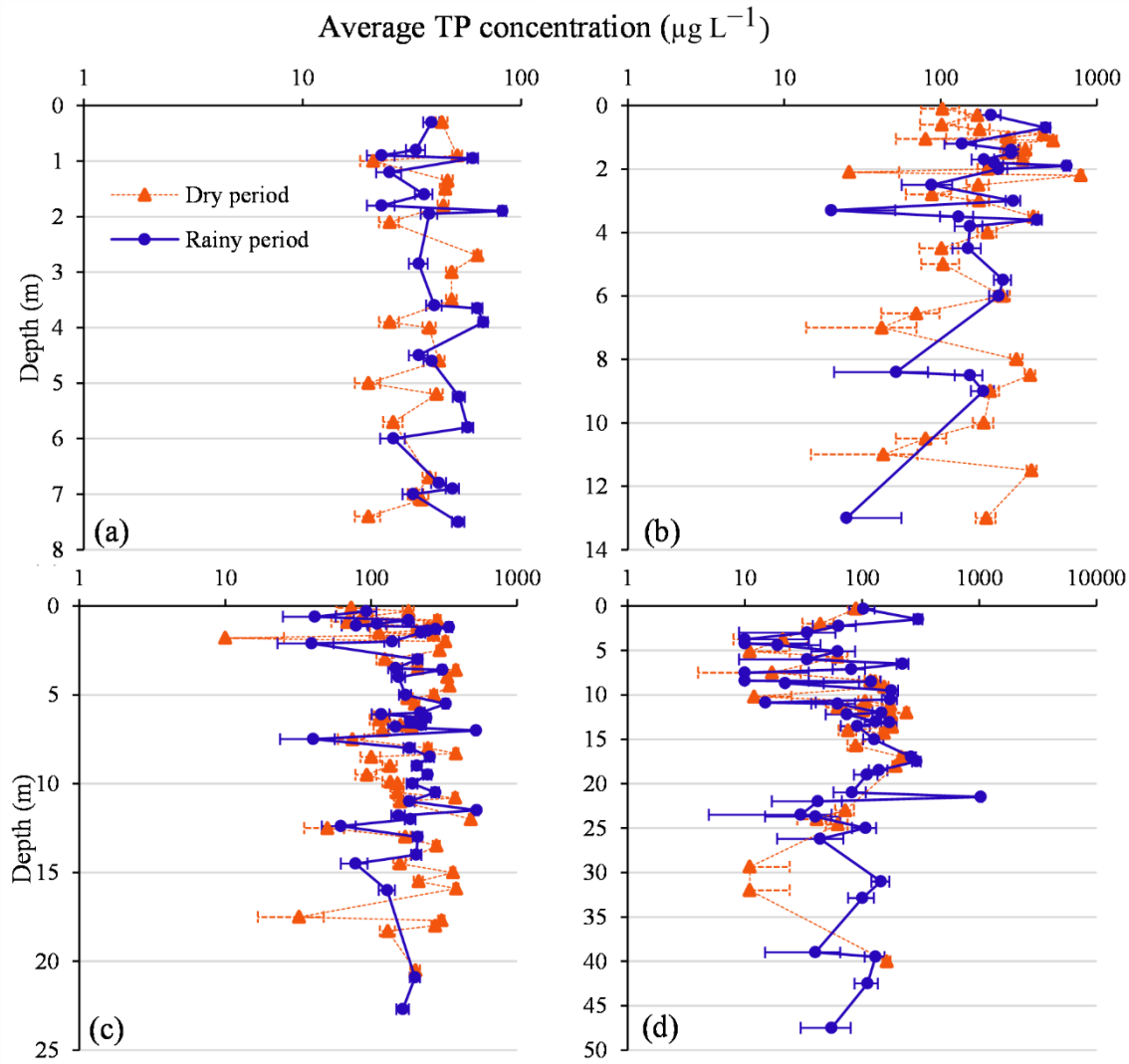

Additionally, the Mann-Whitney and Kruskal-Wallis tests performed between the values in the upper surface (0.3 m deep) and the values in the other depths presented significant p-values for 50% of the reservoirs (p<0.05). This suggests that some reservoirs have a marked mixing behavior and similar TP concentration between upper and lower layers as shown in Figure 2.3. It is important to highlight that the mixing state, mainly in polymictic lakes, might be variable among years (Nürnberg, 2009). Specifically, in the Castanhão reservoir, previous studies indicate that TP concentration measurements present similar values between surface and bottom waters, but with a slight increase towards the bottom (Lacerda et al., 2018).

High tributary inputs of P and release from anoxic sediments might be sources of contribution to the vertical variation of phosphorus concentration in the water column (Nürnberg et al., 2013). P released from sediments has the potential to increase phosphorus

concentration from processes such as diffusion and/or water column mixing and, especially under anoxic conditions, when it can also mix into the epilimnion (Nikolai and Dzialowski, 2014). Particularly for the studied period, while a drought event was in course, stronger mixing conditions occurred. The reduction of volume during drought events and the consequent decrease in water depth might have led to breaking of the thermocline due to wind forcing and contributed to the mixing in the entire water column (Lacerda et al., 2018). Additionally, the effect of wind shear under relatively shallow water conditions potentially caused wind-induced resuspension of sediment and phosphorus, as already pointed out by Araújo et al., (2019) and Mesquita et al., (2020). It is important to highlight that the analysis in the present study was performed for the sampling points near the dams. Hence, spatial variabilities might pose differences for other regions of the reservoirs.

2.3.3 Impact of the drought period in the water quality and reservoir volume

Figure 2.4 presents the temporal distribution of volume, inflow, epilimnion TP concentration and wet/dry period loads for the reservoir Edson Queiroz in the studied period. This reservoir was chosen since it presents typical characteristics of all studied reservoirs. Figure A9 present the evolution of the volume and inflow for all the study sites. The period of remarkable low inflows encompassing from 2011 to 2017 is similar to all other reservoirs along with the increase in epilimnion TP concentration. During this period, they all also presented a drastic volume reduction. For the reservoir Edson Queiroz, the remaining volume at the end of 2016 represented 17.6% of the initial volume in 2011, a reduction from 152.5 hm^3 to 26.9 hm^3. The largest and strategic reservoirs Orós, Castanhão and Banabuiú were those which caused more concerns about their volume reduction. At the end of 2016 they reached 14.3%, 5.1% and 0.43% of their total volume, respectively.

The observed depth reduction during the dry season (considering the difference in water level between the two dates on which the TP measurements were performed) was 1.3 m on average, varying from 0.32 m to 5.53 m. The reservoir that showed the highest level variation was Banabuiú (5.53 m between July and November 2014) and Castanhão (3.66 m between August and December 2015). In the dry period, the evaporation loss and the withdrawal for human consumption are mostly responsible for this water level variation. Additionally, drought events can intensify large variations in water levels, which consequently might cause changes in the physical, chemical and biological characteristics of the waterbodies (Moss, 2011).

Figure 2.4 - Time series of volume, inflow, epilimnion TP concentration and wet/dry period loads for the reservoir

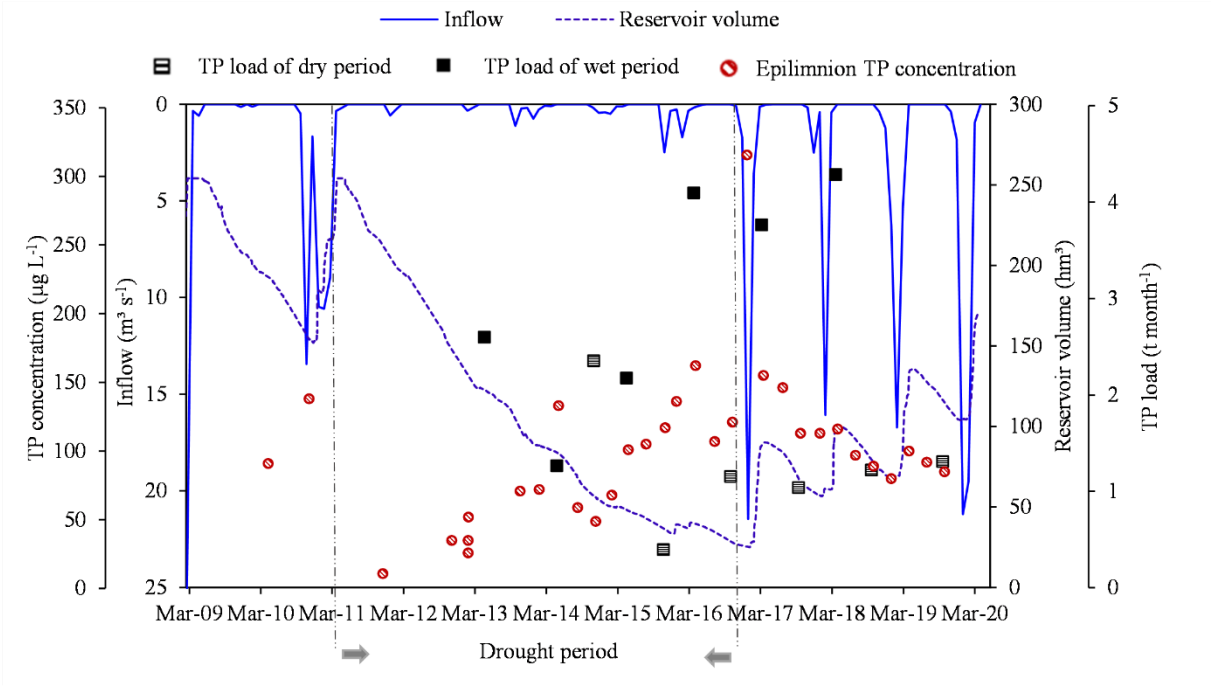

From the wet period of 2017 the inflow pattern increased drastically presenting a peak of 21.46 $m^3\ s^{-1}$ which was 18-fold higher than the average inflow of wet period since 2010. During the wet period of 2017 the highest TP concentration was also measured (314 $\mu g\ L^{-1}$). As already pointed out herein, in waterbodies with a high level of trophy, sediment resuspension by storm events favor nutrient resuspension and increase in nutrient concentration (Seitz et al., 2020). Additionally, higher loads were observed from the increase in inflow as annual external P loading is strongly related to storm events (Carpenter et al., 2014; Rattan et al., 2017).

The TP concentration of the overlying water has showed a pattern of continuous increase from 2011 to 2017, from 34 $\mu g\ L^{-1}$ on February-2011 to 161 $\mu g\ L^{-1}$ on April-2016, while the reservoir volume decreased continuously, as the studied region faced the drought event (Wiegand et al., 2020). Cavalcante et. al (2018) analyzed two semiarid reservoirs during a drought period and observed the highest average TP concentration values during the periods with lower depth. Extended droughts, particularly, have an important role in water quality deterioration due to increasing concentrations of nutrients (Lacerda et al., 2018).

Figure 2.4 also shows the mean modeled TP load for each semester throughout the studied period. As already mentioned, the load during the dry period can be caused by both sediment release and/or resuspension (Moura et al., 2020a). Particularly in shallow lakes, internal loading can promote elevated TP values in the epilimnion (Horppila et al., 2017).

During the drought period, the water level of the studied reservoirs decreased significantly while the TP concentration in the epilimnion increased continuously. Accordingly, higher TP loads were found. The average relation between the load of the wet period and the load of the dry one was about 43% in this period. This might suggest the influence of the low depth in this process. Cavalcante et. al (2018) also reported the highest observed average TP concentration during periods with low depth. Additionally, changes in lake size, depth, and climate potentially affect the level of the critical nutrient and can facilitate a regime shift in the ecosystem (Seitz et al., 2020).

The wet season, on the other hand, presented a load 2.75-fold higher, in average, than that of the dry season. This loading type is highly variable depending on the changes in discharge and is highest during storm events (Song et al., 2017). As observed in Figure 2.4, once the inflow levels started to recover after the intense drought period, higher loads were obtained, with peak values of about 4.33 t $month^{-1}$. Meanwhile, it is known that storm events in the dry period might contribute to over than 80% of the annual external P loading (Carpenter et al., 2015). Furthermore, the higher values of wet period load from 2017 highlight the importance of non-point sources of pollution for the waterbodies in semiarid regions. They are frequently the main external source of nutrients to reservoirs during the rainy season (Medeiros et al., 2015; Cavalcante et al., 2018).

2.3.4 Seasonal and interannual variation in epilimnion total phosphorus and chlorophyll-a concentration

The epilimnion TP concentration and chlorophyll-a concentration measured in the wet and the dry period of each reservoir are presented in Figure 2.5. It is also shown the limiting concentration for Class II according to national standards for lentic waterbodies (Brazil, 2005). The waterbody classification considers to which purpose the water can be used for. Class I indicates the highest water quality level for noble uses and Class III is for consumption after enhanced treatment. All studied reservoirs are classified as Class II with a limiting concentration of 30 μg L^{-1} for TP and Chl-a.

Figure 2.5 - Seasonal and interannual variability in (a) measured epilimnion TP and (b) Chlorophyll-a concentration

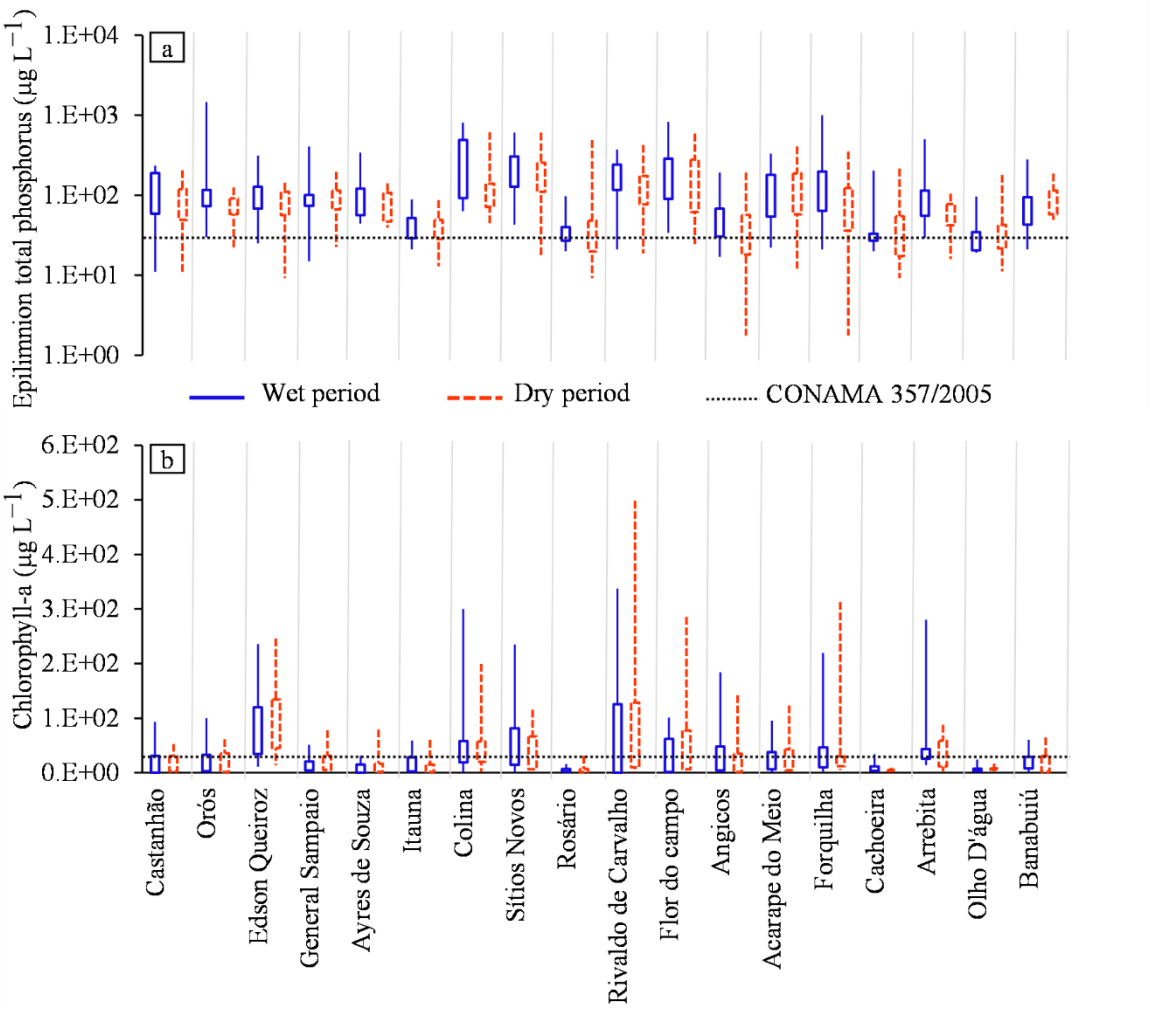

The reservoirs remained eutrophic or hypereutrophic during great majority of the studied period (Ceará, 2021). The epilimnion TP concentrations for the dry period varied from 2 to 194 µg L^{-1} in Angicos. This reservoir showed the highest percentage of good trophy state remaining over than 47.8% under mesotrophic classification. On the other hand, Colina which had the highest concentrations (44 - 599 µg L^{-1}) remained over than 76.9% of the study period in eutrophic or hypereutrophic classification. The high values of concentration also extend to the wet period. In comparison to the limit of 30 µg L^{-1}, there was a common disrespect to reach this standard. As can be observed in Figure 2.5, only 16.7% of the waterbodies have roughly 30% of their dataset under this limiting value.

The Kruskal-Wallis test performed between the concentrations in the wet and dry periods for each reservoir presented significant p-values only for the reservoir Colina (p<0.05) which presented the concentrations in the wet period higher than in the dry one. Colina is the shallower studied reservoir, then it is highly susceptible to drastic water level increase after rainy periods. These events may promote a strong mixing process and increase water column

TP concentration combined with the contribution from the external load that come with the inflow.

It is important to highlight, then, that the general analysis of the grouped dataset of epilimnion concentration in the wet and dry seasons has not presented statistically significant differences for almost all reservoirs. However, the analysis carried out in an annual timestep in each reservoir for paired concentrations comprised in the dry period showed that the great majority of the pairs presented a slightly higher TP concentration at the end of the dry period. This aspect might be a combined result of the volume reduction, which concentrates the nutrients, as well as an evidence of internal load (Nürnberg et al., 2012; Cavalcante et al., 2018).

Regarding the concentration of chlorophyll-a (Chl-a), its seasonal variability kept similarities with the TP concentration in the sense that it was not observed marked differentiation between the periods. The statistical analysis revealed no significant *p*-value between the Chl-a concentration for the two periods for any reservoir. Indeed, the variation in the trophic state of the studied reservoirs was very narrow and they remained eutrophic or hypereutrophic most part of the study period (Ceará, 2021). The median concentrations ranged from 3.56 µg L^{-1} to 80.98 µg L^{-1} for the wet period and from 2.24 µg L^{-1} to 86.18 µg L^{-1} for the dry period. The maximum values for both periods were observed in Rivaldo de Carvalho (337.63 µg L^{-1} in the wet period and 501.85 µg L^{-1} in the dry period). The higher values observed in this reservoir occurred in 2016-2017 when it remained with an average volume of about 1% of its capacity. As for the accordance with the limiting concentration, the Chl-a measurements followed the national regulation more often than what was observed for TP concentration.

The behavior of Chl-a may be better comprehended in light of the behavior of the epilimnion TP concentration, since their strong correlation is widely recognized. Classical studies have observed P (total and organic forms) as a good predictor for Chl-a concentration (Dillon and Rigler, 1974). In Brazilian reservoirs these relationships were also verified (Carneiro et.al, 2014; Rocha et. al, 2019) as well as in other regions world-wide, even by non-linear models (Filstrup et. al, 2014). In opposite with classical reports, recent studies found that P remains as the limiting nutrient to the ecosystem productivity regardless of the nitrogen/phosphorus ratio (Kolzau et. al, 2014). Then, as P concentration remained relatively similar among periods, so did the Chl-a concentration. Furthermore, as further addressed, the variability observed in these water quality surrogates (TP and Chl-a) may be also linked with the TP loading pattern, which meant high variability in TP load but similar production among

periods. In fact, long-term TP loading play and important role on algal biomass (Tang et. al, 2019).

Data uncertainties regarding sample collection and laboratory preservation or analysis may occur and influence the results (Harmel et al., 2006). However, the data accuracy was evaluated by an outlier analysis and by the order of magnitude of the reported TP concentrations in comparison with values reported in the literature. There was only one measurement over 4000 µg L^{-1} which was excluded as a possible sampling error. Peak values (1500 - 4000 µg L^{-1}) represented less than 0.2% of the dataset and occurred mainly in 2016, during the lowest water depth, or in 2009-2010, after the strongest rainy season of the study period. Overall, the measured TP concentrations of the study sites were within reported ranges in the literature for eutrophic ecosystems (10 - 3300 µg L^{-1}) (Rattan et al., 2017; Han et al., 2018; Li et al., 2020). For the Chlorophyll-a data, only four values (0.5% of the dataset) were exceptionally high and then, removed.

2.3.5 Phosphorus load estimates for the wet and dry periods

The modeled TP load for the wet and the dry periods along with the reference TP load value estimated by COGERH are shown in Figure 2.6. The load of reference was used to strengthen the modeled estimations obtained in the present study.

Figure 2.6 - Seasonal and interannual variations in the modeled TP loads for the wet and dry periods

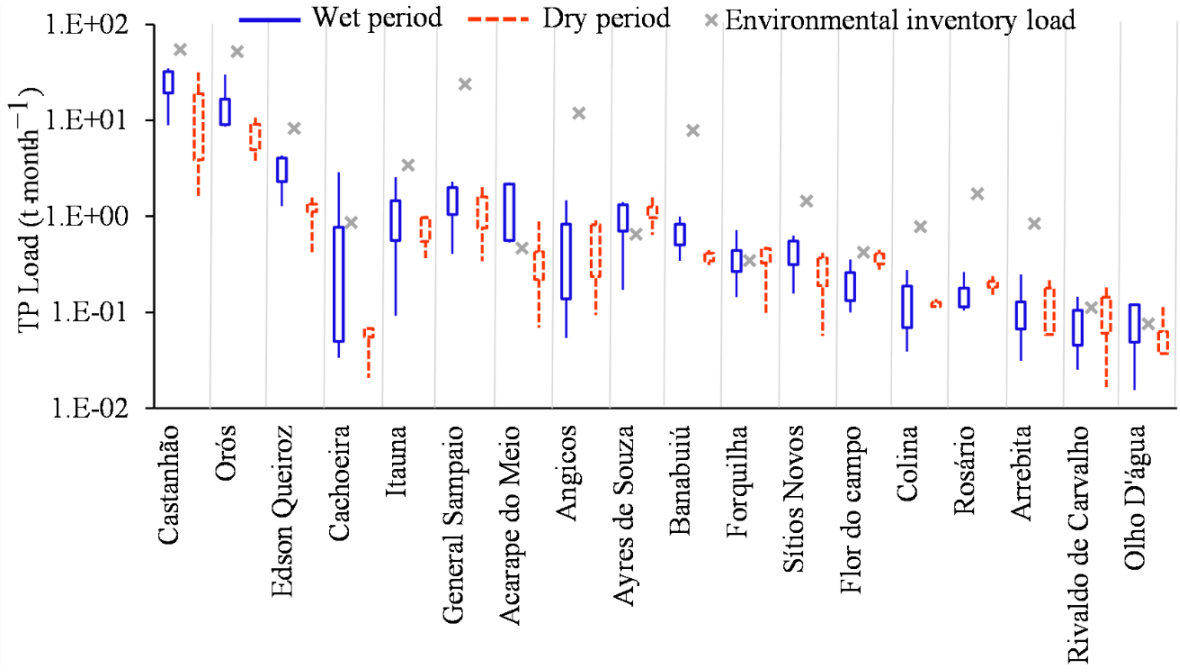

With regards to the loads estimated during the wet season, the values varied from the minimum of 0.015 t $month^{-1}$ in Olho D'água to 34.76 t $month^{-1}$ in Castanhão, with a median value of 2.81 t $month^{-1}$. Some exceptionally high modeled TP load was obtained and their probable causes will be further addressed as the results of a sensitivity analysis of the model. High values were obtained for larger catchments as they have the potential to produce more TP load mostly from nonpoint sources (Marques et al., 2019). Specifically, for the Castanhão catchment, several studies were carried out. The agriculture contribution in this catchment was estimated around 116 t yr^{-1}, in average 9.67 t $month^{-1}$ (Paula Filho et al., 2019). Lacerda et al., (2018) estimated 212 tons as a flux of TP load for the Castanhão reservoir for the six-month of the wet period from measured TP concentration and inflow (about 35.33 t $month^{-1}$), which was very similar to the highest value obtained in this study (34.76 t $month^{-1}$). In some highly eutrophic systems, such as the studied reservoirs, large portion of the load from the wet period possibly settles and becomes recycled within the same year which might impact the internal load estimation by resembling sediment-released P (Nürnberg 2009). Additionally, due to the settling process, only a certain percentage of external load can effectively contribute to lake water TP (Nürnberg et al., 2013).

It can also be seen in Figure 2.6 that the estimated values were slightly under the reference load for the catchments, and more significantly underestimated for 33% of them. For the remaining, the reference value was very close to the value reported by COGERH or in the range of the modeled TP load. The correlation between the mean modeled TP load and the reference load for the reservoirs resulted in a $R^2 = 0.82$ with a bias varying from 2.9% to 96.2% with an average of 65.9%. The underestimation of the TP load in some catchments may be due to the temporally spaced sampling data, only three or four times per year, which tend to underrepresent peak storm or high-flow events. This way, the likely intense phosphorus dynamics in the waterbody that happen at the moment and in a short period after it may not be accounted (Johnes, 2007; Bowes et al., 2009). Moreover, the reference load was estimated in a period with higher inflow levels (from 2008 to 2011 depending on the reservoir) than the average of the studied period, then it has possibly accounted more external load.

Concerning to the load of dry period, the estimates varied from the minimum of 0.016 t $month^{-1}$ in Rivaldo de Carvalho to 31.19 t $month^{-1}$ in Castanhão, with a mean value of 1.09 t $month^{-1}$. The modeling process resulted in 14% of negative estimates in average with a maximum of 48% for the Acarape do Meio reservoir. Positive values indicate that internal P loading occurs in the sediment whereas negative values imply P retention (Song et al., 2017). As can be observed in Figure 2.6, the load estimated during the dry period had similar order as

those of the wet period for the majority of the reservoirs. Lepori and Roberts (2017) suggest that shallow lakes should are more affected by internal loading than deep ones, once deep lakes have a larger volume of water to dilute the P released from the sediments. The studied reservoirs have faced a drastic volume reduction, what may have corroborated to the high values of load produced during the dry season even in once deep reservoirs. Additionally, due to the climatic conditions of the studied area and the complete dryness of the rivers in the dry season, no inflow arrive in this period. Then, significant external inputs of nutrients are not expected (Barbosa et al., 2012). So, internal loading was potentially the main source of P load to the reservoirs during dry periods (Nürnberg, 2009).

Significant differences between the loads produced in the two periods were statistically relevant only for Acarape do Meio and Edson Queiroz reservoirs (p-value < 0.05). They presented wet period loads about 3 and 4-fold higher than the dry period load, respectively. The environmental inventory of these reservoirs reports that the highest annual P input comes from soil and agriculture for Edson Querioz and Acarape do Meio respectively. Additionally, Edson Queiroz has the fourth largest catchment area and the Acarape do Meio has the second highest rainfall index, which enhances external load dominance. For the remaining reservoirs, the statistical test which analyzes the median have not found significant differences, in spite of some reservoirs presenting peak values for the wet period load. The inter seasonal increasing pattern observed in the epilimnion TP concentration in the sampling points corroborates these results. From the beginning to the end of each period the increase in the values may suggest an input of TP load. As observed in Figure 2.5a, the seasonal behavior of epilimnion TP concentrations was similar, such as the one of the loads. Furthermore, beyond the contribution of the volume reduction to increase concentration, as this reduction is less remarkable annually than the long-term interannual volume variation, the occurrence of internal P loading in the dry period is and additional source potentially counterbalancing the external P inputs during the wet period.

The observed among-catchment variation of TP flux for the load of wet period can be largely explained by differentiated net anthropogenic P input as well as seasonal variations of water discharge in the rivers (Han et al., 2018; Hu et al., 2020). For the load of dry period, it may depend on climatic conditions and the level of oxygenation in the water-sediment interface (Cavalcante et al., 2018). Additionally, the existence of aquaculture is another relevant aspect, as it releases nutrients directly to the water column (Santos et al., 2016). This contributes to the water quality deterioration (Oliveira et al., 2015). In the Castanhão reservoir, the aquaculture may contribute to roughly 163 t yr^{-1}, in average 13.58 t $month^{-1}$ (Lacerda et al., 2018). With

regards to the among-season variations, a trade-off between the P mechanisms, notably the physical processes, might contribute to similar estimates. During the wet season, the wind effect is weakened in comparison to the dry season, which might impact wind-induced resuspension. However, the external transport is markedly impactful during the wet period, once there has been no or little outflow/overflow during the dry season. With respect to other mechanisms mainly occurring in the water-sediment interface (such as diffusion, adsorption and desorption), they may be better discussed when gross estimates are obtained, while in this study only net estimates through mass balance were performed.

Following Vollenweider (1968) and Chapra (2008), areal phosphorus loads were obtained, and the rates were expressed in terms of total P. Table 2.2 presents the average values estimated for each reservoir. The areal loads ranged from 0.07 to 1.04 gP m^2 $month^{-1}$ for the wet season and from 0.05 to 0.65 gP m^2 $month^{-1}$ for the dry season. For the dry period, the literature reports rates ranging between 0.11 and 0.30 gP m^2 $month^{-1}$ with higher rates more common in eutrophic water bodies (Nürnberg et al., 2012; Nürnberg et al., 2013; Qin et al., 2016). The annual averages varied from 0.66 to 7.29 gP m^2 yr^{-1}, which is consistent with the ones reported in the literature (0.15 – 7.06 gP m^2 yr^{-1}) (Ahlgren et al., 1988; Nürnberg 1984; Köhler 2005; Nürnberg et al., 2012).

Because of the dense reservoir network of the Brazilian semiarid, the mineral sedimentation (reservoir silting) is only about 20% of the rates observed in other reservoirs globally, as reported by Lima Neto et al., (2011). However, in the reservoirs studied in this work, the net sedimentation rate of total phosphorus ranged from about 60 to 90% of the input load, contrasting with an average of about 40% obtained for temperate lakes and reservoirs (Hejzlar et al., 2006). This higher net sedimentation rate of TP is attributed to the higher water temperature of the Brazilian semiarid reservoirs, which leads to a combined effect of increased P consumption by algae and increased physical sedimentation due to reduced water viscosity, corroborating the results of Toné and Lima Neto (2020). The above results indicate that P retention in the high-density reservoir network is potentially counterbalanced by the higher net sedimentation rates due to higher water temperatures, possibly resulting in similar areal P loads (up to about 7 gP m^2 yr^{-1}), as reported by Ahlgren et al., (1988), Köhler (2005) and Nürnberg et al., (1984, 2012).

Table 2.2 - Mean areal phosphorus load for the wet and dry seasons and total annual load

Reservatório	Areal TP load (gP m² month^{-1})		Areal TP load (gP m² yr^{-1})
	Dry period	Wet period	Annual average
Olho D'água	0.05	0.07	0.66
Rosário	0.05	0.06	0.71
Itauna	0.07	0.08	0.87
Angicos	0.08	0.09	1.01
Arrebita	0.06	0.15	1.28
Cachoeira	0.09	0.22	1.91
Flor do campo	0.26	0.08	2.04
Forquilha	0.15	0.19	2.05
Rivaldo de Carvalho	0.22	0.13	2.16
Colina	0.10	0.30	2.48
Orós	0.13	0.28	2.56
Ayres de Souza	0.16	0.26	2.58
Banabuiú	0.11	0.32	2.86
Edson Queiroz	0.17	0.44	3.54
General Sampaio	0.23	0.49	3.97
Castanhão	0.27	0.54	4.60
Sítios Novos	0.51	0.32	4.98
Acarape do Meio	0.41	0.71	7.29
Statistics			
Minimum	0.05	0.06	0.66
25th	0.08	0.10	1.43
50th	0.14	0.24	2.32
Mean	0.17	0.26	2.63
75th	0.23	0.32	3.37
Maximum	0.51	0.71	7.29

2.3.6 Load of dry season vs. load of wet season over the annual P budget

Figure 2.7 shows the predominance by type of TP load for each reservoir. This estimate represents the average of the estimated values per period in relation to the annual load. The predominance of the dry period load varied from 6.56% in Cachoeira to 62.74% in Flor do Campo. For the reservoir Acarape do Meio, the second with the lowest dominance of dry period load, several studies in its catchment identified the intensity of external input mainly from point sources. Open-air dumps, illegal slaughterhouses and four STW from which three discharge their effluents directly into the main rivers were identified in the catchment of Acarape do Meio (Lima et al., 2016). For the Orós and Castanhão reservoirs, in spite of the intense fish farming practice, they have larger and rural catchments (> 24000 km²) that concentrate the most relevant irrigated croplands of the state. Consequently, there is a high amount of external TP production

from nonpoint sources (Ceará, 2020). Similar analyses were applied for the for the Banabuiú reservoir.

A growing predominance of dry period load is observed in Figure 2.7. From Arrebita reservoir it surpasses 50%. The combination of the volume reduction with a wind-induced complete mixing condition might turn the reservoirs close to shallow polymictic ones and recent literature provides evidence that polymictic lakes are more prone to have high internal P loading rates (North et al., 2015; Orihel et al., 2015; Cavalcante et al., 2018). In the lake nutrient budget, sediment P might have an increasing predominance (Doan et al., 2018). Thus, representing the load produced during the dry season as a percentage of the total annual load is a way to compare it with the load from the wet season and understand its importance (Nürnberg, 2009). Song et al., (2017) highlights that in P enriched agricultural areas internal P loading can be as high as external one. The existence of high internal load production implies that the achievement of a stable mesotrophic condition will not occur until the substantial reduction of these loadings (Lepori and Roberts, 2017). Moreover, it delays the decline of nutrient concentration in the water column as expected once there is a reduction of external load. Meanwhile, it may take a very long time to deplete the internal loading, especially in reservoirs with a long history of pollution (Schindle 2006). It is expected that, in general, changes of the released P depend on the mixing regime of the lake, trophic state and chemistry (Nürnberg, 2009). Additionally, high amount of phytoplankton might be related with the amounts of released P (Kowalczewska-Madura et al., 2019). An assessment of the internal loading percentage over the annual P load budget reported in the literature revealed a range from 2% to 89% (Nürnberg et al., 2012; Nürnberg et al., 2013; Loh et al., 2013; Nikolai and Dzialowski, 2014; Matisoff et al., 2016; Lepori and Roberts 2017; Song et al., 2017; Kowalczewska-Madura et al., 2019), which highlights that the internal TP load can be as high as the external load.

Figure 2.7 - Assessment of the representativeness of the loads produced in the wet and dry seasons in the annual TP load

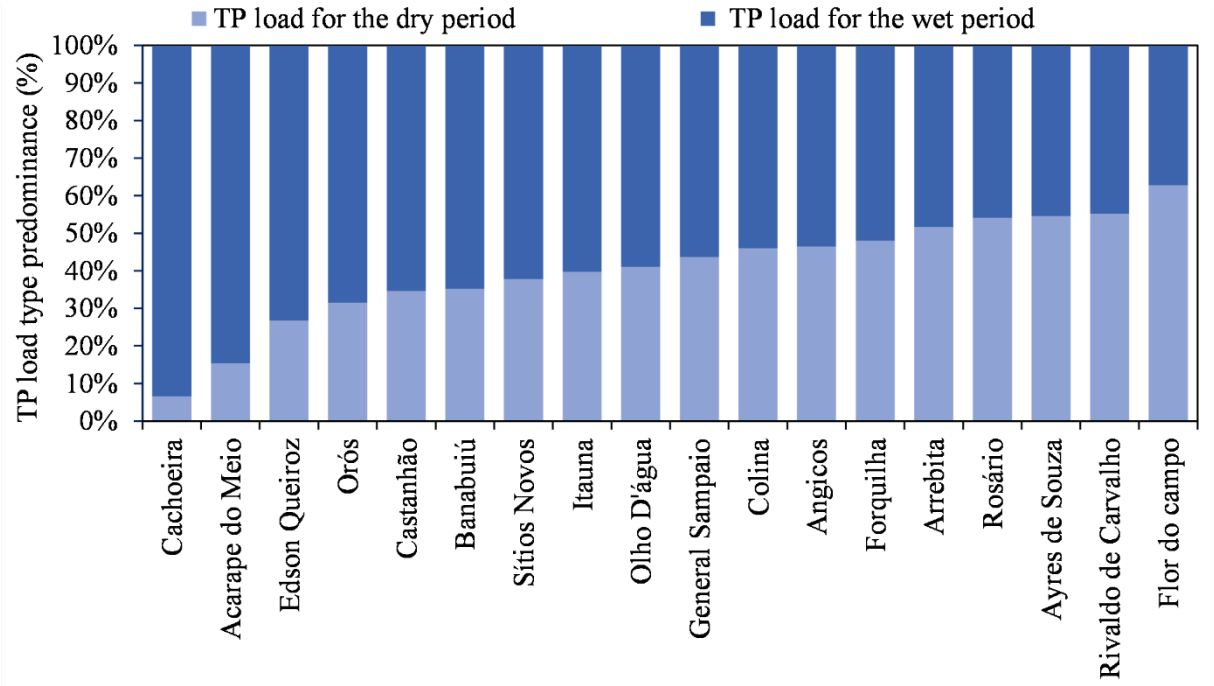

2.3.7 Predictive models for TP load input

Simple predictive models were proposed as an attempt to assess the most correlated characteristics with the TP load. The correlations were developed between the TP load of dry period and volume, TP load of wet period and inflow, TP load of dry period and TP load of wet period, and Total TP load and catchment area. Figure 2.8 presents the models as well as the coefficient of determination for each one. The models were adjusted with mean values to reduce the bias, once the fitting with the entire dataset including the modeled values of all reservoirs presented a large variability. The mean load was calculated as an arithmetic average over the period with data. A satisfactory R^2 was obtained through a power-low curve adjustment. The residual analysis, in order to reinforce the quality of the models, was performed graphically.

Figure 2.8a presents a positive correlation between the TP load of dry period and the reservoir volume ($R^2 = 0.84$). A possible explanation relies on the relation between the reservoir volume and the water-sediment interfacial area. A larger volume enlarges this interface and P production by release under appropriate conditions. Moreover, several aspects may be linked to this result. Larger reservoirs also have larger catchments in the study area. The reservoirs with this characteristic receive significant contributions of external load, and it can be seen in Figure 2.8c that greater load in the wet period implies greater load in the dry period, possibly as a result of a long-term accumulation process.

The positive correlation between the TP load of wet period and the inflow ($R^2 = 0.94$) is largely known (Figure 2.8b). This type of load is adequately explained by seasonal variations of water discharge in the rivers (Han et al., 2018), as stream discharge is a fundamental explanatory variable with a positive influence on external TP load (Rattan et al., 2017). Hydrologic events, such as peak storms, mainly in watersheds dominated by non-point sources, significantly contribute to external TP load (Jeznach et al., 2017). Its rates during peak flow events can be approximately five times higher than under normal conditions (North et al., 2015).

As shown in Figure 2.8c, the dry and wet period loads were directly correlated ($R^2 = 0.98$). The higher the TP inputs during the wet period, the higher those in the dry one. This positive correlation indicates that an abatement of external P sources implies a decrease in the internal load. This also highlights the strong influence of the load produced during the wet period with that produced during the dry period. According to Nürnberg (2009), the wet period load is more susceptible to settle and be recycled within the same year in highly eutrophic systems. As the studied reservoirs remained highly eutrophic during the studied period, this aspect strengthens the obtained correlation. In contrast, an inverse correlation between these variables was already found (Nürnberg et al., 2012).

Finally, the catchment area was shown as an important predictor of the total TP load entering a waterbody ($R^2 = 0.86$), as depicted in Figure 2.8d. It is commonly expected and observed that larger catchments might produce more TP load, especially if there is an intensive agriculture exploitation on the lands (Marques et al., 2019). Additionally to agriculture, soil erodibility also plays an important role in the mobilization of pollutants (Li et al., 2020). Poorly drained soils can transfer the most diffuse P load (Greene et al., 2011), particularly in semiarid watersheds (Paula Filho et al., 2019).

Figure 2.8 - Proposed models for the (a) TP load of dry period as function of the volume, (b) TP load of wet period as function of the inflow, (c) TP load of dry period as function of the TP load of wet period and (d) Total TP load as function of the catchment area

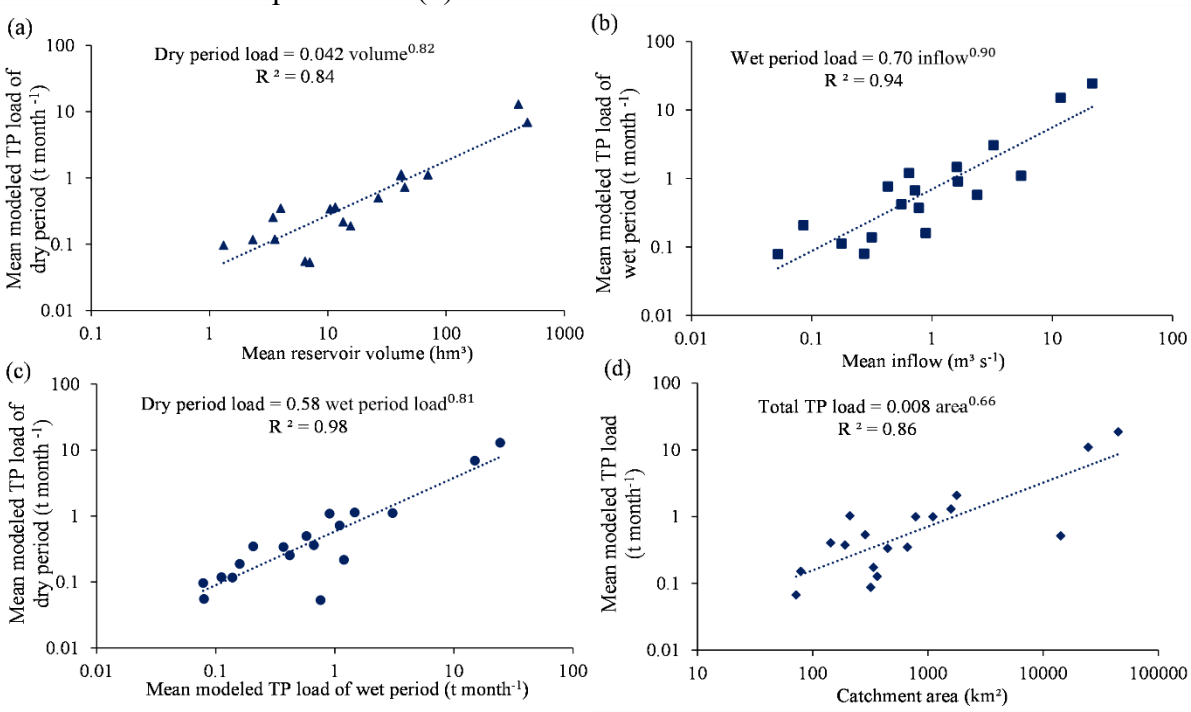

The ultimate analysis performed was the estimation of the TP load through a concentration - flow relationship particularly for the Castanhão reservoir. Thus, a comparison between the load obtained through calibration of the Equation (2.1) with the one obtained through the concentration - flow relationship was performed. Figure 2.9 presents the comparison of the modeled loads encompassing the period from 2013 to 2019. The estimated loads varied from 0.002 to 51.03 t month^{-1} for the concentration - flow relationship modeling approach and from 0.24 to 34.99 t month^{-1} for the mass balance approach. The NSE between the models was 0.67, which turned the quality of the adjustment satisfactory (Moriasi et al., 2007).

The most distant result between the models was obtained for the estimation in 2015. In the dry period of this year, the reservoir presented a very low volume and high measured epilimnion TP concentrations. This implied a higher load estimate by the model of Vollenweider. On the other hand, the low flow rates measured in the river resulted in lower load estimates by the flow-concentration model. Combined, these factors enlarged the difference between the models. However, considering the overall comparison of the results, the classic predictive model of Vollenweider is properly capable to perform a good estimation for the load of the wet period, once this load type has formed the basis of development for this model (Schauser and Chorus 2009).

Figure 2.9 - Comparison of the total TP load input to the Castanhão reservoir by using two different approaches

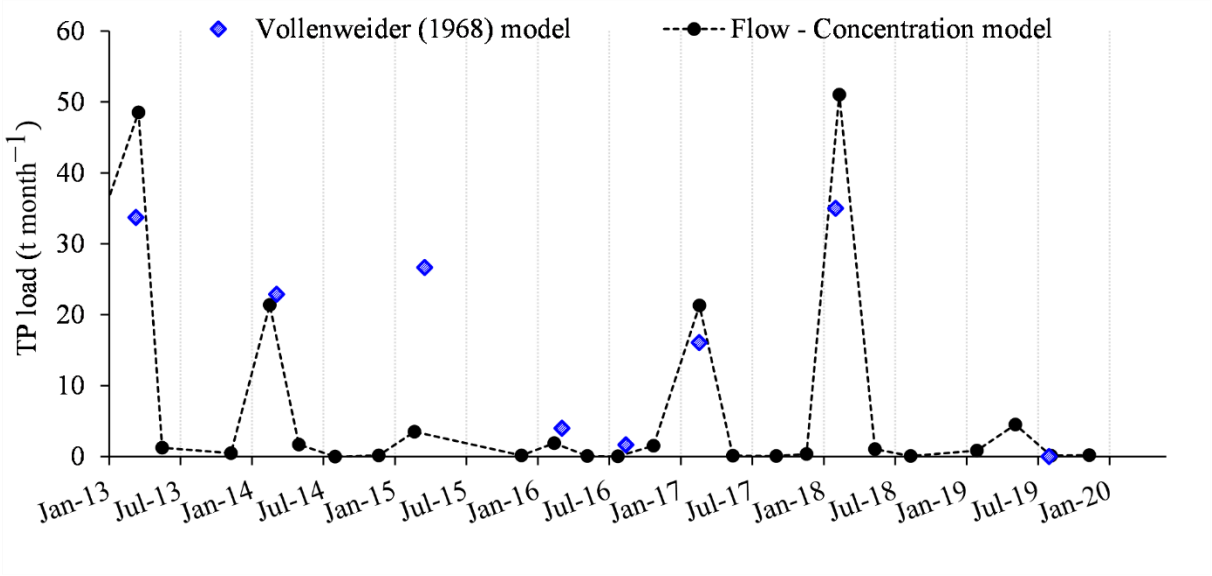

2.3.8 Model implications, uncertainty and sensitivity analysis

The results of the sensitivity analysis showed that the elapsed time (t) and the ratio TP(t)/TP0 had an important influence regardless of the loading type. Short t between measurements resulted in higher estimated loads. However, the impact of t was more pronounced combined with the ratio TP(t)/TP0. As expected, if considerable average TP increase is observed, especially if it occurs in a short interval, peak load events might have induced this increase. Dropping t by half resulted in a mean deviation from the original estimate of 20% when TP(t)/TP0 < 2 and 50% when TP(t)/TP0 > 4. Then, paired concentrations with elapsed time less than one month were not considered, although this situation was rarely observed in the dataset. Considering only the effect of the ratio, for TP(t)/TP0 = 1.5 the mean deviation accounting all estimated loads reached about 40%. As for the impact of the inflow, the tested range of variation (30%) resulted in an average deviation of the wet period load of about 10%, considering all reservoirs' estimates together. However, as it was observed and as further detailed, for some reservoirs marked interannual differences in the inflow, that far surpassed this percentual, caused large differences in the estimates between years. For the volume influence, a deviation of ±30% resulted in a mean deviation of the same magnitude for the dry period load. For the wet period load the volume variation influence was smaller (about 20% in average).

Knowing the sensitive parameters of the modeling and their impact on the estimates turns possible to evaluate the variability of the modeled loads. The coefficient of variation (CV) ranged from 0.40 to 2.08 with mean of 0.99 for the load of wet period and from 0.09 to 2.03

with mean of 0.70 for the load of dry period. Although these values appear to be high, they were only a few estimates influenced by uncommon conditions which elevated the median values. For the wet period load, the CV of 2.08 was obtained for the reservoir Sitios Novos accounting the load estimated for 2011, the highest inflow among the years, whose measurements presented a TP(t)/TP0 ratio of 1.9. The reservoir Cachoeira presented the second highest CV of 2.07. Similarly, it was obtained for the estimate of 2014, which had the highest inflow of all years and TP(t)/TP0 ratio of 4. Disregarding these peak values would drop the average CV to 0.77 and the maximum to 1.0. For external loads, the literature reported CV ranges of 0.05-0.71 (Kulasova et al., 2012; Chapra and Dolan, 2012). Then, the average CV of this study is very close to these reports. The high interannual climatic variability typical of semiarid conditions may be largely responsible for this slightly elevated average. The ratio between the inflow of the rainiest year with the driest one for the studied period resulted in a median value of 6.2. In fact, due to the drought period, the inflow during the period 2008-2011 was markedly superior than during 2013-2016.

For the estimated load of the dry period, the maximum CV of 2.03 was obtained for the reservoir Acapare do Meio as a result of a peak estimate in 2009. In this year, the TP(t)/TP0 was 6.4 (from 62 μg L^{-1} to 399 μg L^{-1}). The reservoirs Sítios Novos and Castanhão also presented peak estimates for the years 2008 and 2010, respectively. The first one was mainly influenced by the high TP(t)/TP0 ratio of 7.2. The second was majorly due to the short elapsed time between the TP measurements. By disregarding these peak estimates the CV range would change from 0.09 to 1.24, with average of 0.58. For internal load, reported CV ranged from 0.33 to 0.83 (Spears, 2012; Nürnberg, 2009, 2012, 2019; Horpilla, 2017). Thus, the values obtained here are in accordance with the literature. Moreover, for some higher variation still remaining, the interannual variation in the volume reduction and the rapid deterioration under drought conditions strongly influence the estimates of the dry season. Furthermore, for the years with strong rainy seasons, the possible water mixing during elevated inflow events and rapidly volume increase during the wet season resulted in following dry periods with higher water column TP concentration. The water level variation and inflow turn the internal TP load estimation particularly challenging in complex managed reservoirs (North et al., 2015), especially in the study sites under a tropical semiarid climate.

Regarding to the reference TP load, previous studies that have already applied the ECM reported a maximum mean error of 31%, as already mentioned. Then, for the catchments whose reference load was underestimated this range of mean error in computing the reference TP load might be taken into consideration. Besides, for the most distant results, variations in the input

data to the modeled load may have had greater influence on this difference. For seasonal and spatial data, the monitoring frequency, quality and quantity significantly contribute to the accuracy of the load assessment (Nürnberg, 2009). Error exclusively due to variability of P concentrations is at least 20% on average for lake samples (Nürnberg et al., 2012).

Existing limitations are mainly related with TP load estimation, since the developed models rely on the accuracy of the extensive field study carried out by COGERH. It has to be highlighted, though, that the data limitation on the studied area largely reduce the range of possible useful alternatives to perform a data comparison and validation. Additionally, sampling interval, analysis and data quality manipulation inaccuracies in reservoirs' data can have an impact in the load estimation process and in the modeled outputs. Moreover, in the data frequency of roughly twelve years of sampling in reservoirs, high flow events remained under-represented. Only five years in the studied period presented precipitation indexes roughly above the average in all catchments. Thus, low to medium flow were more frequent in the study dataset which may have reduced the possible amount of TP load produced in the wet season.

Finally, addressing the main implications of the method developed in this research, mainly regarding the issue of controlling phosphorus production, the contributions can be evaluated at the individual level per reservoir or encompassing the integrated network of reservoirs. The modeling of scenarios to assess the impact of mitigation measures regarding external inputs, such as the expansion of sanitation coverage on the catchment or the regulation and inspection on the application of phosphorus-enriched fertilizers in agriculture, may be a tool to assist reservoir management. Additionally, regardless of the loading type, the required load reduction may be evaluated so that the TP concentration of upper layers reach the limits established by national water quality standards. Lastly, a target phosphorus concentration may be defined during the occurrence of extreme hydrological scenarios, such as drastic reduction in volume and inflow, to determine the associated maximum phosphorus load. This assessment would assist an efficient integrated management of the reservoirs and their prioritization by type of water uses.

2.4. Conclusions

The analysis of seasonal epilimnion TP concentrations between the wet and dry periods resulted in insignificant differences (p>0.05) for more than 90% of the reservoirs, which was attributed to a trade-off between the hydrological/limnological processes occurring in the two seasons. However, a slightly higher overlying concentration at the end of the dry period was observed. The statistical tests performed between the concentrations in the upper surface (0.3 m depth) and in the other depths also revealed no significant p-values for 50% of the reservoirs (p>0.05). This suggests that many reservoirs tended to present a well-mixed behavior. Then, a complete-mix mass balance model was applied. For the dry period, the modeling process resulted in only 14% of negative TP load estimates on average. While negative values imply P retention, positive ones indicate that internal P loading occurred. The results also indicated that a high amount of load from the dry period contributed to the annual budget, with estimates varying from 0.016 to 31.19 t month^{-1}. The predominance of the dry period load over the annual TP input varied from 6.56 to 62.74%. This suggests that the eutrophic state and shallow water condition of the studied reservoirs have possibly contributed to the settling and recycling of the external load within the same year. The areal TP load estimates ranged from 0.66 to 7.29 gP m^2 yr^{-1}, consistently with the literature (0.146 - 7.06 gP m^2 yr^{-1}). This implies that TP retention in the dense reservoir network is potentially counterbalanced by the higher net sedimentation rates due to higher water temperatures.

Power-law curves were adjusted between internal TP load and volume, internal and external TP loads, external load and inflow, and total TP load and catchment area, resulting in satisfactory R^2 of 0.84, 0.98, 0.94 and 0.86, respectively. Despite the uncertainties involved in the estimations, the findings from this work are novel as the quantification of external and internal P loads was approximated by the estimation of the loads produced during the wet and dry periods, respectively. Additionally, their relative importance to the annual input load was evaluated and predictive correlations were proposed. This study not only advanced the knowledge of P dynamics in tropical semiarid reservoirs, but also provided evidences of important internal loadings to these systems. Furthermore, the methodology applied in the study might be directly applicable to water bodies with similar characteristics in other dryland regions.

CHAPTER 3

Modeling flow-related phosphorus inputs to tropical semiarid reservoirs[2]

3.1. Introduction

Phosphorus is a critical nutrient with regards to primary productivity in water bodies (Ansari and Gill, 2014; Le Moal et al., 2019). Identifying the main contribution sources of total phosphorus (TP) load is a first step to understand relevant P inputs to rivers and reservoirs, and guides water quality management strategies (Sharpley, 2016; Lun et al., 2018). However, the relation between catchment characteristics and TP concentration remains poorly understood in regions such as the Brazilian semiarid, where many reservoirs are failing to meet national water quality standards (Pacheco and Lima Neto, 2017; Lima et al., 2018; Mesquita et al., 2020; Lira et al., 2020; Wiegand et al., 2021). An additional challenge comes from the high-density reservoir network (one per about 5 km²) and mostly intermittent rivers (Lima Neto et al., 2011; Campos et al., 2016; Mamede et al., 2012, 2018).

A catchment-based approach is required to understand the delivery pathways of TP sources entering rivers, lakes and reservoirs and to further address P-related water quality problems (Chen et al., 2015b; Krasa et al., 2019). Natural and anthropogenic TP point sources (PS) and non-point sources (NPS) have fundamental differences, distinct transfer pathways and contrasting relationships with flow rates (Bowes et al., 2008). Nutrient wash-off in runoff, erosion processes and river bed remobilization can increase TP concentration in water bodies located in NPS dominated catchments (Jarvie et al., 2010; Moura et al., 2020). Otherwise, high TP concentrations during low flow rate indicate PS dominated catchments (Jarvie et al., 2013; Sharpley et al., 2013). There are also more complicated catchments that contribute significantly with the two types of sources (Greene et al., 2011).

The absence or scarcity of water quality data, however, imposes serious difficulties for TP load estimation (Johnes, 2007; Chen et al., 2015). Hence, nutrient balance in a catchment becomes an available option (Han et al., 2018). Physical-based and empirical models are widely applied for TP load estimation and simulation with good accuracy (Mockler et al., 2017). However, physical-based approaches are of difficult implementation in data-scarce regions (Bowes et al., 2009), and then empirical models may be an alternative with acceptable precision (Rattan et al., 2017). The Export Coefficient Modeling (ECM) approach is an empirical model

---

[2] The content of this chapter has been published in Journal of Environmental Management (https://doi.org/10.1016/j.jenvman.2021.113123)

widely applied for P load estimation in the State of Ceará, Brazil (Ceará, 2020) and other regions world-wide (Johnes, 1996; Ding et al., 2010; Matias and Johnes, 2012; Delkash and Al-faraj, 2014; Greene et al., 2015; Tsakiris and Alexakis, 2015). The combination of the Loss Coefficient Method (LCM) with the Nutrient Losses Empirical Model (NLEM) is another approach based on export coefficients to estimate TP load (Zhang et al., 2020). Meantime, it should be noted that indirect methodologies such as calibration processes in a coupled reservoir-catchment approach remain little explored as a viable alternative.

Vollenweider (1968) started pioneer studies on TP modeling in lakes by proposing a mass-balance model applied to well-mixed lakes, allowing transient analysis when multi-year TP concentration and flow data are available. The model's predictive ability was tested over the past decades and additional improvements were performed in recent studies (Chapra and Dolan, 2012; Shimoda and Arhonditsis, 2015; Chapra et al., 2016; Katsev, 2017; Araújo et al., 2019; Lira et al., 2020). Additionally, for the Brazilian semiarid, the occurrence of a diurnal mixing cycle with weak stratification patterns turns plausible a complete-mix hypothesis (Lima Neto, 2019). Also, for data-scarce regions, this parsimonious model stands out as a feasible solution.

Estimating the catchment production of P load in regions such as the Brazilian semiarid can contribute to understand the patterns of P input to water supply reservoirs (Chaves et al., 2013; Wu et al., 2016; Paula Filho et al., 2019). Subsequently, to the development of concentration-flow relationships. This approach is of particular interest in regions with intermittent rivers (von Schiller et al., 2017; Chaves et al., 2019), where reservoir related issues are of great concern for water quality management (Lopes et al., 2014; Lacerda et al., 2018; Wiegand et al., 2021).

The nutrient-flow relationship is described by a power-law function that can be applied to a dataset comprised of paired TP concentration and inflow measurements (Bowes et al., 2008, 2009). This methodology has been successfully applied to perennials rivers throughout the globe (Bowes et al., 2009b, 2010, 2014; Bieroza and Heathwaite, 2015). The coefficients of the flow-nutrient model contribute to the understanding of dominant P inputs (Bowes et al., 2008; Chen et al., 2015a), as the model stands on fundamental hydrological differences between PS and NPS dominated catchments. The application of this model covering paired mean TP concentration and discharge at reservoir inlet is still a new approach to be verified for semiarid environments.

Thus, the objective of this study was to evaluate and discuss the main external TP input sources to reservoirs from Brazilian semiarid catchments and develop concentration-flow relationships for their intermittent rivers. The specific goals are: (i) to provide a methodology

to estimate and evaluate average TP load and concentration at reservoirs' inlet through a mass-balance approach, (ii) to extend the application of TP-discharge relations to regions of intermittent rivers, (iii) to improve the understanding of flow conditions on TP concentration at reservoirs' inlet, and (iv) to provide a tool to address the TP issue in water bodies in data scarce regions.

3.2. Material and methods

3.2.1. Study area

As depicted in Figure 3.1, the study includes twenty reservoirs located in the State of Ceará, Brazilian semiarid, monitored by the Water Resources Management Company of the State of Ceará (COGERH). Their capacities range from 0.3 to 6,700 hm^3 and their catchments present different TP sources. The smallest reservoir, called Santo Anastácio, is located in the capital of the State, closer to the coastal zone. The main water uses of these reservoirs are human supply, aquaculture and irrigation. According to COGERH, fish farming is practiced in 40% of these reservoirs (Ceará, 2020). Regarding the ecological protection of these ecosystems, specifically fauna and flora, the adverse climatic conditions imposed upon them, the priority use given to human supply and the incipient regulatory measures in this field, make them self-managed. In extreme drought periods, many reach their lowest volume or a complete dryness, destroying almost all life in the ecosystem. When they are very polluted, eutrophication triggers an intense proliferation of aquatic macrophytes. The reservoirs with a relevant practice of aquaculture are those that receive more attention in mitigating the potential impacts of volume and water quality changes, mostly due to economic losses. Thus, these management issues regarding life in the ecosystems still need thorough attention.

Table 3.1 summarizes important data of the catchments and reservoirs. The total catchment area of these reservoirs reaches 89,296 km^2, which represents about 60% of the state's area. These catchments are characterized by mild slopes varying normally from 0 to 15°. Only the catchments of the reservoirs Arrebita e Angicos present steeper slopes of 30 and 75º, respectively. The soils are not deep as they are located in the crystalline geological formation and the most representative soil types are the red-yellow argisol, litolic neosol and chromic luvisol (Jacomine et al., 1973; Araújo and Medeiros, 2013). These conditions favor the inexistence of perennial rivers and practically no base flow. The precipitation indexes vary from about 600 $mm.yr^{-1}$, in the Flor do Campo reservoir catchment, to about 1,400 $mm.yr^{-1}$, in the Santo Anastácio reservoir catchment. Details of the rainfall patterns are available in the

appendix, Figure A1. As typical of semiarid regions, there are two marked periods: the rainy season and the dry season. The rivers are intermittent with flows primarily occurring during the rainy season. In a special situation, the Santo Anastácio reservoir receives an almost constant flow of untreated sewage through an urban drainage channel, even during the dry season (Fraga et al., 2020). More details of the physical characteristics of the catchments and their land uses can be found in Ceará (2020).

Figure 3.1 - Study sites location in the State of Ceará – Brazil highlighting the different TP sources of pollution of the catchments. Catchment and reservoir details presented in Table 3.1

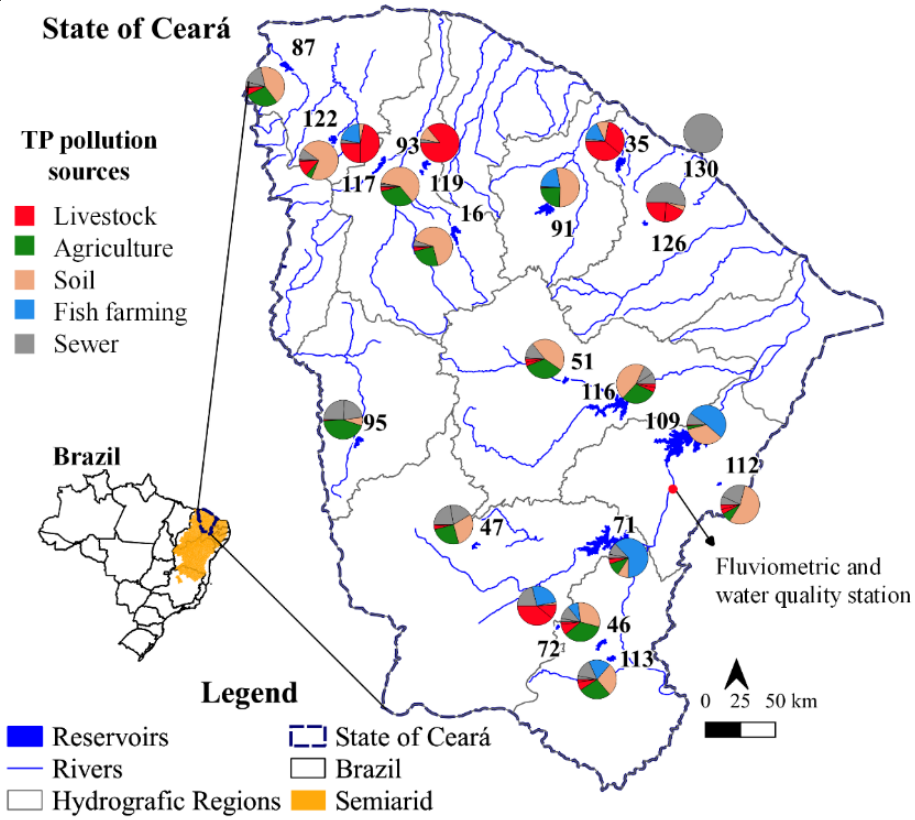

High-quality agricultural land use with irrigated crop production can be found in the Jaguaribe river basin, which covers about 40% of the catchments of the studied reservoirs. However, subsistence agriculture and animal husbandry, such as cattle, pig and poultry farming, is extensively practiced by the dispersed rural population. In spite of being essentially rural, there are some cities in the catchments with population densities ranging from 1.8 to 7,204 inhab.km^{-2}, as shown in Table 3.1. Note that the highest population density refers to a neighborhood of the city of Fortaleza, where the Santo Anastácio reservoir is located, the only with an urban catchment.

Table 3.1 - Physical characteristics of the reservoirs, catchments and the period of available water quality data.

ID	Reservoir	Catchment area (km^2)[a]	(Inhab km^{-2})[b]	Reservoir capacitiy (hm^3)	Average depth (m)	Catchment average precipitation (mm yr^{-1})	Data period	Environmental inventory date [b]
16	Edson Queiroz	1778	24.1	254	15.5	687	2008-2020	2011
35	Sítios Novos	446	854	126	11.1	899	2008-2020	2008
46	Rosário	337	171	47.2	15.3	1036	2010-2020	2011
47	Rivaldo de Carvalho	318	220	20.1	9.0	657	2008-2020	2011
51	Quixeramobim	7005	10.3	7.9	10.6	705	2009-2020	2011
71	Orós	24538	5.4	1940	26.3	728	2008-2020	2011
72	Olho D'água	72.0	485	19	13.0	948	2008-2020	2008
87	Itaúna	781	67.4	72.6	8.2	1176	2011-2020	2011
91	General Sampaio	1582	3.9	322	18.0	729	2008-2020	2011
93	Forquilha	191	91.9	50.1	9.1	726	2008-2020	2008
95	Flor do campo	663	71.4	105	5.4	615	2010-2020	2011
109	Castanhão	44800	1.8	6700	38.2	836	2008-2020	2011
112	Canafístula	329	62.5	13.1	6.5	830	2008-2020	2011
113	Cachoeira	143	356	34.3	14.7	983	2008-2020	2011
116	Banabuiú	14200	6.3	1601	20.5	671	2010-2020	2011
117	Ayres de Sousa	1102	209	96.8	19.1	1125	2010-2020	2009
119	Arrebita	79.0	255	18.5	9.0	801	2008-2020	2011
122	Angicos	286	122	56.1	12.2	1119	2008-2020	2011
126	Acarape do Meio	210	524	29.6	19.7	1292	2008-2020	2008
130	ASA	4.0	7204	0.3	5.0	1042	2013-2019	-

[a] Ceará (2021)
[b] Ceará (2020)
[c] Araújo et al., (2019); Mesquita et al., (2020)

3.2.2. Reservoir Modeling

3.2.2.1. Total phosphorus input load modeling

Equation (3.1) presents the transient complete-mix model proposed by Vollenweider (1968) (Chapra, 2008). The model requires parameters related with water balance, morphometry and TP dynamics. Due to the elevated interannual and seasonal variations in the morphometric parameters of semiarid reservoirs, this model is particularly suitable. The required data to perform the modeling was provided by COGERH (Ceará, 2021). For Santo Anastácio reservoir, the data was obtained from Araújo et al., (2019) and Mesquita et al., (2020).

$$TP_r(t) = TP_{r,o} e^{-\left(\frac{Q_s}{V}+k\right)t} + \frac{W}{Q_s + kV}\left[1 - e^{-\left(\frac{Q_s}{V}+k\right)t}\right] \quad (3.1)$$

in which $TP_r(t)$: TP concentration at reservoir outlet in a given time (kg m^{-3}); $TP_{r,o}$: Initial TP concentration (kg m^{-3}); t: Elapsed time (yr); V: Average reservoir volume for a specified period (m^3); W: TP load (kg yr^{-1}); Q_s: Released water (m^3 yr^{-1}); k: TP decay coefficient (yr^{-1}).

The application of Equation 3.1 consisted of taking paired TP measurements made by COGERH during the rainy period. These measurements are generally collected four times a year, two of them during the rainy period and analyzed according to APHA (2005). They are usually measured in January or February and, then in May or June, encompassing the beginning and the end of the wet period. These measurements were classified according to date as $TP_{r,o}$ and TP_r (t) and the elapsed time was calculated. The volume (V), released flow (Q_s) and decay coefficient (k) are the required additional parameters to estimate the TP load. It is expected that, once the elapsed time between the measurements encompasses almost the entire rainy season, the estimations significantly account the load entering the water body through inflow. Ultimately, particularly for the Santo Anastácio reservoir, once there are available TP concentration and inflow data measured directly at the reservoir's inlet, the TP load was estimated from the product of these two variables.

3.2.2.2. Retention time (RT) and phosphorus decay coefficient (k)

In line with the assumed complete-mix hydraulic behavior, the real residence time was replaced by the theoretical hydraulic residence time (V/Q). V is volume and Q the inflow, both averages of the measurement elapsed time (Salas and Martino, 1991; Castellano et al., 2010). This assumption is considered consistent once Brazilian semiarid reservoirs present a very weak thermal stratification which breaks-up on a daily cycle (Lima Neto, 2019). Furthermore, for relatively well-mixed lakes, simpler approaches to obtain this parameter have demonstrated good accuracy (Pilotti et al., 2014).

The phosphorus decay coefficient (k) was calculated by applying Equation (3.2), as function of the RT. This empirical correlation was adjusted and validated by Toné and Lima Neto (2020) for several Brazilian semiarid reservoirs and also validated by Lima (2016) and Araújo et al., (2019) for the Acarape do Meio and Santo Anastácio reservoirs, respectively. It is noteworthy that similar empirical relations were developed for temperate and tropical lakes by Vollenweider (1976) and Salas and Martino (1991), respectively. However, this particular correlation (Equation 3) intended to account the effect of higher water temperatures of the Brazilian water bodies (~30ºC) in comparison with temperate (~10ºC) and tropical lakes

(~20ºC). This increased water temperature results in increased consumption rate by algae and decreased water viscosity, which favors faster TP sedimentation rates, as proposed by Castagnino (1982) and Toné and Lima Neto (2020).

$$k = \frac{4}{RT^{1/2}} \quad (3.2)$$

3.2.2.3. Total phosphorus measurements and water balance data

The reservoirs were selected according to the availability of TP concentration and TP load information. Excepting for the Santo Anastácio reservoir, which measurements of TP_r and W were taken from Araújo et al., (2019) and Mesquita et al., (2020), the remaining 19 reservoirs integrate a continuous monitoring program by COGERH. Their catchments have an environmental inventory also prepared by COGERH with TP load data estimated by the ECM methodology (Ceará, 2020). It accounts for the main TP source contributions in an annual timestep. The details regarding TP load calculation methods are available in Ceará (2020).

The last required parameters were: reservoir's volume (V), reservoir inflow (Q), evaporation (E), and released flow (Q_s). The volume V was obtained through daily water level measurements and level-volume curves provided by Ceará (2021). The values of Q and Q_s were obtained from COGERH on a monthly basis and then converted to a daily average. Finally, the evaporated volume E was calculated from the product of the average surface area of the reservoir by the evaporated height, available from the climatological station of each reservoir (Brazil, 2021). The reservoir surface area was also obtained from level-area curves provided by Ceará (2021).

3.2.2.4. National standards of water-column TP concentration for water quality protection

The issues related with water quality, limiting nutrient concentration and classification of water bodies are regulated by the Brazilian National Environment Council (Brazil, 2005). The level of water quality in order to ensure the appropriate water uses is deliberated through the classification of the water bodies. A reservoir may be classified as Special Class and Classes I, II and III. The Special Class defines water bodies with a high water quality level destined for the preservation of aquatic environments and the natural balance of aquatic communities. Class I ensures safety for human primary contact, human consumption after conventional treatment and irrigation. Lastly, Classes II and III describe less noble usage and the human supply is

allowed after advanced treatment. Each class poses limiting TP concentration. For lentic environments, the limits for classes I, II and III are 20, 30 and 50 μg L^{-1}, respectively. For lotic environments, the limits are 100 μg L^{-1} for classes I and II, and 150 μg L^{-1} for class III. The studied reservoirs and their tributaries are framed as Class II. Then, the measured and modeled TP concentrations were evaluated in accordance with these standards.

3.2.3. Riverine TP concentration

The TP concentration at the reservoirs' inlet (TP_{in}) was calculated through the ratio between the modeled loads (W) and the inflows (Q) for each period. Then, a dataset of paired TP_{in} and Q was constructed for each reservoir. Whenever available, measured riverine TP concentrations were also considered. It is noteworthy that the methodology applied in this work intends primarily to estimate the flow-related TP load during the rainy season (i.e., external load), not accounting for the internal TP contributions in the overall TP balance. Note that the high inflow rates of the wet period favor the assumed well-mixed behavior in the reservoirs and weaken the already subtle stratification patterns, potentially reducing the risk of internal load (Lima Neto, 2019; Rocha et al., 2020). The literature reports that the external load is more significant during the rainy season, especially in semiarid regions (Song et al., 2017; Cavalcante et al., 2018; Barbosa et al., 2019), while internal loading is more impactful in the dry period (Coppens et al., 2016). Moreover, since the studied catchments are mostly rural with high NPS dominance, one expects significant nutrient wash-off from external sources (Jiang et al., 2019). In addition, during the wet period, the water level is higher and wind velocity smaller (Jalil et al., 2019), reducing the effect of wind shear in deeper water layers and minimizing P resuspension from bottom sediments (Bai et al., 2020).

3.2.3.1 Flow-concentration model development

The flow-concentration approach is mainly useful in data-scarce regions for integration of water resources management and/or further calibration of more complex models. Once the relationship is satisfactorily calibrated, the empirically-fitted model is a feasible tool to analyze the catchment land use contribution to the water quality and predict TP concentration (Chen et al., 2015). The TP_{in} concentration can be expressed as presented in Equation (3.3), accounting for the contribution of PS pollution (first term) and NPS pollution (second term), as proposed by Bowes et al., (2008).

$$TP_{in} = A.Q^{B-1} + C.Q^{D-1} \quad (3.3)$$

The four fitting parameters A, B, C and D in Equation (3.3) were calibrated using the non-linear least squares regression procedure PROC NLIN of the SAS statistical analysis package (SAS, 2018). The A and C coefficients have unit of load while B and D are dimensionless. Two constraints were applied to provide reliable solutions. First, it was assumed $0 \leq B \leq 1$, which implies that the TP concentration from PS-derived TP load will decrease with increasing river discharge (Q). Second, $D > 1$, as NPS-derived TP load and concentration will both increase with increasing Q (Bowes et al., 2008). Furthermore, parameters A and B were both constrained as greater than zero. Particular constraints such as a total PS dominance (C=D=0) or NPS dominance (A=B=0) were not considered as the studied catchments present significant proportions of the two main sources (Ceará, 2020). The Nash–Sutcliffe Efficiency (NSE) was calculated to each fitted model as a performance indicator (Moriasi et al., 2007).

In order to analyze TP patterns depending on the inflow and catchment influence, the data was not grouped by seasonal periods. The intermittent regime of the semiarid rivers was another relevant aspect to avoid this grouped analysis. Furthermore, the discharge at which the estimated PS and NPS TP inputs are equal ($Q = Q_e$) was calculated using the coupled A, B, C, and D parameters according to Equation (3.4). When $Q < Q_e$, PS inputs dominate the TP load as compared to NPS. Conversely, NPS inputs dominate the TP load when $Q > Q_e$.

$$Q_e = \left(\frac{A}{C}\right)^{\frac{1}{(D-B)}} \quad (3.4)$$

3.2.4. Application and validation of the flow-concentration model for the Castanhão reservoir

The Castanhão reservoir, the largest in the State of Ceará, has fluviometric and water quality stations managed by COGERH located near its main entrance (see Figure 3.1). Thus, particularly for this reservoir, a comparison between the daily inflow from the water balance and the fluviometric station was possible, for which the indicators NSE and R^2 were calculated. Furthermore, the flow-concentration model for the TP_{in} concentration was applied for the entire study period using the inflow data from the fluviometric station. Then, the modeled concentrations were compared with a subset of the measured values in the water quality station and evaluated by the same indicators (NSE and R^2).

3.2.5. Uncertainty analysis and validation

The fundamental data used to develop the nutrient-flow relationships were the TP load. However, the load estimation process discussed arise uncertainties mainly related with water quality and quantity data (Hollaway et al., 2018). Then, an uncertainty analysis along with the validation of the estimated loads were performed. The validation was possible through the evaluation of the R^2 and the bias between the mean modeled TP load and the reference load calculated by COGERH. Furthermore, as several TP loads were estimated throughout the studied period, the coefficient of variation was calculated for each catchment and an analysis of this statistics was carried out in light of available literature. Ultimately, reported mean error values for the ECM methodology was gathered to perform a comparison of the range of variation of the modeled TP load with the range of variation of the reference TP load.

3.3 Results and discussion

3.3.1. Catchment hydrology and water quality characterization

The volume variation, inflow regime, sampled TP_r and estimated TP_{in} concentration for the studied period are presented, respectively, in Figs. 3.2a, 3.2b, 3.2c and 3.2d, along with the limits of TP concentration according to national standards. The interannual variability of the volume is shown in Figure 3.2a. One can see a wide range of volume variation among reservoirs, with maximum reductions spanning from about 50% to 5% of the maximum observed volumes. For instance, the volume of the Castanhão reduced from 5,192 to 289 hm^3, while the volume of the Canafístula from 10.6 to 0.06 hm^3. The small reservoirs usually present an annual cycle due to their frequent “emptying process”, while the larger ones sustain water for several years (Lopes et al., 2014; Lacerda et al., 2018). The volume of the Santo Anastácio is approximately constant (0.3 hm^3) since it receives continuously sewage from a drainage channel. In the wet season, though, the volume increases to about 0.5 hm^3 due to urban runoff (Fraga et al., 2020).

Figure 3.2b shows a marked variability in the mean inflow to the reservoirs during the wet seasons of the study period. The reservoir Olho D’água presented the lowest inflow, from 0.01 to 0.7 $m^3\ s^{-1}$, while the highest values were observed in the Castanhão reservoir, from 2.1 to 74.7 $m^3\ s^{-1}$. The seasonal and interannual variabilities of volume and inflow are highly influenced by changes in precipitation levels, particularly in the State of Ceará (Broad et al., 2007). While a decline in the mean inflow is expected during dry periods in most regions (Zhang et al., 2015), due to the semiarid condition of the studied area, the inflow is completely

interrupted during the dry season. Additionally, the high-density reservoir network strongly contributes to this inflow interruption in downstream reservoirs (Mamede et al., 2012, 2018). Conversely, the inflow to Santo Anastácio reservoir had a lower variation of 0.1 - 1.6 $m^3 s^{-1}$, even in the dry season.

The measured TP concentrations in the reservoirs (TP_r) are shown in Figure 3.2c. The ranges were: 10 – 400 μg L^{-1} (minimum values), 27 – 2,011 μg L^{-1} (median values) and 89 - 7,181 μg L^{-1} (maximum values). The Orós and General Sampaio reservoirs presented the lowest (about 6 times) and highest (about 100 times) variations, respectively. The water quality deterioration (TP_r = 2,145 μg L^{-1}) observed in the General Sampaio reservoir was associated with large NPS pollution due to the heavy precipitations in 2009, mainly considering its proximity to the city of General Sampaio (Chaves et al., 2013). Contrastingly, the values of TP_r in the Santo Anastácio reservoir ranged from 225 to 7,181 μg L^{-1}, as a result of massive untreated sewage input from its drainage channel.

With regards to the accordance with Brazilian standards for water quality, most reservoirs had their concentrations over the limiting value of 30 μg L^{-1} for their classification (see Figure 3.2c). The reservoirs which better performed were Rosário, Cachoeira and Olho D'água, with 46%, 56% and 52% of the TP_r measurements under this limit. The implications of exceeding these limits rely mainly on triggering eutrophication processes, for which TP is a critical nutrient (Le Moal et al., 2019), and intensifying the water quality degradation. The recovery of the water quality related to this nutrient has been a natural process with no measures taken by environmental regulatory agencies on record. TP_r is strongly affected by changes in hydrological parameters (Zhang et al., 2020). For the studied period, the lower the volume, the higher the concentration in the water column for all reservoirs, which is an expected behavior for this nutrient (Wu et al., 2016). Furthermore, the input TP load variability is another explaining factor for TP_r variation through time.

The different variations in the water quality of the reservoirs may have several causes related to the catchment and the reservoir itself, such as: seasonal patterns and variations in the flow regime (Rattan et al., 2017), different land uses (Lun et al., 2018), variable water retention time (Chaves et al., 2013) and significant water level variation (Sharpley et al., 2013). Previous studies in lakes and artificial reservoirs have found TP_r concentrations ranging from about 1 to 3,270 μg L^{-1} (Matias and Johnes., 2011; Rattan et al., 2017; Han et al., 2018; Li et al., 2020), which are of the same order as those observed in the present study.

Figure 3.2 - Variation range of (a) volume, (b) Inflow, (c) measured TPr (d) estimated TPin along with the limits of TP concentration according to national standards. * Measurements from Araújo et al., (2019) and Mesquita et al., (2020)

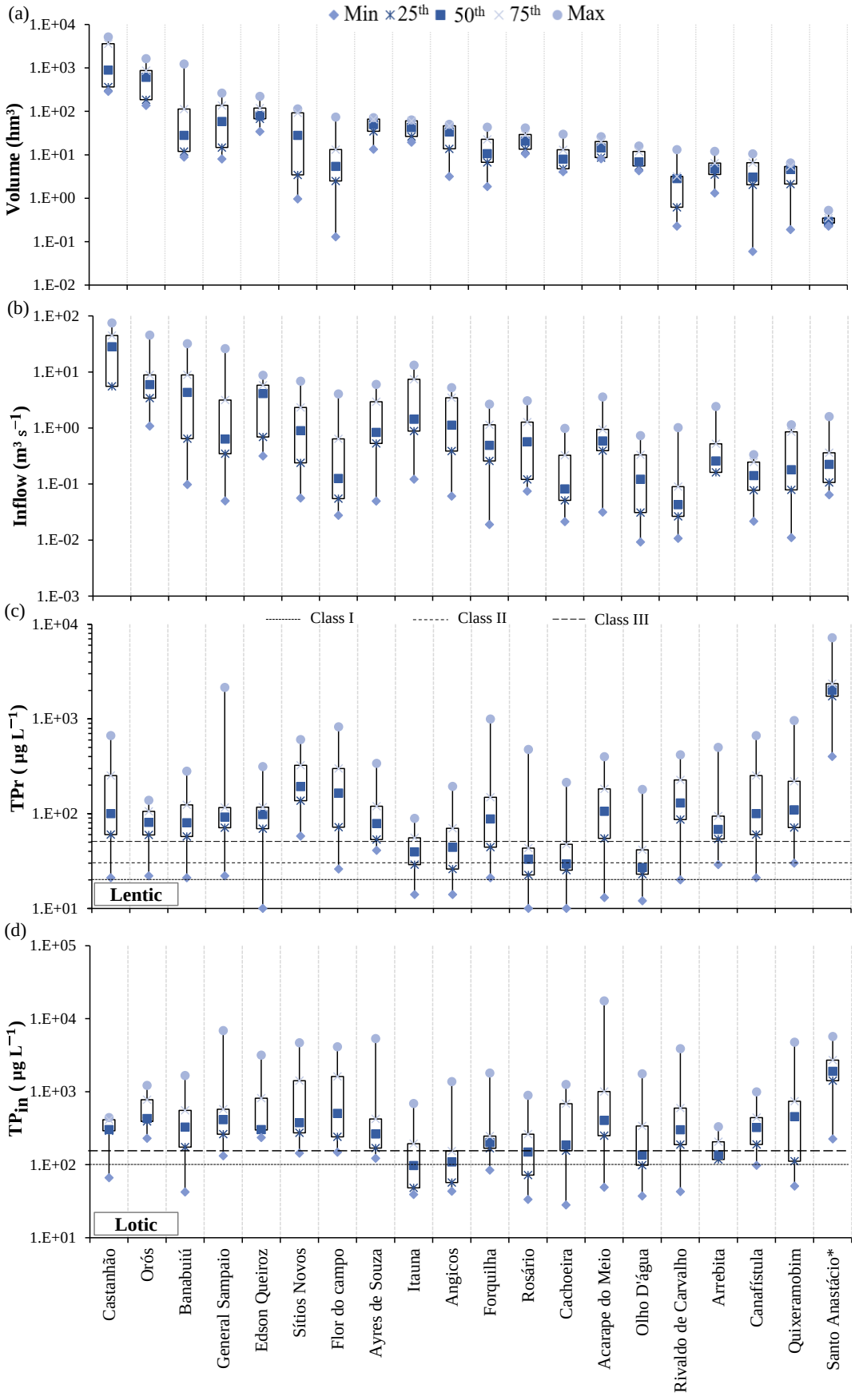

Ultimately, the TP concentration modeled at the reservoirs' inlet as an average of its tributaries (TP_{in}) is presented in Figure 3.2d, along with the limiting concentrations. An overall description shows that the lowest value was 28 μg L^{-1} (Cachoeira) and the largest was 17,515 μg L^{-1} (Acarape do Meio), 2.56-fold higher than the second highest value of 6,839 μg L^{-1} for the General Sampaio inlet waters. The maximum TP_{in} concentrations were considerably high during low flow period (0.001 - 0.2 m^3 s^{-1}). The 75th percentile, though, reached more usual values ranging from 154 to 2,707 μg L^{-1}, while the flow varied from 0.09 to 45 m^3 s^{-1}. The median concentrations ranged from 98 to 1,897 μg L^{-1}. As for the limiting concentrations, the TP_{in} of the reservoirs Santo Anastácio, Edson Queiroz and Orós resulted in all estimated values over the established limit for both classes. Angicos, Itaúna and Rosário, though, better met the standard, with 64%, 62% and 50% of the estimated values under the limit concentration for Class II, respectively. For the remaining, only the modeled values between the minimum and the 25th percentile fell below the reference concentration of 100 μg L^{-1}.

The estimated TP_{in} concentration values were very far from those reported by Chen et al., (2015) (10-200 μg L^{-1}), Bowes et al., (2009) (400 μg L^{-1} in average), Bowes et al., (2015) (85-447 μg L^{-1}), Greene et al., (2011) (500 μg L^{-1} in average), and Mouri et al., (2011) (540 μg L^{-1} in average). In contrast, they were closer to those observed by Rattan et al., (2017) (55-1,740 μg L^{-1}), Bowes et al., (2014) (20-2,000 μg L^{-1}), Bieroza and Heathwaite (2015) (10-2,000 μg L^{-1}), Bowes et al., (2010) (~0-4,000 μg L^{-1}) and Bowes et al., (2008) (~0-8,000 μg L^{-1}). Remarkably, TP_{in} values superior than 16,000 μg L^{-1} were found during low flow periods of a Mediterranean intermittent river with an arid catchment highly dominated by PS pollution (Perrin et al., 2018). These hydrologic regimes and climate condition are quite similar to the ones of the studied area as well as the high TP_{in} concentrations.

The major inflows of the reservoirs come from intermittent rivers, except for Santo Anastácio, whose inflow come from an urban drainage channel. For the rural reservoirs, higher TP_{in} values were obtained in the alternation of wet and dry phases, a low flow period denominated hydrological contraction (von Schiller et al., 2017), before the river complete dryness. This aspect might be associated with a lack of dilution of TP from point sources during low flow rates (Bowes, et al., 2009). Contrastingly, the bioavailability of P compounds in the sediments of intermittent rivers on drying potentially contributes to eventual peak concentration during high flow events (von Schiller et al., 2017). In addition, aspects such as the enlargement of P delivery from land to water bodies through a high hydrologic connectivity (Chen et al., 2015b; Rattan et al., 2017), high concentrations of suspended algal material (Bowes et al.,

2009), catchment urbanization (Mouri et al., 2011; (Rattan et al., 2017) and the low water quality of the reservoir during the modeling period can contribute to high TP_{in} estimations.

3.3.2. Modeled TP load

The estimation of the TP load produced in the catchments was achieved by the application of Equation (3.1). The variability presented in Figure 3.3 results from changes in TP_r and water balance parameters for each modeled interval. The reservoirs with the largest variations in the estimated TP load were also those with the largest variability in their inflows, such as the General Sampaio and Acarape do Meio reservoirs (see Figure 3.2b). The reference TP load values estimated by COGERH through the ECM approach is also shown in Figure 3.3.

Figure 3.3 - Estimated TP load by mass balance and reference TP load by the ECM modelling approach. * Estimated TP load from measured data of TPin and inflow (Araújo et al., 2019; Mesquita et al., 2020)

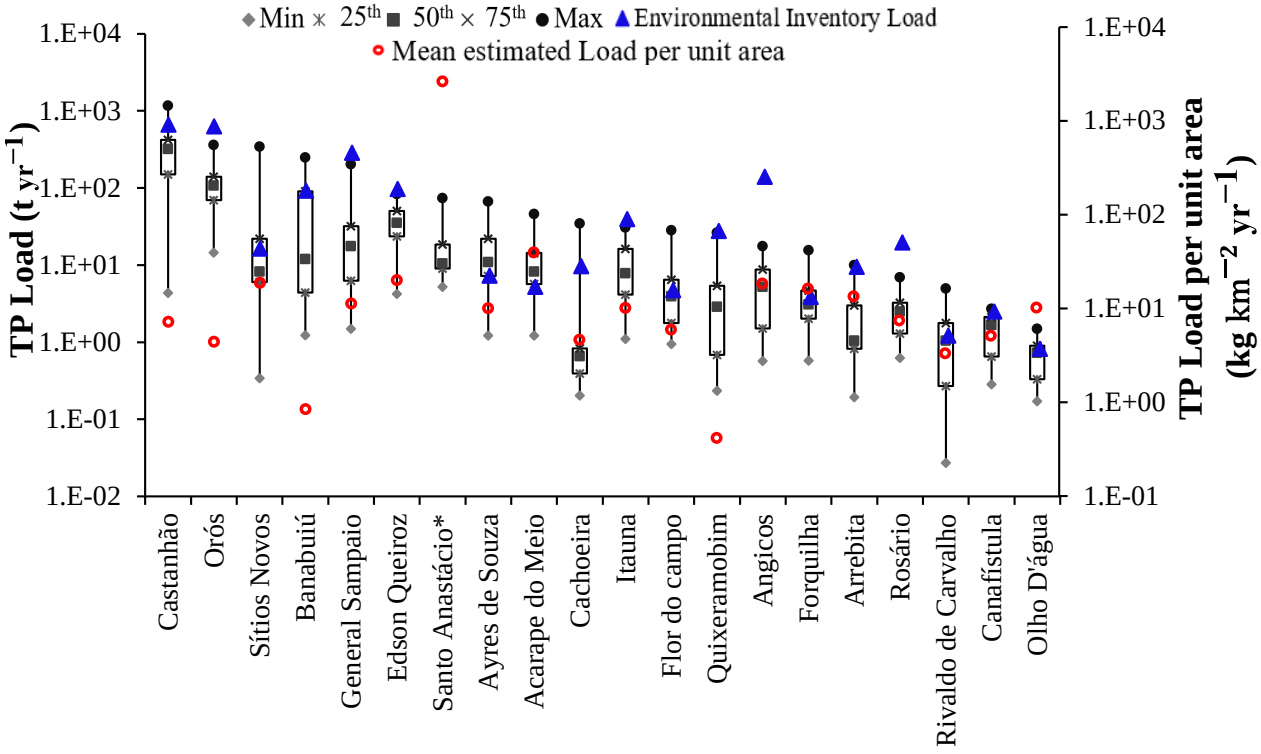

The estimated annual TP loads ranged from 0.03 t yr^{-1}, for the catchment of the Rivaldo de Carvalho reservoir, to 1,164 t yr^{-1} for the Castanhão catchment. Considering only the Orós and Castanhão catchments, the median value was 214 t yr^{-1}, while including all 19 reservoirs managed by COGERH, the median drops to 7.2 t yr^{-1}, which turns these first two catchments the largest TP producers. It is interesting to stress, however, that even being much smaller, the

Santo Anastácio reservoir receives annually an average TP load of about 16.6 t yr^{-1} (Araújo et al., 2019), which is twice higher than the median value for the above-mentioned reservoirs.

As can be seen in Figure 3.3, the estimated TP loads were slightly under the reference values for 25% of the catchments, and more significantly underestimated for only 10% of them, represented by the catchments of the reservoirs Orós and Angicos. For 35% of the catchments, the reference load and the median estimated load were the closest, while, for the remaining, the reference value was somewhere between the range of modeled loads. The temporally spaced measured data might have contributed to the underestimation of the TP load. Low sampling frequency during the rainy season tends to underrepresent peak storm or high-flow events and the intense phosphorus dynamics right after (Johnes, 2007; Bowes et al., 2009). Besides, particularly for the larger catchments, the high density of reservoirs also plays an important role in regulating upstream P retention (Hu et al., 2020). Bowes et al., (2009) evaluated the impact of sampling frequency influence on annual TP load estimation. Their estimation with monthly measurements produced a mean deviation of -21 to 35% from the one carried with weekly measurements. Therefore, improved load estimates are produced from more frequent sampling, which highlights the challenge of dealing with low data availability. In the meantime, as water quality or quantity data are not carried out frequently, modeling with the available data remains the possible option in data-scarce regions, such as the Brazilian semiarid.

The reconstruction of TP load through different modeling approaches was widely performed in the literature. Rattan et al., (2017) obtained values of 117 t yr^{-1} in Canada. Chen et al., (2015) found TP loads around 357 t yr^{-1} in China. Zhang et al., (2020) obtained TP loads reaching peak values over 2,700 t yr^{-1} in China. Mockler et al., (2017) assessed annual TP emissions for 16 major river catchments with values up to 3,000 t yr^{-1}. Lastly, Han et al., (2018) evaluated the great Three Gorges Reservoir basin and estimated TP load of about 43,977 t yr^{-1}. In comparison, the studied catchments do not present a so intense TP load production (see Figure 3.3). A plausible explanation may be the existence of a dense reservoir network, which potentially contribute to P retention, as observed for the sediment production (Lima Neto et al., 2011; Mamede et al., 2018).

The TP load production from NPS pollution is expected to be higher in larger catchments (Marques et al., 2019). However, the activities' intensity developed in the basin plays a more important role. Rural areas where predominate livestock and agriculture produce about four times more TP load than urban areas (Li et al., 2020). The catchments of Castanhão and Orós concentrate the most relevant irrigated croplands of the study area and the first one shows the highest amount of TP production (656 t yr^{-1}) (Ceará, 2020). The TP load from

fertilizers is another concern to be considered for the catchment of Orós, the second largest TP producer (624 t yr^{-1}). Agriculture and soil contribute with 80% of NPS pollution in this catchment. Indeed, cultivated lands can be a major secondary pollutant to surface waters (Li et al., 2020).

With respect to the among-catchment variation of the input load, specific anthropogenic uses of each catchment play an important role in this variablity (Hong et al., 2012; Chen et al., 2015b; Hu et al., 2020), while the intervariation of TP load may be better explained by its relation with seasonal variations in rivers discharge (Han et al., 2018). Stream discharge fundamentally influences annual TP load along with the river's own nutrient retention capability (Torres et al., 2007). Also, hydrologic events (Jeznach, 2017), such as peak storms (Chen et al., 2012), mainly in NPS dominated. Besides, legacy P remobilization during slow flow paths may be taken into consideration as a relevant aspect (Sharpley et al., 2013).

The TP loads per unit area were also presented in Figure 3.3 to support a comparison among catchments. Despite the high TP loads estimated for Orós and Castanhão catchments, their values per unit area were relatively low: 4.4 and 7.2 kg km^{-2} yr^{-1}, respectively. On the other hand, the catchment of Acarape do Meio presented the highest value, 39.3 kg km^{-2} yr^{-1}, possibly as consequence of its relatively small area and potentially high river connectivity. This catchment presents the highest precipitation index, which also favors higher TP runoff. Contrastingly, Lun et al., (2018) found a net soil P budget for Brazilian croplands of about 500 $kg.km^{-2}.yr^{-1}$. Although the loads in the studied catchments come from more uses than croplands, the values are very low compared to this national average. Lower precipitation indexes and the intermittent regime of the rivers, potentially reducing TP runoff, contribute to these low estimates. Additionally, the TP retention in the numerous small upstream reservoirs within the catchment impacts this result (Lima Neto et al., 2011; Mamede et al., 2012, 2018). Contrastingly, the Santo Anastácio reservoir presented a TP load per unit area of 2,626 kg km^{-2} yr^{-1} (Araújo et al., 2019), significantly higher than the above-mentioned national average. This is a combined result of the high precipitation indexes in a small urban catchment that additionally disposes untreated sewage into the reservoir.

3.3.3 Assessment of TP point and non-point sources to the catchments

To describe the proportions of TP load from different sources in each catchment and further contrast with the behavior of the nutrient-flow relationships, Figure 3.4 shows the percentages of contributions from agriculture, soil, fish farming, livestock and sewer sources

according to the environmental inventory of each catchment (Ceará, 2020). Note that for the Santo Anastácio reservoir, it was assumed the sewer discharge as the main TP source (Pacheco and Lima Neto, 2017). It is noteworthy that some simplified hypothesis adopted when the environmental inventories were elaborated might bring uncertainties. They might be primarily related with empirical parameters such as loss coefficients from soil and pasture, as well as TP load per capita. This uncertainty analysis, however, is later addressed.

The NPS loads refer to animal husbandry, agriculture and soil erosion, while PS loads refer to fish farming and sewer production. The total NPS load exceeded PS loads in seventeen catchments, except the Castanhão, Orós and Acarape do Meio reservoirs. This accounts for a NPS dominance in 86% of the catchments. Forquilha and Arrebita reservoirs presented the highest NPS contributions (97% and 97%, respectively), while Orós and Castanhão the highest PS contributions (76% and 62%, respectively). The representative sewage contribution for the Orós reservoir is justified by the location of a large city (>100,000 inhabitants) in its surroundings. Its low coverage of sanitation facilities largely leads to untreated sewage inputs (Barbosa et. al 2012; Ceará, 2020). For the Castanhão reservoir, Paula Filho et. al (2019) have estimated the P contribution of 28% of the catchment as 340 t yr^{-1}. Furthermore, in the rural areas of the State of Ceará, septic tank systems are the main method for disposal of human wastes. Lastly, although not monitored, the approximation for sewer contribution as the most significant TP source for Santo Anastácio is consistent with the characteristics of its catchment as well as previous studies (Araújo et al., 2019).

Overall, sewer contributed the most as PS load in 77% of the catchments, while fish farming accounted significantly for the PS load produced in the Orós (64%) and other reservoirs as shown in Figure 3.4. Regarding the representativeness of NPS, livestock dominated in 25% of the catchments, while soil contribution prevailed in 55% as the most significant non-point source. Agriculture, then, predominated in the remaining catchments. The predominance of NPS over PS in the study area highlights the importance of animal husbandry and agriculture for the local population. Furthermore, the among-catchment heterogeneity of TP sources is largely explained by differentiated anthropogenically-sourced load, agricultural intensity, cattle density and soil type (Ceará, 2020).

Regarding the soil influence on NPS contribution, soil erodibility plays an important role in the mobilization of pollutants (Li et al., 2020). Poorly drained soils can transfer the most NPS contribution (Greene et al 2011), particularly in semiarid regions (Paula Filho et. al 2019). This process might be driven by rainfall through runoff events (Greene et al., 2011) as well as the soil type (Jacomine et al., 1973). The rainy season in Brazilian semiarid, well-defined from

January to May, accounts for more than 80% of annual precipitation and 90% of annual erosivity (Araújo and Medeiros, 2013). In addition, riparian ecosystems are important to control NPS pollution from soil and sediments (Guo et al., 2014), providing a TP load reduction of up to 30% (Zinabu et al., 2017). In the studied area, these ecosystems are severely degraded, particularly for some water bodies such as Orós (Chaves et al., 2019). Ultimately, soil erodibility can also make available legacy P, although quantifying the real contribution of this TP input is very difficult (Sharpley et al., 2013).

Together, the aforementioned aspects related with high TP concentrations (see Figure 3.2c), the estimated TP loads (see Figure 3.3) and their main sources (see Figure 3.4), arise the problem of how to reduce this nutrient source. This is particularly important considering human supply as the main use of water for these reservoirs. Among the non-point sources of pollution, the soil contribution is one of the most representative and difficult to address. It depends mainly on the condition and characteristics of the local vegetation, the degree of exposure to processes such as erosion and desertification, the land use by the diffuse rural population and the action of natural phenomenon. Thus, focusing on this source of pollution is more impractical, at least in a mid-term perspective. With regard to agriculture, undefined standards or widespread fertilizer application might increase the availability of TP to be carried out in run-off events, which can be addressed mainly through regulation by environmental agencies. Ultimately, the sewer pollution is the pressing P source through which is possible and necessary to take reduction measures. This approach, however, requires mostly a governmental effort to expand sanitation facilities, which currently cover only 41% of the urban areas of the state (Ceará, 2018). These measures may, in the medium and long term, help decrease the transfer of P from the catchment to water bodies and possibly contribute to the improvement of water quality.

Figure 3.4 - Total phosphorus point source and non-point source load characterization for the studied catchments in the State of Ceará

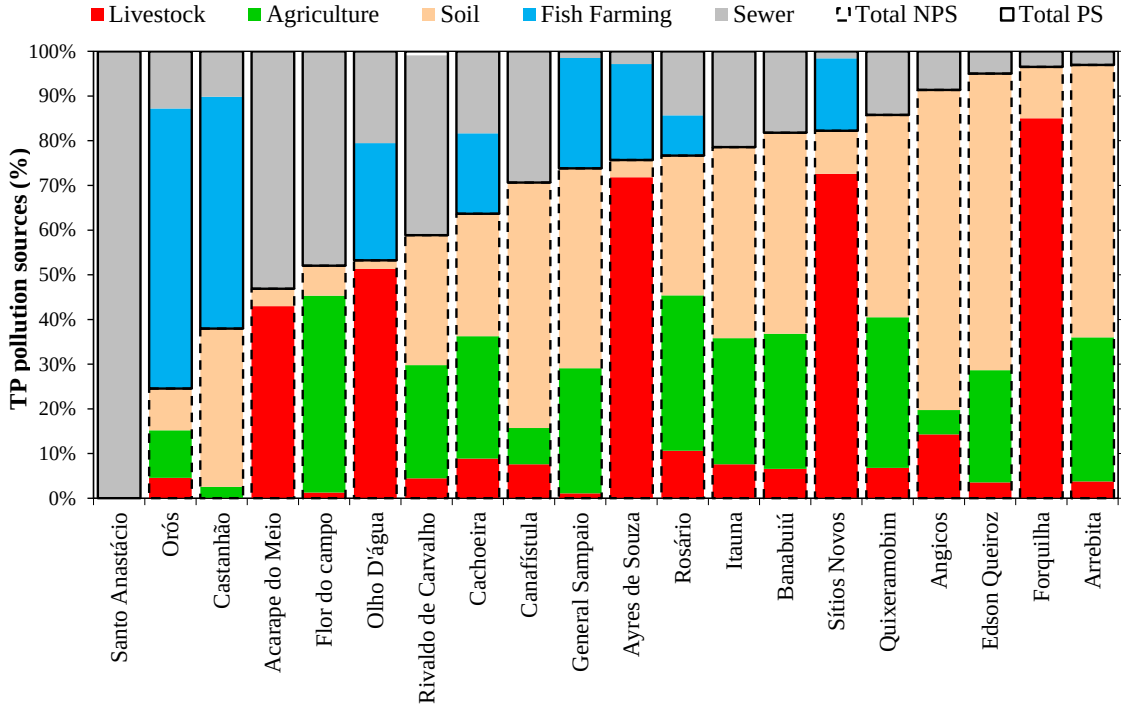

* Data on P sources by catchment obtained from Ceará (2020).

3.3.4. Adjusted nutrient-flow relationships

The fitted models encompassing average inflow and TP concentration at reservoir's inlet are presented in Figure 3.5, while their modeling parameters are shown in Table 3.2. Three main nutrient-flow patterns should be highlighted: an inverse curve, when PS dominance occurs, representing a dilution pattern; a linear or exponential curve, for NPS dominance where a combined increase in flow and concentration is more likely; and, a u-shaped curve for PS and NPS codominance (Greene et al., 2011). These curves describe the existing relations with four parameters (A, B, C and D).

Analyzing the adjusted models along with the catchment sources of contribution of TP load reveal that the relationships presented a consistent shape form for the majority of the studied sites, with only few particularities. The adjusted curve for the reservoirs Castanhão, Forquilha and Sítios Novos presented clear u-shaped forms. Consistently, the percentage of TP load from NPS contribution is 97% and 82% for Forquilha and Sítios Novos, respectively. In contrast, Castanhão, with 38% of non-point source dominance, also presented a strong pattern of NPS dominated catchments. This can be attributed to eventual inaccuracies in the load estimation process in its environmental inventory, mainly due to the difficulty to account accurately non-point sources of pollution in a large catchment (44,800 km²). Still, as the model for this reservoir present several TP_{in} measurements, the result is assumed to be reliable. None

of the studied sites presented a single linear or exponential curve, except the Santo Anastácio reservoir, which presented only a dilution pattern. This is in line with the high contribution from point sources as well as the predominantly urban usage of the catchment.

Many sites presented a slightly u-shaped pattern with a decrease in TP_{in} as flow increases followed by an increase in concentration as flow increases. This aspect reveals a PS dominance for low flow rates and a NPS dominance for high flow rates, in line with which is expected since the catchments present contributions from point and non-point sources in significant proportions. At these sites, the discharge at which the estimated PS and NPS TP inputs are equal (Q_e) marks the inversion of the curve. Furthermore, it is important to highlight that the highest TP concentrations occurred during flows below the Q_e value in 90% of the catchments.

A high variability in the TP_{in} was observed in the fitted models of the Banabuiú and Quixeramobim reservoirs, which impacted in the adjustment of the model. This scatter in the estimated values may suggest large hysteresis patterns during some storm events (Bowes et al., 2014). For the Banabuiú, high TP_{in} derived from estimated TP loads with markedly different values in the pair $TP_{r,0}$-$TP_r(t)$, with elevated $TP_r(t)$ measurements. Sporadic peaks in TP_{in} concentration during low flow rates suggests the existence of a pollution source neither continuously constant nor diffuse, such as a random pollution event (Bowes et al., 2008). Cattle access points and local effluent thrown into rivers, for instance, might work as sporadic PS contributions (Jarvie et al., 2010). This aspect also elucidates the contrasting dilution pattern observed in these rural catchments.

The fitted model for the Acarape do Meio reservoir (with loads coefficients A = 183, B = 0.07, C = 47, and D = 2) derived from the largest TP_r dataset and also presented measured TP_{in} data by Lima et al., (2018). Prevails in the model low flow rates and a dilution pattern. The catchment present significant PS pollution near the tributaries, such as sewage treatment stations from which three discharge their effluents directly into the main river of the catchment (Lima et al., 2018). Its A coefficient, which accounts for PS contribution, is accordingly higher than 60% of the others.

With regards to the A and C fitting parameters shown in Table 3.2, they describe for each model the relevance of PS and NPS contributions, respectively. The A coefficients varied from 18 to 1,858 with a median of 100.4, while the C coefficients varied from 0 to 137, with a median of 34.7. The adjusted model for the Orós presented the largest A coefficient (A = 1858) and, accordingly, its catchment presented the second highest PS contribution. The D coefficient, the flow-dependent one, describes the changing rate of the load with flow and remains greater

than one to account for NPS contributions. D ≈ 1.0, however, suggests the poor ability of the model to predict only the mean TP concentration. Physical phenomena such as P remobilization into the river bed potentially lead to superior D values (Bowes et al., 2008). The best fit for two models in this work, however, presented D = 1. This difficulty to detect input signals from NPS contribution was also reported by Bowes et al., (2008). Regarding the B coefficient, the values always greater than zero indicate a PS load removal from water such as losses to river sediment through sorption process. This is particular intensified in slow water velocity, low flow, and when the sediment P sorption capacity is not saturated (Sharpley et al., 2013; Jarvie et al., 2013). Consumption and deposition are other intensifying processes of TP removal from the water (Ansari and Gill, 2014; Gargallo et al., 2017; Braga et al., 2019). Thus, the low flow levels during the studied period may have largely contributed to B parameters less than 1.

The majority of the fitted models were realistic with respect to the data, with modeled TP_{in} concentration versus average daily discharge showing satisfactory Nash–Sutcliffe coefficients. NSE coefficients over than 0.20 are considered satisfactory for NPS dominated catchments as highlighted in previous applications (Greene et al., 2011; Chen et al., 2015a). The fitted model for Ayres de Souza presented the best NSE (0.73). For those models with a poor performance metric (Canafístula and Itaúna reservoirs), their NSE was sensitively affected by isolated TP_{in} peak value. The NSE for Canafístula would change from -0.43 to 0.15 without this peak value. Similar analysis applies for the Itaúna reservoir. Ultimately, the indicators for the models of the reservoirs Quixeramobim and Banabuiú reservoirs have presented a low performance mainly due to the variability of the estimated TP_{in} in spite of the good overall pattern of the curve.

Table 3.2 - Parameters of the TPin-inflow adjusted models (A, B, C and D) along with the model performance indicators (NSE and R^2) and the inflow that equalizes point and non-point loads (Qe)

Catchment's reservoir	Main river	Model parameters				Q_e ($m^3.s^{-1}$)	NSE	R^2
		A	B	C	D			
Ayres de Souza	Jaibaras	291.4	0.10	61.0	1.13	4.6	0.73	0.75
Forquilha	Riacho Oficina	85.0	0.13	23.0	3.40	1.5	0.60	0.94
Edson Queiroz	Groaíras	569.0	0.10	70.0	1.47	4.6	0.58	0.62
General Sampaio	Curu	390.0	0.26	23.0	1.77	6.5	0.56	0.61
Rivaldo de Carvalho	Rivaldo de Carvalho	40.3	0.10	50.0	2.00	0.9	0.56	0.60
Flor do campo	Poti	143.4	0.31	80.0	1.40	1.7	0.44	0.78
Santo Anastácio*	Drainage channel	406.9	0.16	0.0	0.00	-	0.41	0.53
Orós	Jaguaribe	1858	0.10	21.0	1.70	16.4	0.37	0.66
Sítios Novos	São Gonçalo	184.0	0.24	53.0	2.15	1.9	0.37	0.84
Rosário	Rosário	39.3	0.02	34.3	1.00	1.2	0.32	0.37
Castanhão	Jaguaribe	40.6	0.68	26.5	1.55	1.6	0.32	0.46
Acarape do Meio	Pacoti	183.0	0.07	47.0	2.00	2.0	0.29	0.52
Olho D'água	Machado	18.0	0.05	31.0	1.50	0.7	0.27	0.38
Arrebita	Sabonete	27.0	0.04	80.0	1.20	0.4	0.16	0.25
Cachoeira	Caiçara	20.0	0.01	35.0	2.00	0.7	0.10	0.21
Angicos	Juazeiro	55.0	0.02	18.0	1.75	1.9	0.07	0.15
Quixeramobim	Quixeramobim	67.0	0.17	47.5	1.90	1.2	-0.28	0.02
Canafístula	Foice	30.4	0.10	137.7	1.33	0.3	-0.43	0.06
Itaúna	Timonha	115.7	0.02	9.0	1.73	4.4	-0.91	0.10
Banabuiú	Banabuiú	320.0	0.03	12.0	1.77	6.6	-2.89	0.17

Figure 3.5 - Fitted models between mean TPin and average inflow for the twenty studied reservoirs: dot (modeled concentration), asterisk (measured concentration), dashed line (changing flow) and continuous line (adjusted model)

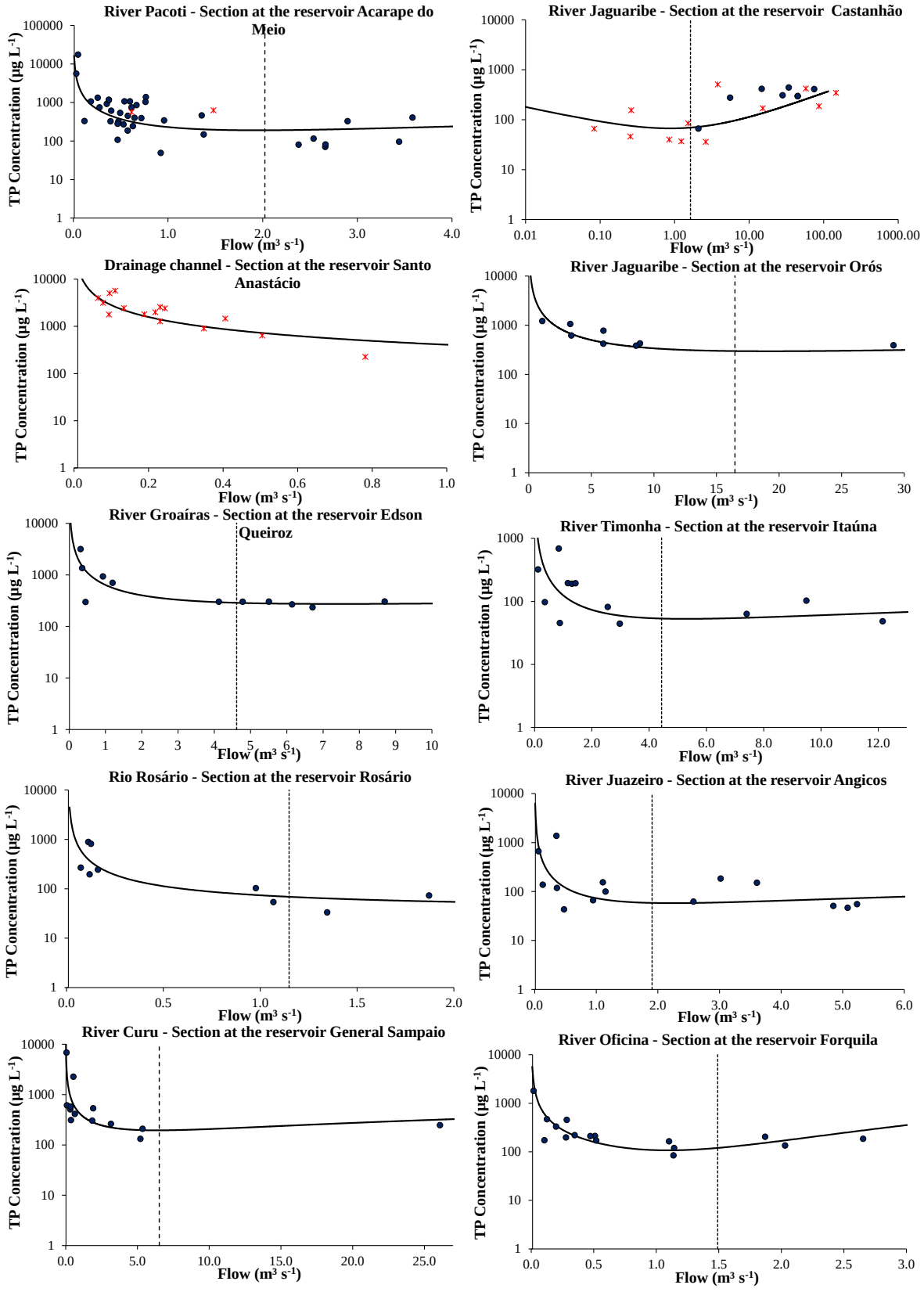

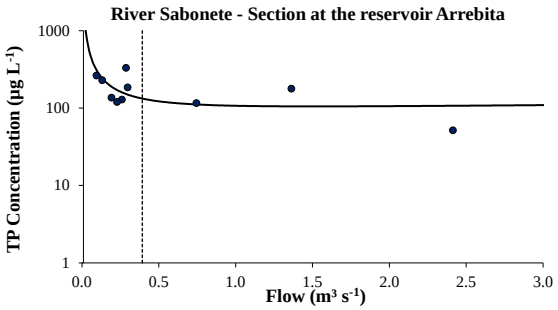
River Sabonete - Section at the reservoir Arrebita
TP Concentration (µg L-1)
Flow (m³ s-1)

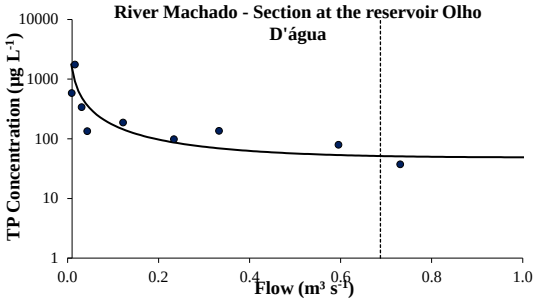
River Machado - Section at the reservoir Olho D'água
TP Concentration (µg L-1)
Flow (m³ s-1)

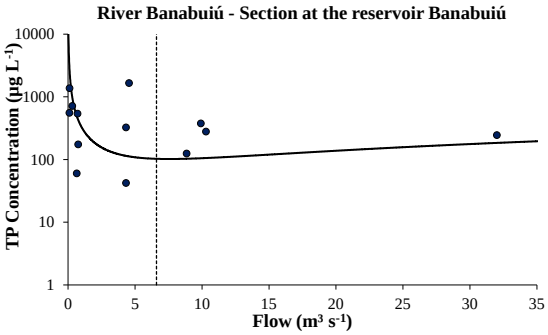
River Banabuiú - Section at the reservoir Banabuiú
TP Concentration (µg L-1)
Flow (m³ s-1)

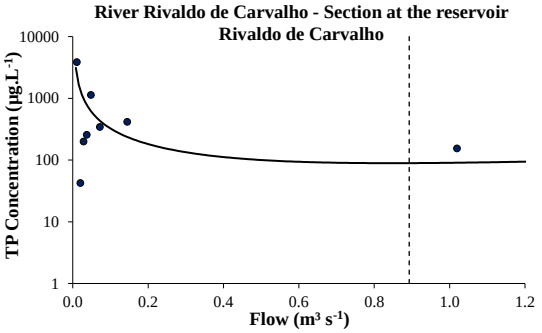
River Rivaldo de Carvalho - Section at the reservoir Rivaldo de Carvalho
TP Concentration (µg L-1)
Flow (m³ s-1)

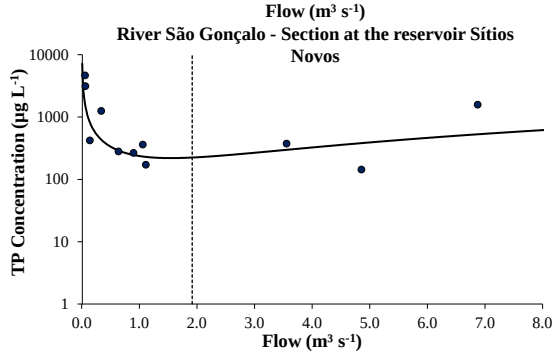
River São Gonçalo - Section at the reservoir Sítios Novos
TP Concentration (µg L-1)
Flow (m³ s-1)

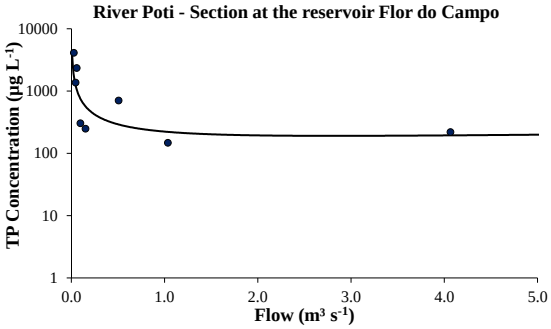
River Poti - Section at the reservoir Flor do Campo
TP Concentration (µg L-1)
Flow (m³ s-1)

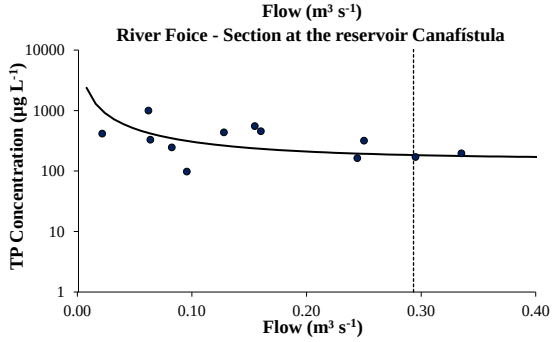
River Foice - Section at the reservoir Canafístula
TP Concentration (µg L-1)
Flow (m³ s-1)

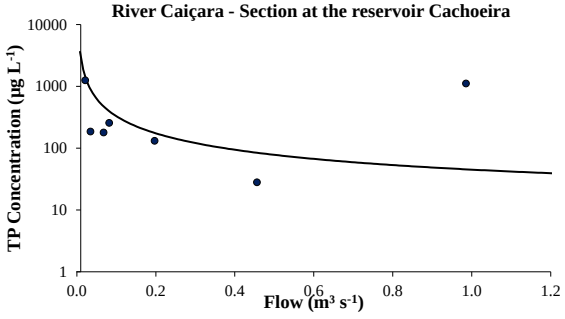
River Caiçara - Section at the reservoir Cachoeira
TP Concentration (µg L-1)
Flow (m³ s-1)

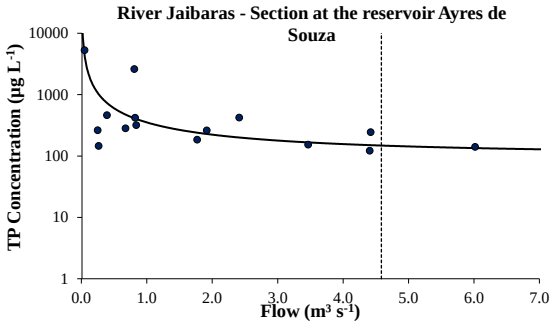
River Jaibaras - Section at the reservoir Ayres de Souza
TP Concentration (µg L-1)
Flow (m³ s-1)

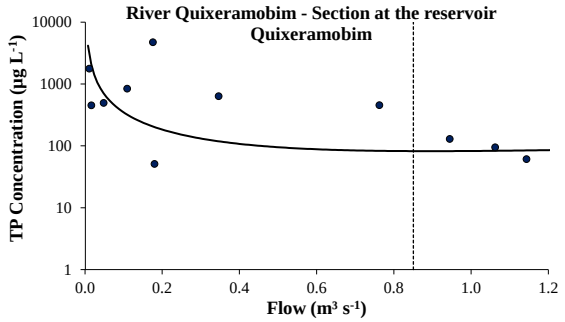
River Quixeramobim - Section at the reservoir Quixeramobim
TP Concentration (µg L-1)
Flow (m³ s-1)

The model developed for the Castanhão reservoir (with loads coefficients A = 40.6, B = 0.68, C = 26.5, and D = 1.55) was applied to estimate TP_{in} from measured flow data. The available measured riverine TP concentration was used to evaluate the model's performance. Figure 3.6 presents the results of this modeling along with the national standards for water quality. Additionally, the measured and estimated flow are shown. The comparison between modeled and measured TP concentration resulted in a Nash coefficient of 0.63 and a R^2 of 0.70. As can be observed, the validation of the model included both low and high flow periods. However, some unusual low concentrations were not reached by the model, which may be due to the unrepresentativeness of this low concentration pattern in the entire dataset (< 10%).

During high flow events higher concentrations are obtained as a result of the u-shape pattern of the model to reflect strong NPS contribution from wash-off. In the meantime, as low flow rates prevailed during the studied period, the dilution pattern of the model (for $Q < Q_e$) stood out and low concentrations were observed. Even under these conditions, only 53% of the estimated values were under the limit of Class II. Ultimately, the comparison between measured and estimated flow resulted in a NSE of 0.81 and a R^2 of 0.82, which highlight the quality of the flow data obtained from the water balance. This result reinforces the application of the flow estimated from water balance as a workaround to the inexistence of fluviometric stations at the inlet of several studied reservoirs.

Figure 3.6 - Modeled TP_{in} concentration for the inlet of the Castanhão reservoir by the application of the adjusted flow-concentration curve

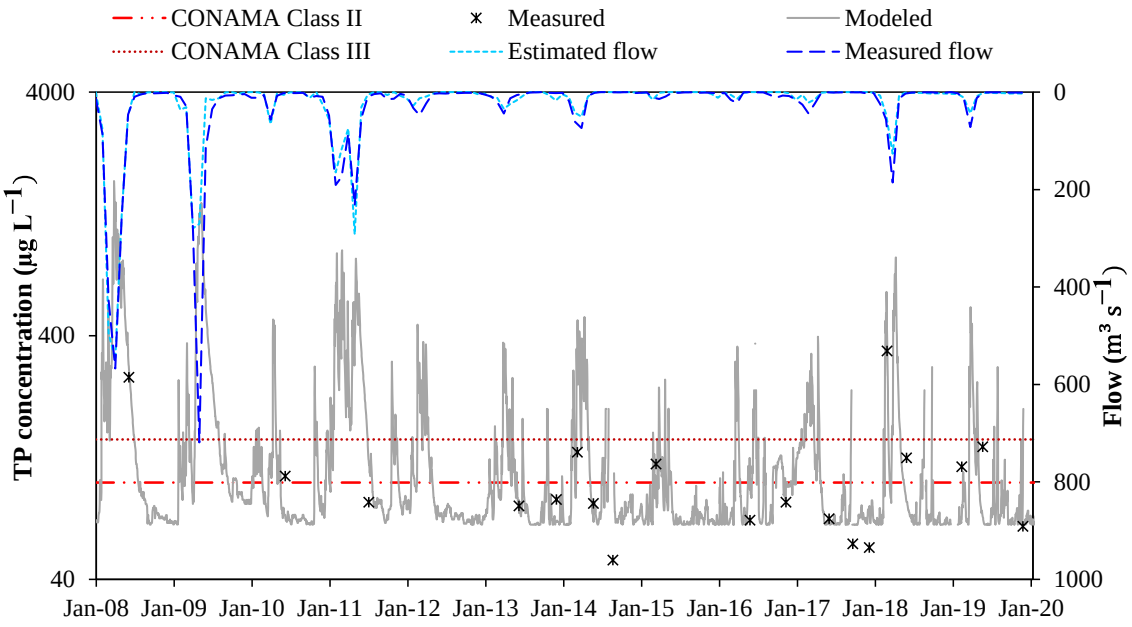

3.3.5. Evaluation and comparison of the proposed models

The proposal and analysis of TP concentration-inflow relationships were carried out previously by several authors (Bowes et al., 2008, 2009b, 2010, 2014,1015; Greene et al., 2011; Bieroza and Heathwaite, 2015; Chen et al., 2015a). The detailed description of the parameters presented by the first four researches was, then, compared with the ones obtained in the present study. It is noteworthy that, even though the relationships reported by Bowes et al., (2009b) were developed with soluble reactive phosphorus concentration, once the fraction represented more than 65% of the TP load (Bowes et al., 2009b), their coefficients are likely to represent an order of magnitude reliable to perform the comparison. The compared studies were performed in perennial rivers and the general statistic, minimum, median and maximum values of the parameters are presented in Table 3.3. Bowes et al., (2008, 2009b, 2010) highlight the relevant influence of human occupation and PS contribution in their studied catchments, while Bowes et al., (2014) presented relationships with both TP load dominance.

The highest A coefficient shown in Table 3.3 was 11,776, about six times higher than the value of 1,858 obtained in this study, suggesting a stronger influence of PS pollution. With regards to the A coefficient, the values reported by Bowes et al., (2014) were similar to those obtained in the presented study. As aforementioned, the similarities rely mainly in the NPS contribution to the catchments. The C coefficient, which mostly characterizes NPS contribution, reached the minimum values in this study in comparison with the others. In median terms, it was closer to the results obtained by Bowes et al., (2014). The minimum C value was fitted for the catchment of the Santo Anastácio reservoir. Accordingly, high C coefficients are not expected in urban catchments. Some particularities, such as $B \geq 1$ and $D \leq 1$ observed by Bowes et al., (2008), were not observed in the present study. The D and B coefficients were those more similar in all the studies. Particularly for the Santo Anastácio, the parameters related with the NPS pollution were nill. The model stated this way, accounting mainly PS contributions, reached the best performance. Additionally, this behavior is widely supported by the studies that highlighted sewer as the main TP input source for this water body (Pacheco and Lima Neto, 2017).

Table 3.3 - Comparison among the parameters of the TP concentration-discharge relationships

Statistics	A coefficient			B coefficient			C coefficient			D coefficient		
	Min	Med	Max	Min	Med	Max	Min	Med	Max	Min	Med	Max
This study	18.0	237	1,858	0.01	0.2	0.7	0.0	45.2	138	0.00	1.7	3.4
Bowes et. al (2008)	0.01	316	11,776	0.0	0.0	1.1	0.9	84.6	490	0.97	1.5	4.0
Bowes et. al (2009b)	193	368	464	0.0	0.0	0.0	11.8	29.9	47.7	1.1	1.4	1.7
Bowes et. al (2010)	10.5	1,765	6,613	0.0	0.2	1.0	10.6	20.9	41.6	1.0	1.4	2.0
Bowes et. al (2014)	0.00	71.0	4,806	0.0	0.0	0.0	9.0	61.0	585	1.0	1.4	1.8

3.3.6. Uncertainty analysis

The three main approaches that integrate this research present some degree of related uncertainties that were evaluated to ensure the effectiveness of the methodology. Those three refer to the use of the reference load estimated by COGERH to validate the modeled loads, the TP load modeling process itself and associated errors and the uncertainties with the TP_{in} concentration-flow relationships. With regards to the reference load, the concerning aspects with the ECM methodology are the adequacy of the coefficients to each catchment as well as the precision in determining total population, land use and soil type. Literature reports a range of mean error in the application of this methodology varying from 4.3% to 31% (Johnes, 1996; Ding et al., 2010; Matias and Johnes, 2012; Delkash and Al-faraj, 2014; Tsakiris and Alexakis, 2015). Then, a comparison was carried out between the reference TP load with a maximum range of variation of 31% and the modeled load with its related range of variation.

For the catchments whose reference load was underestimated in modeling, increasing or decreasing the reference load by a percentage of error did not significantly enhanced the already obtained deviation. This analysis suggests that the reference load and its variability due to some inherent percentage of error is largely covered by the greater variability of the estimated loads. Furthermore, the variability in the input data to the modeled load might have a large influence on this deviation, as previously discussed. The correlation analysis between the mean modeled load and the reference load, though, reached a $R^2 = 0.74$. This result was considered satisfactory to the quality of the modeling process (Moriasi et al., 2007).

The coefficient of variation for the modeled loads ranged from 0.6 to 2.4 with mean of 1.1. Kulasova et al., (2012) reported a range 0.05-0.2, significantly lower than that obtained in this study. Uncertainties associated with discharge measurement, sample collection and laboratory analysis significantly contribute to this result. Sample collection, only, adds an uncertainty of 109% in the worst scenario for TP concentration and data aggregation, such as average measures, adds 13% of uncertainty (Harmel et al., 2006, 2009). Also, the range of variation in the estimation process of NPS loads vary from 30% to 110% (Harmel et al., 2006).

The sampling interval between TP measurements might also imply uncertainties to the developed concentration-discharge relationships and their applicability. Quarterly average concentration-flow relations might reach from 10% to 20% uncertainty in load estimation (Dolan et al., 1981). Moreover, for the top 5% of flows, the uncertainties associated with the applied traditional power law fit might achieve even higher percentages (Hollaway et al., 2018).

3.3.7. Model implications and limitations

The methodology introduced in this research coupled catchment and reservoir. Designed from the modeling of average TP concentration at reservoirs' inlet from reservoirs inside characteristics, nutrient-flow relationships were adjusted. This methodology is replicable to semiarid regions with intermittent rivers where strategic water supply reservoirs are of greatest concern. It has the advantage of enhancing the understanding of the most relevant TP sources to a water body, evaluate the patterns of TP concentration coming from the catchment and predict the influence of inflow rates in water quality. Its main purpose is help addressing the TP issue in regions highly affected with lack of measured data in rivers and mostly monitored data in reservoirs. This methodology also provides means to evaluate seasonal TP concentrations only by classifying the levels of observed flow, with the advantage of simplicity to easily estimate averaged riverine TP concentration. Furthermore, it might be directly applicable in other regions with similar characteristics.

The development of relationships between TP concentration and river discharge to address PS or NPS influence of external P sources is widely reported. However, it was mostly applied to perennial rivers, a contrasting reality with the one of the studied area, with intermittent rivers and reservoirs for human supply. Thus, the approach adopted in the current paper tries to address the characteristics of the inlet waters of reservoirs as these water bodies are of utmost importance for semiarid regions. Additionally, nutrient-flow relationships can be used to address and understand the impacts of the catchment in the water quality of the reservoir.

Existing limitations related with the TP load estimation occur due to the utilization of simple relationships for the retention time RT and TP sedimentation rate k, as well as the reference TP load to guide the estimation process. However, the data limitation on the studied region strongly reduces the available alternatives to carry out a data comparison or validation. As previously presented, inaccuracies related with the sampling interval, analysis and data quality manipulation might impact the load estimation process and the modeled outputs.

Another limiting aspect is related with the under-representation of high flow events during the studied period with only five years of precipitation indexes above average. This way, low flow events were more representative. This might have impacted the total TP load estimated from non-point sources. Moreover, the models indicated that, despite the studied catchments being rural, point sources were more influential than non-point sources. This may be due to aspects such as the proximity of the cities to the water bodies or because the streams remained with low flow conditions. Note that a dilution pattern prevails during low flow rates.

3.4. Conclusions

This research aimed to investigate the flow-related TP input load to semiarid reservoirs and obtain phosphorus-discharge relationships pairing average inflow and TP concentration at reservoir's inlet (TP_{in}). This was reached through the application of a simple modeling approach to predict TP_{in} from hydrological data and water quality measurements inside the reservoir. This model was particularly designed to support the issue of phosphorus pollution in semiarid data-scarce regions of intermittent rivers where artificial water supply reservoirs prevail as the most important water body.

The TP load produced in the catchments and delivered to the reservoirs was estimated throughout the application of a mass balance model. The modeled loads were considered satisfactory with only 10% of underestimated results in comparison to the reference TP load and a correlation between modeled and reference load with $R^2 = 0.74$. The estimated TP input loads per unit area of the rural catchments ranged from about 4 to 40 kg km^{-2} yr^{-1}, which were significantly lower than the national average of about 500 kg km^{-2} yr^{-1}. This was attributed to lower precipitation indexes and the intermittent regime of the rivers, which potentially reduce TP runoff. Additionally, the high-density reservoir network promotes TP retention in the thousands of small reservoirs distributed over the catchments. On the other hand, the average TP input load per unit area of a urban catchment was significantly higher (2,626 kg km^{-2} yr^{-1}), which was a result of its relatively small area, higher precipitation indexes and low sanitation coverage.

The existing among-catchment variation of TP flux was mainly due to differentiated activities' intensity carried out in each basin. In general, a predominance of NPS over PS was observed in sixteen of the twenty catchments. The main non-point source of TP load were animal manure, agricultural production and natural soil erosion, whereas point source loads went from fish farming and sewer. With regards to TP_{in} estimation, remarkably high values

were obtained, especially during low flow periods. This aspect suggests that PS pollution was more significant during the period, even when the catchments markedly presented rainfall related pollution dominance.

The TP-discharge models were realistic, with modeled TP_{in} concentration versus average daily discharge showing acceptable Nash–Sutcliffe coefficients. For the Castanhão reservoir, the concentrations resulting from the application of the model compared with measured riverine concentration achieved an NSE of 0.63. The predominance of NPS over PS of phosphorus supply in a great majority of the catchments was markedly reflected in three TP-discharge relations, with a strong u-shaped form behavior. For the others, only a slight NPS signal was observed prevailing a dilution pattern. Additionally, peak values in TP_{in} concentration sensitively affected the fitting of the models.

Regarding to the parameters of the model, the comparison between the ones obtained in this study with those from others researches highlighted the quality of the adjusted curves. Similar characteristics related to the range of the values of the four fitting parameters A, B, C and D were observed. The empirically-fitted models, once calibrated to the local data, have presented themselves as a feasible tool to analyze the phosphorus supply from the catchment to the reservoirs. It is expected that the simple methodology presented in this paper will help understand the TP issue in arid/semiarid regions and assist integrated water quality management actions in strategic water supply reservoirs.

CHAPTER 4

Assessment of internal phosphorus loading and driving factors in the dry period of Brazilian semiarid reservoirs[3]

4.1. Introduction

Understanding the role of sediment-water interactions and nutrient release from the sediment in reservoirs is a necessary step to assess important limnological processes (Wang et al., 2021). According to the history of phosphorus (P) pollution in a waterbody, the impact of the internal load can vary from nearly irrelevant to higher than the external inputs on an annual P budget (Orihe et al., 2017). The effect of the internal phosphorus loading can last for several years after significant reductions in external inputs delaying the recovery of waterbodies from poor water quality conditions (Katsev, 2017). Furthermore, even small release rates may cause significant disturbances in water column total phosphorus concentration (TP_w) (Horppila et al., 2017; Moura et al., 2020).

The internal P loading can be described as two different fluxes from sediment: a net internal loading rate and a gross phosphorus flux (Nürnberg et al., 2012). The net rate of P release is estimated through modeling, commonly by a whole-lake mass balance, representing the balance, on an annual or seasonal basis, between upward and downward flux of P from the water column (Barbosa et al., 2019). Contrastingly, the gross rates are the P rates directly released from sediment, which are usually measured from sediment incubation experiment (Orihe et al., 2017). As positive net rates are obtained, internal load is likely contributing to TP_w (Nikolai and Dzialowski, 2014).

The continuous accumulation and releasing of P from sediment results from several physical and biogeochemical mechanisms (Li et al., 2013; Katsev and Dittrich, 2013; North et al., 2015; Cavalcante et al., 2018; Tammeorg et al., 2020). More importantly, the relevance of the mechanisms driving internal P loading relies mainly on the time scale evaluated (Katsev et al., 2006; Markovic et al., 2019). To determine net retention or release rates on an annual or seasonal basis, short-term P fluxes from sediment may not be so relevant (Orihe et al., 2017). In that perspective, physical and environmental drivers are suitable to correlate and explain internal P loading in a long-term budget (Wang et al., 2015; Huang et al., 2021). They may also

[3] The content of this chapter has been published in Journal of Environmental Management (https://doi.org/10.1016/j.jenvman.2022.114983)

act as indicator surrogates more easily measurable to facilitate management goals (Hunter et al., 2016).

Physical aspects such as wind disturbance, inflow-outflow relationship, lake morphometry, mixing degree, light and water/ambient temperature strongly influence P dynamics (Håkanson,l 2005; Matisoff and Carson, 2014; Zhang et al., 2016; Lun et al., 2018; Huo et al., 2019). Additionally, data on climate and reservoir morphometry are strong predictors for P release and usually easier to access in comparison with sediment data (Zhang et al., 2017; Zhang et al., 2020). The trophic state is another determining factor in sediment P release (Liu et al., 2018; Nürnberg et al., 2019). Hypereutrophic water bodies are more susceptible to present higher release rates than eutrophic or mesotrophic ones (Kowalczewska-Madura et al., 2015, 2019; Ostrofsky and Marbach, 2019). This is especially impactful in semiarid regions where eutrophication is a serious issue in drinking water reservoirs (Wiegand et al., 2021). Factors such as prolonged drought periods, irregular precipitation cycle and high evaporation rates incur great water losses and water level fluctuation (Santos et al., 2016a). Consequently, the reservoirs become shallower, eutrophic and vulnerable to internal loading effects (Freire et al., 2009; Coppens et al., 2016; Lira et al., 2020; Cavalcante, 2021).

The internal loading quantification in artificial reservoirs is a relatively new subject, less addressed than in natural lakes, especially in semiarid regions (Rocha and Lima Neto, 2021a; Lima Neto et al., 2022). However, in dryland regions reservoirs are strategic waterbodies which highlights the importance of these quantification in such environments (Noori et al., 2018; 2021a). Furthermore, lakes and reservoirs are inherently different regarding, among other aspects, the hydraulic residence time, the susceptibility to faster regime shifts, productivity level, anthropogenic usage in catchment and water level fluctuation (Noori et al., 2021b). The practice of aquaculture in reservoirs with fish-farming byproducts entering the limnetic environment is also an additional source upon the P budget (Johansson and Nordvarg, 2002; Santos et al., 2017). Combined, these factors differentiate the internal P loading estimation in reservoirs. Particularly in the Brazilian semiarid, over the past century a high-density reservoir network (one per about 5 km²) has been built to provide human supply (Lima Neto et al., 2011). Then, allied with the aforementioned conditions, the water quality management of these reservoirs has become a major challenge.

Despite the internal loading relevance in these environments, efforts towards its quantification is still incipient, especially under sediment data scarcity (Nurnberg, 2009). Furthermore, as a detailed measurement of P exchanges in sediment-water interface (SWI) is very time and cost demanding and still a punctual representation of the phenomenon, an overall

assessment of P release may be suitable as a first attempt of quantification. Then, to achieve a broader comprehension of the phenomenon in larger timescales, one may apply an approach that requires as few fitting parameters as possible (Katsev, 2017 ; Xu et al., 2020). Additionally, under resource constraints in monitoring the development of expeditious predictive models for sediment P release may assist with valuable support decision tools. The use of surrogates instead of *in situ* measurements is often necessary to achieve a cost-effective yet useful way to assess ecosystem responses and key ecological processes (Lindenmayer et al., 2015).

This research aimed to quantify the internal phosphorus load produced during the dry period and identify the most influencing factors on this loading in water supply reservoirs of the Brazilian semiarid. Specifically, the goals were: (i) estimate gross release rates from sediment data and water quality parameters through regression approaches, (ii) estimate averaged net release rates from mass balance, (iii) statistically connect the net rates with single factors (P external fluxes, physical and environmental drivers, trophic state index) and coupling factors (mean lake level fluctuation and wind speed/volume ratio) and (iv) propose a new surrogate indicator to predict TP release rates. This work innovates in evaluating the internal P loading potential of semiarid reservoirs under data constraints while elucidating relevant driving factors affecting P release in dryland regions.

4.2. Methodology

4.2.1 Site description and reservoir selection

Thirty reservoirs located in the State of Ceará, Brazilian semiarid, were selected to carry this study. The selection considered, firstly, the strategic importance of the reservoirs into the network that supplies water for human, industrial, and agricultural uses in the state. Secondly, if the reservoir is under the continuous monitoring program of water quality, quantity, and catchment characterization of the Water Management Company of the State of Ceará (COGERH). The selection also covered morphologically different water bodies scattered over the state (Figure 4.1) and captured a trophic-state gradient representative of the region as detailed in Table 4.1 with additional information in Table A3. While most of the reservoirs are eutrophic ecosystems, copping measures to recover water quality are still incipient. Regarding water uses, priority is given to human supply and aquaculture. Concerning water-depth, Table 4.1 presents the maximum average depth ($\overline{H_{max}}$) measured at the dam of the reservoir during the dry period over the years 2010-2020. Ten reservoirs presented $\overline{H_{max}} \leq 10$m and seven showed

10m<$\overline{H_{max}}$≤12m. During the driest years (2013-2016) (See Figure A6) the reservoirs became even shallower with seventeen presenting a $\overline{H_{max}}$<10m (Table A3).

Due to the semiarid climate and the susceptibility to droughts, the water level, surface area, and water storage varies significantly. According to the Köppen classification, 90% of the State of Ceará is under a dry, hot semiarid climate with annual average temperature between 23º and 28 °C (Wiegand et al., 2021) and annual average evaporation rates of about 2 m yr^{-1} (Brazil, 2021). Summarizing important climatic aspects, semiarid reservoirs are under a high and relatively constant incidence of solar radiation, small seasonal variations in water temperature, wind influence and greater temperature variability occurring in a 24-hour period (Souza Filho et al., 2006; Meireles et al., 2007; Dantas et al., 2011; Lemos, 2018; Lima Neto, 2019). Then, regarding the mixing regime, this aspects suggest that the study sites can be considered mostly polymictic reservoirs with a diurnal mixing cycle (up to 5 ºC from bottom to top).

Figure 4.1 - Study sites and meteorological forcings in the State of Ceará, Brazil

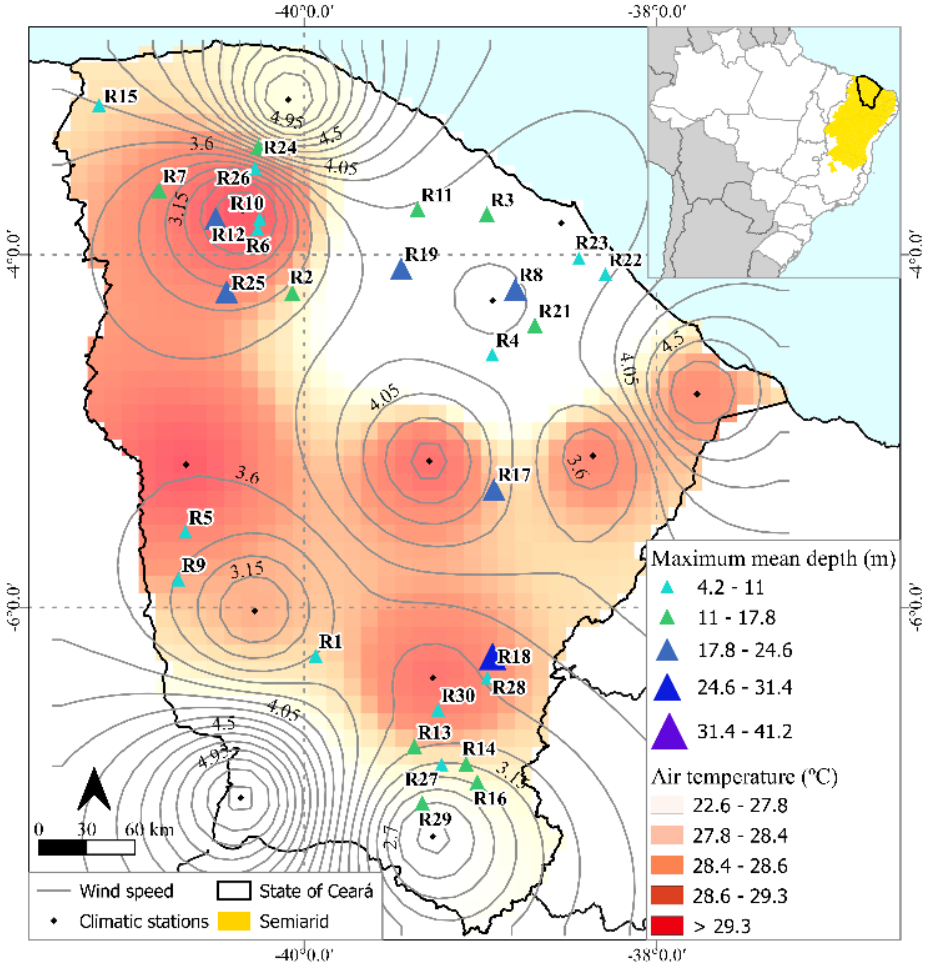

Table 4.4 - Physical characterization of the reservoirs and water quality conditions

ID	Water surface area (km^2)[a]	Maximum mean depth (m)[a]	Reservoir age[b]	Miminum surface TP concentration ($mg\ L^{-1}$)[a]	Average surface TP concentration ($mg\ L^{-1}$)[a]	Maximum surface TP concentration ($mg\ L^{-1}$)[a]	Representative trophic state[c]
R1	1.5	8.9	55	0.010	0.124	0.417	Eutrophic
R2	13.8	17.5	34	0.010	0.081	0.145	Eutrophic
R3	15.6	10.2	22	0.033	0.158	0.453	Eutrophic
R4	1.7	7.3	24	0.044	0.154	0.442	Eutrophic
R5	5.0	6.4	22	0.026	0.175	0.574	Eutrophic
R6	2.3	9.4	29	0.022	0.059	0.107	Oligotrophic
R7	7.3	12.1	23	0.015	0.051	0.194	Eutrophic
R8	1.6	18.3	97	0.010	0.111	0.285	Eutrophic
R9	1.0	7.1	23	0.044	0.120	0.599	Eutrophic
R10	4.9	9.1	94	0.021	0.092	0.347	Eutrophic
R11	8.5	12.0	59	0.032	0.075	0.206	Eutrophic
R12	7.8	19.6	85	0.037	0.079	0.142	Eutrophic
R13	1.3	11.7	23	0.010	0.042	0.278	Eutrophic
R14	4.9	15.1	20	0.010	0.052	0.475	Eutrophic
R15	12.6	8.0	20	0.014	0.038	0.089	Eutrophic
R16	2.6	14.5	21	0.010	0.041	0.118	Mesotrophic
R17	37.2	29.3	55	0.046	0.122	0.280	Eutrophic
R18	79.8	28.4	60	0.010	0.080	0.142	Eutrophic
R19	10.3	18.3	86	0.010	0.109	0.473	Mesotrophic
R20	162.5	41.2	18	0.015	0.103	0.219	Eutrophic
R21	7.5	17.1	18	0.026	0.056	0.112	Eutrophic
R22	4.0	10.8	18	0.027	0.179	0.364	Eutrophic
R23	2.6	7.9	19	0.040	0.169	0.431	Eutrophic
R24	1.2	11.7	98	0.023	0.044	0.072	Eutrophic
R25	20.1	24.2	63	0.025	0.091	0.183	Eutrophic
R26	4.7	10.2	114	0.015	0.045	0.073	Oligotrophic
R27	0.3	4.2	63	0.020	0.101	0.354	Eutrophic
R28	6.7	7.7	97	0.031	0.100	0.208	Eutrophic
R29	1.0	19.6	36	0.014	0.058	0.230	Mesotrophic
R30	3.4	10.3	22	0.023	0.058	0.104	Eutrophic

[a] From measurements taken during the dry period (01/jul – 31/dez) in the study period (2008-2020)

[b] From the year of conclusion of the construction to 2021

[c] Calculated from how many times the TSI was attributed to the reservoir over the total number of TSI classifications in the study period (2008-2020). For each field campaign carried out by COGERH a TSI is attributed to the reservoirs.

4.2.2 Data sources

COGERH provided the datasets of TP_w, water temperature (T), pH and dissolved oxygen (DO). The data was quarterly collected from in situ measurement using a multiparametric probe, previously calibrated with respective standard solutions, covering the ranges of values ordinarily recorded in the reservoirs. The laboratory analysis followed APHA (2005). During the dry period, the sampling frequency is usually in July/August and November/December and the sampling point is located near the reservoir's dam. Datasets on chlorophyll-a concentration (Chl-a) and Secchi depth (z_{secchi}) were also provided. Additional

water surface data at 0.3 m deep of phosphorus ($TP_{surface}$), Chl-a and z_{secchi} was publicly available in Ceará (2021). A data consistency was performed to identify possible sampling errors. Data in other depths to provide a vertical profile of TP in the water column, however, was less frequent in the last four years and the available data have not achieved the deepest layers for most reservoirs. Despite limitations, the dataset of TP concentration in other depths provided important information on the temporal variability of vertical TP concentration. Additionally, it supported the calculation of TP_w whenever possible.

Sediment measurements were performed in 2016 in the reservoirs R20 to R30 and were available in the environmental inventory of each one (Ceará, 2021). Total phosphorus (TPs), ion (Fe_s) and aluminium (Al_s) concentrations in the sediment were quantified. A detailed speciation of the P fractions was not available for the study sites. However, previous work in the study area and in other regions world-wide support the quantification of the internal loading as a mass of total phosphorus (Nürnberg 2009, 2012, 2013; Rocha and Lima Neto, 2021a). Furthermore, although sediment measurement data were not performed in the remaining reservoirs, all reservoirs have a detailed quantification of the external TP load produced by their catchments, which was also used for model validation. The TP load contribution from the catchment is detailed in the supplementary material (Table A3 and Figure A8).

The dataset of the trophic state index (TSI) of the reservoirs was also available in Ceará (2021). TSI was calculated from TP_w, z_{secchi} and Chl-a through the method proposed by Toledo et al. (1983). This method has been adapted considering specific characteristic of tropical systems, such as the low water transparency due to the high mineral turbidity (Lima Neto et al., 2011; Klippel et al., 2020). The datasets comprised the period of 2008 to 2020. Data related with reservoir morphometry and operation (volume, water level, surface area and released flow) were obtained from Ceará (2021). The climatic characterization was performed from twelve climatological stations scattered across the study area (see Figure 4.1). The climatic variables were obtained from the nearest station of each reservoir. The dataset covers a thirty-years monitoring period (1981-2010) of the National Meteorological Institute to settle representative monthly averages to each station. The wind intensity was measured by an anemometer at 10 m high (Brazil, 2021).

4.2.3 Internal load modeling

4.2.3.1 Assumption for fish contribution

Fish farm emissions may be accepted as a fast-sinking particulate fraction which in a short-term mass balance is momentarily transported to the sediment (Johansson and Nordvarg, 2002). However, in a long-term perspective, the origin of the P released fraction might be difficult to track, especially the undercage release (Kelly, 1993). In this study, nine reservoirs with aquaculture practice were incorporated among the study sites. This was necessary in order to not exclude of the study the largest and more strategic reservoirs of the state (R18 and R20) (Ceará, 2018). Based on this criteria, reservoirs R18, R20 and the remaining medium-sized and small reservoirs with such practice were considered. Furthermore, the study of reservoirs through an approach that separate the load of the aquaculture from the seasonal budget is an alternative. On the contrary, the study of the internal P loading in such waterbodies would be neglected in face of the difficulty to address the aquaculture contribution.

To quantify the TP load from aquaculture was necessary to separate fish contribution. This quantification involved the delimitation of the area of fish cages, farming productivity, P concentration in the fish feed and the coefficients related with feed conversion and apparent digestibility. Detailed information on the P load from aquaculture and the estimation process is presented in Ceará (2021). Then, to perform the P budget in this study, the fish contribution was assumed to be constant over the years, equal to the field estimate reported by COGERH and was deducted from the modeled P load following the methodology proposed by Nürnberg et al. (2012). Although this estimate may not precisely relate to specific years, it attempted to remove the average fish contribution from the seasonal balance when performing the budget (Nürnberg et al., 2012).

4.2.3.2 Phosphorus budget for net internal load

The dry period of the Brazilian Northeast is characterized from mid-June to December, covers the seasons Winter and Spring and has negligible precipitation indexes (Costa et al., 2020). Therefore, irrelevant rainfall-related inflow to the reservoirs is expected. Furthermore, due to the shallow soils over crystalline rocks, base flow is also negligible, and the rivers are intermittent (Ceará, 2011). Under these conditions it is possible to quantify with less interference possible the actual internal load. Equation (4.1) presents the one-box mass balance model proposed by Vollenweider (1968) applied to estimate the average net P loading from TP_w. As the elapsed time between TP measurements covers the dry period, the modeled load is

assumed to represent the averaged net internal TP load produced over this period. The average TP_w was used whenever available hypolimnetic water samples. When not, the surface concentration was used assuming a complete-mixed behavior (Rocha and Lima Neto, 2021a). Results to support this hypothesis are presented and discussed in results section.

$$TP_w(t) = TP_{w,o} e^{-\left(\frac{Q_s}{V}+k\right) t} + \frac{W}{Q_s + kV}\left[1 - e^{-\left(\frac{Q_s}{V}+k\right) t}\right] \quad (4.1)$$

Where $TP_w(t)$: TP concentration at the reservoir outlet at a given time (kg m^{-3}); $TP_{w,o}$: Initial TP concentration (kg m^{-3}); t: Elapsed time (month); V: Average reservoir volume (m^3); L: TP load (kg $month^{-1}$); Q_s: Released flow (m^3 $month^{-1}$); RT: Theoretical hydraulic residence time ($month^{-1}$).

The settling loss rate ($\frac{4}{\sqrt{TR}}$) is an empirical model validated for semiarid reservoirs (Lima, 2016; Araújo et al., 2019; Toné and Lima Neto, 2019; Rocha and Lima Neto, 2021b; Lima Neto et al., 2022). Regarding RT, it was calculated as presented in Equation (4.2) as an adaptation for the study region. Since there is virtually no inflow during the dry period and, in most years nor outflow, it was not possible to apply traditional equations. Then, the inflow was replaced by the sum of the released and evaporated rates to keep RT with a coherent order of magnitude (Rocha and Lima Neto, 2021a).

$$RT = \frac{V}{Q_s + E} \quad (4.2)$$

Ultimately, the net areal P loading (L_net) was calculated by the ratio $L.A^{-1}$, where A is the mean lake surface area of the period. As the unit representation for this estimate varies widely in the literature depending on the study period (mg m^{-2} $summer^{-1}$, mg m^2 $season^{-1}$, mg m^{-2} $Aug\text{-}Sep^{-1}$, mg m^{-2} yr^{-1}) (Nürnberg et. al, 2019), in this work a new unit representation (mg m^{-2} dry $period^{-1}$) was adopted to accurately describe the particularity of tropical semiarid regions.

4.2.3.3 Gross sediment fluxes and active sediment release factor

The gross internal P loading (L_gross) in shallow lakes may be estimated from the product of the gross fluxes of P release (RR in mg m^{-2} day^{-1}) by the actively releasing area of the sediment modeled as the anoxic factor (AF in day per dry period) (Nürnberg, 2005). In this work, the definition of anoxia (DO < 2 mg L^{-1}) and hypoxia (3-5 mg L^{-1} DO) follows Nürnberg

(2019b). L_gross was estimated for the dry season of the years in the study period in which there was available data. To obtain RR, the literature provides several predictive models validated in different regions world-wide. They apply different variables, such as sediment TP concentration (TP_s), reductant-soluble P fractions or lake water quality data. For this work, as TP_s was available for 37% of the reservoirs, four different models were tested to estimate RR: Equations (4.3) (Nürnberg et al., 1986), (4.4) (Cheng et al., 2020), (4.5) (Carter and Dzialowski, 2012), (4.6) (Moura et. al, 2020) and (4.7) (Chapra and Canale, 1991; Lira et al., 2020). Equation (4.7) requires TP_s while the remaining methods attempted to correlate RR with water quality data or other physical parameters directly obtained from the study sites. Assuming that Equation (4.7) results the most accurate estimates since it applies sediment data, RR_5 was correlated with the other models to validate and obtain the estimates for R20-R30. Then, the model with the best correlation was applied to calculate L_gross for all reservoirs.

$$RR_1 = 12.116 \cdot \log(TP_w) - 9.708 \quad (4.3)$$

$$RR_2 = 10^{[-0.54 + 0.827 \cdot \log(TP_{surface})]} \quad (4.4)$$

$$RR_3 = 0.3332 \cdot Age \quad (4.5)$$

$$RR_4 = 1.0482 \cdot RR1 \cdot \exp[0.099 \cdot (T - 20)] \quad (4.6)$$

$$RR_5 = vr \cdot \rho s \cdot TPs \quad (4.7)$$

Where RR_i: TP release rate (mg m^{-2} day^{-1}); ρ_s: Dry-bulk density (kg m^{-3}); v_r: coefficient of phosphorus recycled mass-transfer from sediments to the water (m $month^{-1}$); Age: Reservoir age (yr); T: Water temperature (ºC).

Eq. (4.6) was applied combined with Equation (4.3) as it was developed for temperate lakes. Equation (4.6) was developed experimentally considering flowing overlying water with low velocity plus static sediments. It also considers a correction of RR from estimates at 20 ºC to any arbitrary temperature, which is a relevant aspect as Brazilian water bodies have higher water temperatures (~30 ◦C). For the model presented in Equation (4.4), although it was also developed for temperate lakes, it requires only measured surface TP data, which is largely available in the study sites and turns it the most practical model to apply. Equation (4.5) express a novel approach designed with data of semiarid reservoirs to estimate RR from reservoir age. Correlations between P release rate and lake/reservoir age are widely known (Shinohara et al., 2017; Cavalcante et al., 2018). In Equation (4.7) the parameter v_r applied was calibrated by Lira et al., (2020) (v_r = 0.00097 m $month^{-1}$) to a reservoir located in the study region. This value was also very close to the that reported by Chapra and Canale (1991) (v_r = 0.00096 m $month^{-1}$).

Assuming that Eq. (4.6) results the most accurate estimates since is applied sediment data, the Pearson correlation coefficient (r^2), the Mean absolute percental error (MAPE) between the medians, and the relative index of agreement (r_d) were evaluated to validate the release rates. The relative index of agreement was developed by Willmort (1981) to overcome the insensitivity of correlation-based measures. The r_d was calculated as presented in Eq. (4.8) for each method described from Eq. (4.3) to Eq. (4.7) considering RR_5 and the median of the respective method for the reservoirs R20-R30. These reservoirs were considered as there was available measured sediment data. Then, the model with the best metrics was applied to calculate L_gross for all reservoirs.

$$r_{d,j} = 1 - \frac{\sum_{i=1}^{11} \left(\frac{RR_{5,i} - RR_{j,i}}{RR_{5,i}} \right)^2}{\sum_{i=1}^{11} \left(\frac{\left| RR_{j,i} - \overline{RR_5} \right| + \left| RR_{5,i} - \overline{RR_5} \right|}{\overline{RR_5}} \right)^2} \quad (4.8)$$

Where $r_{d,j}$: Relative index of agreement of the method j; $RR_{5,i}$: TP release rate of the i^{th} reservoir estimated by Eq. (4.7) (mg m^{-2} day^{-1}); $RR_{j,i}$: TP release rate of the i^{th} reservoir estimated by the method j (mg m^{-2} day^{-1}); $\overline{RR_5}$: Average RR_5 estimates considering all reservoirs (R20-R30).

Equation (4.9) describes AF as proposed by Nürnberg (1995). AF is one of the several ways to quantify oxygen depletion chosen in accordance with the available data. It intends to quantify the spread and duration of anoxia or hypoxia events. It is a ratio that represents the number of days in a period that a sediment area equal to the lake or reservoir surface area is anoxic or hypoxic (Nürnberg, 2019b). It is predictable from TP_w and reservoir morphometric data considering that the actively P releasing area may not be restricted to those overlain by anoxic water, especially in polymictic lakes (Nürnberg, 2019b). The unit is commonly expressed as day per $summer^{-1}$ or day per $season^{-1}$ which was adapted here as day per $dry\ period^{-1}$. This equation has already been validated to eutrophic shallow and mixed lakes (Nürnberg, 2009) and applied to lakes world-wide including arid environments (Townsend, 1999; Kiani et al., 2020; Tammeorg et al., 2020; Lima Neto et al., 2022).

$$AF = -36.2 + 50.1 \log (TP_w) + 0.762 \times \frac{Z}{A^{0.5}} \quad (4.9)$$

Where TP_w: Average concentration in the water column during the period (μg L^{-1}); Z: Lake mean depth (m); A: Lake surface area (km^2).

4.2.4 Driving factors on P release rates

4.2.4.1 Surrogates for climatic factors

The variables wind speed, insolation and air temperature were selected as surrogates for climatic factors that potentially influence the internal loading. The paired dataset encompassing all reservoirs of RR and the respective average climatic variable calculated for the same period of the RR estimate was divided in subsets according to three ranges predefined for each variable. Then, to assess significant differences in RR depending on the ranges of the environmental variables, pairwise statistical analyses were performed by the Kruskal-Wallis (K-W) and Mann-Whitney (M-W) tests considering a significance level $\alpha = 0.05$ (Cleophas and Zwinderman, 2016). The null hypothesis considers RR independent of the magnitude of the environmental variable. Additionally, box plots were presented with the adopted thresholds beyond which RR might be significantly affected.

4.2.4.2 Trophic state and lake level influence

Analyzing the influence of the trophic state followed similar approach of the climatic surrogates aforementioned. To test for differences in P release rates among trophic states, the grouped datasets encompassing the release rates of all reservoirs by trophic state type were statistically analyzed with the K-W and M-W tests. The unequal length of observations within each subset favored the application of this non-parametric tests. The statistical tests were also performed for each reservoir. However, as the reservoirs remained with one trophy level for most part of the study period (see Table 4.1), they presented short subsets for the non-representative trophic state type which turns the results on the single reservoir level less reliable. An algorithm in Python language was designed in order to test each group against all the other groups. Then, post-hoc tests were not necessary.

The behavior of P release rate over time and its relationship with the level variation was additionally evaluated. The fluctuation in the reservoir's level intends to evaluate the long-term interannual stability of a system, the average strength of the seasonal fluctuation and may also serve as a proxy for bottom-up driven processes (Kolding and van Zwieten, 2012). Then, the ratio between the daily lake level and half of the maximum depth of the respective dry period of each year was calculated. This indicator range from 0 to 2 and visually helped to evaluate the reservoirs drying up and this impact on P release.

4.2.5 Predictive model for internal P loading

Previous studies have attempted to use several lake morphometric characteristics combined as predictors for internal P loading (Tammeorg et al., 2017, 2020). Others have already applied combinations of morphometric and environmental characteristics, such as the ratio of wind speed to lake depth (Håkanson, 2005; Zhang et al., 2017; Jalil et al., 2019; Huang et al., 2021). In this study, the P release rate was logarithmically correlated with the wind speed to reservoir volume ratio for each lake. The ratio of wind speed to mean reservoir volume was adopted here as a suitable surrogate. Firstly, because the effect of wind-induced shear stress to enhance the advection-diffusion transport of chemicals across SWI is considered. Secondly, this surrogate considers the influence of the volume in the stability, productivity and increasing in nutrient concentration of the reservoir (Gownaris et al., 2018). The coupling of these variables turns into a potential indicator to explain the release process (Hunter et al., 2016). For each statistical model adjusted, the goodness of fit was evaluated through the metrics coefficient of determination (r^2), adjusted coefficient of determination (r_a^2) and the Mean Absolute Percentual Error (MAPE). Additionally, the analysis of the homoscedasticity of the model residuals was performed graphically assessing whether the residuals fit linear, quadratic, or exponential curves.

4.2.6 Uncertainty and sensitivity analysis and model validation

Data accuracy and outlier analysis were performed followed by removal of non-specific values below the detection limit (TP < 0.01 mg L^{-1}). Additionally, a sensitivity analysis to identify the impact of the modeling most influencing parameters was performed as descripted by Rocha and Lima Neto (2021a). It was verified that the volume and the difference in TP_w between the elapsed time in the modeling interval ($TP_{w,t}/TP_{w,0}$ ratio) more strongly influence the results. Then, an analysis on these parameters was performed in light of the threshold reported by the above-mentioned authors. The coefficient of variation of the estimated loads was calculated and compared with others reported in literature to assess the model variability. Moreover, since the complete mix hypothesis is commonly accepted for the reservoirs in the study region as already presented (Lima Neto et al., 2022), eventual statistically significant differences between $TP_{surface}$ and those measured in other depths was evaluated for each reservoir by K-W and M-W tests (α = 0.05). Finally, considering the available data, the best way found to validate the P release estimates was by comparing the results of the method assumed to be more reliable, whose rates were obtained from measured sediment data (RR_5),

with the estimates of the remaining models. The Pearson correlation coefficient and the bias between the estimates was calculated for the reservoirs R21 to R30.

4.2.6.1 Comparison with gross external P loading

The study sites present an environmental inventory elaborated by COGERH, which estimated the gross external TP load according to the Export Coefficient Modeling (ECM) approach (Ceará, 2020). It accounted for the main external TP sources (agriculture, livestock, soil, sewer and aquaculture) in an annual timestep (t yr^{-1}). Therefore, in order to assess and reinforce the order of magnitude of the estimated internal P loads, they were compared with the external load excluding fish contribution (L_ext). To keep consistency between units, gross, net and external loads were converted to a monthly average (t $month^{-1}$).

4.3. Results and discussion

4.3.1 Water quality characterization

4.3.1.1 TP and DO variation among and within reservoirs

Filled contour plots with polynomial smoothing based on TP and DO concentration profiles indicate the mixing status regarding these nutrients in the study sites from 2009 to 2019 (Figure 4.2). The hatched area limits anoxic waters. The definition of anoxia (DO < 2 mg L^{-1}) and hypoxia (3-5 mg L^{-1} DO) follows Nürnberg (2019b). The reservoirs in Figure 4.2 were selected as they cover from the shallowest to the deepest ones. However, the profiles for all reservoirs along with pH and water temperature plots are available in the appendix (Figures A2 to A5). For most reservoirs, increasing TP_w has been noted during the driest years (2013-2016). (Jepson et al., 2021). As expected, water quality rapidly deteriorates under drought events (Cavalcante et al., 2021; Zou et al., 2020). At the end of 2016, eighteen reservoirs were below 10% of the maximum capacity and twenty-four below 20%.

The variation in TP_w among reservoirs is remarkable. R15 presented the lowest average concentrations (0.02-0.09 mg L^{-1}) while R9 presented the highest ones (0.06-0.90 mg L^{-1}). Accordingly, R15 presented the highest DO values while R9 presented the lowest ones. In average, the concentration considering all reservoirs was about 0.11 mg L^{-1} (± 0.12) which is within the ranges reported in literature for eutrophic ecosystems. Huo et. al (2019) found a limiting TP concentration as a threaten criterion for Chinese lakes as 0.021 mg L^{-1}, which is about 6-fold lower than the observed values in the study sites. Uncommonly high TP

concentrations (> 4 mg L^{-1}) were excluded as probable measurement errors considering that the TP concentration in sewer is about 4 mg L^{-1} (Sperling, 2007). Eventual peak values (1 – 4 mg L^{-1}) were observed in R20 in 2016, when the reservoir was with a very low volume, and in reservoirs R9, R11, R18, R19 in 2009-2010, which was after the last strong rainy season of the past twelve years (Jepson et al., 2021). As influencing factors in the inter-reservoir variation may be highlighted the size and form (Håkanson, 2005), variable water retention time (Chaves et al., 2013), evaporation rates, volume variation and drought response (Coppens et al., 2016), inflow and input load during the prior wet period (Rattan et al., 2017), aquaculture practice (Gurgel-Lourenço et al., 2015) and climatic forcings (Zhang et al., 2020).

A marked interaction between surface and bottom TP concentration was observed in reservoirs R17 and R18. R18 presented high concentrations in the deeper layers from 2016 that lasted and increased while the water-depth reduced. This high concentration also spread to upper layers (See Figure 4.2). Accordingly, DO concentration decreased from 2016 remaining under 2 mg L^{-1} from then on. In 2019 anoxic conditions (DO < 2 mg L^{-1}) were observed even in the surface layers. High TP concentration in deep layers under anoxic conditions is a strong indicator of internal loading effect (Lopes et al., 2014; Andrade et al., 2020). Internal P loading may account for about 54% in TP_w increase (Ding et al., 2018). Studies suggest that deep-water hypoxia frequently develops in SWI of eutrophic ecosystems and is accelerated in warmer climates (Fukushima et al., 2017). Furthermore, the deeper layers may remain anoxic favoring P release even after the reservoir began to mix (Nikolai and Dzialowski, 2014). During the pre-drought years, high water depth may act as a protective mechanism trapping P in deep layers (Kowalczewska-Madura et al., 2019b). However, as the reservoir became shallower, short-term changes may also be influenced by wind shear and wave action potentially contributing to this P increase (Lepori and Roberts, 2017).

The behavior observed in R20 with simultaneously high concentrations in surface and deep layers with a transition zone between these layers may be influenced by factors such as aquaculture presence and anoxic/hypoxic events which widely occurred in the study period (See Figure 4.2). Moreover, this reservoir has a strong fish farming production which might have contributed to sediment enrichment, high concentrations in the upper layers, and, combined with the water velocity, the dispersion of related pollutants in a broader area around fishcages (Molisani et al., 2015; Lacerda et al., 2018). Additionally, the results reported by Molisani et al. (2015) highlighted that the external sources still induce worst water quality conditions than aquaculture. In fact, the L_ext of this reservoir is about 600 t yr^{-1} (Ceará, 2021).

Reservoirs R9 and R15 presented a markedly mixed vertical profile of TP concentration, mainly during 2012-2015. The worst condition was observed in R9, the shallowest reservoir, with average TP_w around 0.52 mg L^{-1} (± 0.25). Shallow waterbodies and also the littoral zone of deeper lakes are more susceptible to wind-induced water column mixing and increasing nutrient concentration driven by resuspension (Cyr et al., 2009). Furthermore, as low DO concentration was observed, despite the low depth, not only physical releasing processes might have occurred. Even in shallow reservoirs under aerobic conditions (R15), significant amounts of P may be released driven by turbulence. The turbulence induces mixing and an increase in the in-lake flow velocity, which may cause a gradient of phosphate concentration at the SWI increasing P release (Kowalczewska-Madura et al., 2019b). Additionally, warmer SWI adequately oxygenated might favor microbially-mediated mineralization of organic P (Nicholls, 1999).

Regarding the vertical pattern and mixing status of the TP concentration and its variation over the study period (See Figure 4.2 and Figure A2), one can first highlight the impact of depth on the differentiation between concentrations in the deeper and surface layers. Only by evaluating these figures, it can be observed that the reservoirs with a depth less than 20 m showed similar concentrations throughout the vertical profile during the study period. The result of the statistical tests performed between TP measurements in the surface and in other depths revealed no significant differences in 70% of the reservoirs at a 95% confidence level. Part of the reservoirs with significant differences were also those with a more unbalanced dataset towards surface measurements, which might have biased the results.

However, in reservoirs with depths greater than 20 m (R8, 11, 17, 18 and 20), the greater depth combined with a low DO concentration (See Figure A3) potentially favored events of phosphorus release from the sediment. Meantime, due to the depth, the high concentrations remained in the deeper layers. When these reservoirs became shallower (See R17, 18, 20 in Figure 4.2), these high concentrations at the bottom spread to the entire water column, highlighting an intense mixing process at lower depths. Overall, the mixing pattern observed in the study sites may be driven by several factors such as the increasing wind forcing effect and the temperature impact on DO concentration as the reservoirs become shallower (Santos et al., 2016; Katsev, 2017).

Figure 4.2 - Contour plots for the vertical profile of TP concentration (mg L^{-1}) and DO (mg L^{-1}) in the sampling point of the study sites over the period of available data

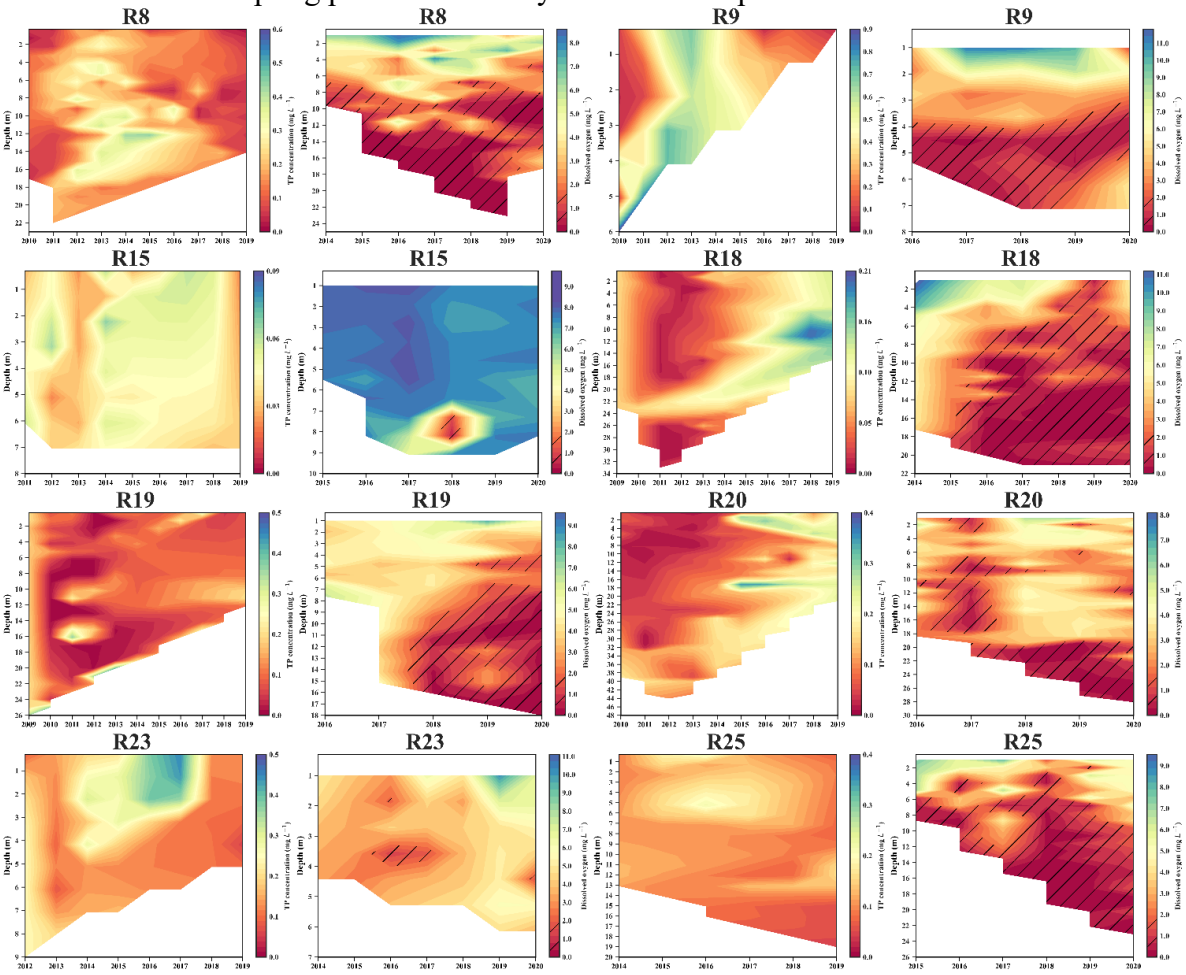

4.3.1.2 Water transparency and chlorophyll-a concentration

Figure 4.3a synthesizes the parameters Chl-a, $TP_{surface}$ and z_{secchi} for all study sites plotted against the water depth in the day of the sample collection along with the grouped data of z_{secchi} (Figure 4.3b) and Chl-a concentration (Figure 4.3c) by year. Chl-a and $TP_{surface}$ were negatively correlated with water depth as z_{secchi} was positively correlated as expected (Carneiro et al., 2014). Chl-a values reached 0.69 mg L^{-1} with average of 0.048 mg L^{-1}. For z_{secchi}, the values ranged from 0.1 to 4.20 m with average of 0.99 m. Consistently, the reservoirs with the highest z_{secchi} values were those with better water quality conditions. As for the temporal pattern, in 2009 the average z_{secchi} was about 1.5 m. This average value decreased continuously until 2014 when reached 0.5 m. From 2014 to 2016 the average z_{secchi} remained stable around 0.5 m. Then, from 2017 an increase in this average was observed reaching 1.0 m in 2020. Chl-a average values also responded over time on a similar trend as z_{secchi}, but with an inverse behavior.

These water quality surrogates presented a consistent pattern in response to the water level variation of the reservoirs over the study period, representing a continuous water quality degradation of these environments. As the reservoirs became shallower over the years, they also became particularly susceptible to wind action, resuspension of bottom sediments and reduction in water transparency, especially during the dry period (Freire et al., 2009). Accordingly, Chl-a concentration tends to increase with increasing wind speed and air temperature (Huang et al., 2021; Stefanidis et al., 2021). From analyzing the grouped dataset of TP_w by month, more frequent high measurements (0.20 – 0.40 mg L^{-1}) were observed at the end of the dry period. Similarly, peak Chl-a values were also more frequent at the end of the dry period, and, as shown in Figure3, in the years 2014-2016. In the recent literature several predictive models for internal P loading incorporated z_{secchi} and Chl-a as explanatory variables (Spears et al., 2012; Carter and Dzialowski, 2012).

Internal loading (Spears et al., 2012), increased turbidity (Zou et al., 2020) and turnover events such as algal blooms (Wang et al., 2021) are usually associated with Peak TP concentration. Additionally, in highly eutrophic ecosystems the link between TP and algal is mutually reinforced under the internal loading perspective. This loading is more bioavailable, then more influential on algal biomass. Particularly in shallow water bodies, a continuous mixing at the sediment-water interface ensures P availability for the algal growth (Tammeorg et al., 2020). In contrast, bloom-forming cyanobacteria have a high phosphorus release potential during their decline period (Wang et al., 2021).

Figure 4.3 - (a) Water-depth related patterns of the water quality indicators Chl-a, TPsurface and zsecchi* and temporal trends of (b) zsecchi and (c) Chl-a concentration over the study period.

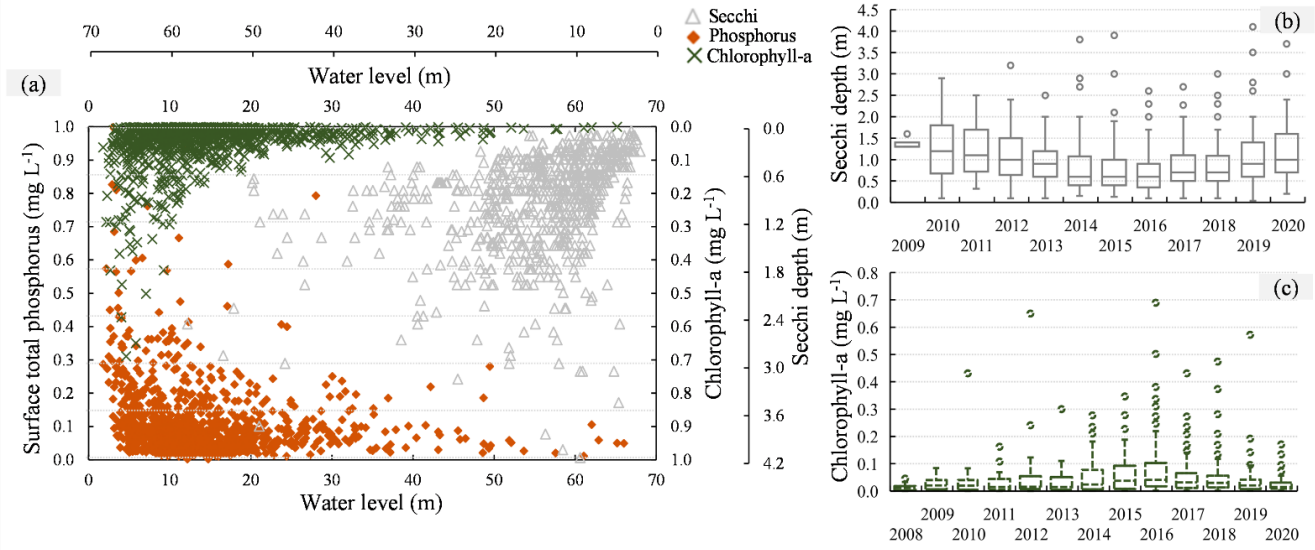

* z_{secchi} data plotted in the third floating x-axis and y-axis.

4.3.2 Phosphorus release rate and internal P load quantification

4.3.2.1 Net internal load and gross internal load estimation

The results of the daily gross release rates are presented in Figure 4.4a while net, gross and external loads averaged over the dry period are shown in Figure 4.4b. It can be firstly highlighted the variability among the models. RR_1 and RR_2 estimates resulted in similar values in median terms, though the second one was more variable. On the contrary, RR_3 presented the lowest in-lake variability and the largest among-lakes one. This is mostly due to the reservoirs' age, that varied from 6 (R21) to 113 (R26) years. As for RR_4 estimates, although they showed higher values than those previously mentioned, the highest estimates were obtained when TP_s data was applied (RR_5).

TP_s ranged from 118.25 to 3,020 mg kg^{-1} with 50^{th} percentile of 1,024 mg kg^{-1}. The highest values were observed in the older reservoirs (>900 mg kg^{-1} in reservoirs older than 58 years at the measurement date). TP_s values in other reservoirs of the Brazilian semiarid were about 600 mg kg^{-1} (Cavalcante et al., 2021) while in other regions world-wide reached 1,424 mg kg^{-1} (Kim et al., 2004; Li et al., 2013; Zhang et al., 2016). As RR_5 directly incorporated these high TP_s data (Eq. 5), high estimates were obtained accordingly. Exceptionally for R22, R23 and R25, TP_s was 2,040, 1,600 and 3,020 mg kg^{-1} which resulted in RR_5 estimates of 67, 86 and 127 mg m^{-2} day^{-1}, respectively (not shown in Figure 4.4a). Consistently, R22 and R23 have a highly urbanized catchment and showed the highest $TP_{surface}$ values (Table 4.1). Similarly, for R25 a district of about 20,000 inhabitants is located near the reservoir dam with small settlements in the margins of its main tributaries. Thus, an accumulation of the intense external P pollution is occurring in the sediments of these ecosystems.

From the correlation analysis between RR_5 and the other estimates, RR_4 best performed with an r^2 of 0.36, a r_d of 0.78 and a MAPE of 39%, which were considered satisfactory indicators (Moriasi et al., 2015). The effect of the temperature, not considered in the other models, has strongly impacted RR_4 and turned Equation (4.6) the more representative model for the region. RR_4 estimates ranged from 5.29 to 52.58 mg m^{-2} day^{-1} while the 50^{th} ranged from 17.64 to 35.99 mg m^{-2} day^{-1}. In comparison with other studies, the release rates of the study sites were higher in average. However, the range observed in the searched literature varied from 1 to 77,83 mg m^{-2} day^{-1} (Arunbabu et al., 2014) with higher estimates (>50 mg m^{-2} day^{-1}) usually found in hypereutrophic ecosystems (Nürnberg, 1988). Then, considering RR_4 representativeness for the validated reservoirs, it was applied along with AF to calculate the seasonal averages (Figure 4.4b)

The AF values reached 97.33 days dry period^{-1} with average values ranging from 40.35 to 75.71 days dry period^{-1}. The lowest values were observed in the reservoirs with better water quality conditions (R3 and R13). Other studies reported values reaching 26.6 days summer^{-1} (Nürnberg et al., 2013), 34.3 days Aug–Sep^{-1} and 60 days summer^{-1} (Nürnberg et al., 2019; 2019b) and ~70 days season^{-1} (Snortheim et al., 2017). The results suggested anoxic periods that, in some years, lasted longer than observed in other regions. Aspects such as historical anthropogenic P supply, long periods with low DO concentration allied with lake morphometry are generally associated with hypolimnetic anoxia (Nürnberg et al., 2019). Furthermore, air temperature and wind speed are additional drivers positively correlated with AF (Nürnberg et al., 2019b). It is also noteworthy the possibility of under/overestimated AF values. Overestimation occurs in shallow lakes since its sediment often exhibits narrow anoxic layers (Tammeorg et al., 2020), while underestimation occurs in deep lakes when the anoxic areas extend into shallow zones (Nürnberg et al., 2019b).

The average seasonal estimates (Figure 4.4b) varied from 0.02 to 11.35 t month^{-1} with average of 0.26. The comparison with the external load (L_ext) for reservoirs R1 to R20 showed that L_ext was over the 75th of L_net estimates in 90% of the study sites, except R10 and R12 where L_ext was over the 50th percentile. Most catchments of the study sites are majorly rural and P external sources are the main pollution sources in the annual P budget (Rocha and Lima Neto, 2021b). Specifically, R18 and R20 have the largest catchments (>24,000 km²) with livestock production, subsistence farming and relevant irrigated croplands for the state (Ceará, 2021), which support their high external TP production. Intensive cropland practice in a catchment favors sediment P accumulation in the waterbody in a long-term perspective (Carter and Dzialowski, 2012). However, the ratio between median L_int and L_ext ranged from 1% to 47% as already reported by Rocha and Lima Neto (2021a), highlighting the relevance of the internal sources to the total P budget.

Unmentioned aspects so far such as sediment heterogeneity, physical characterization and size distribution may had contributed with the high estimated rates. Smaller particles have greater specific surface area for pollutant adsorption which enhances resuspension ability (Zhu and Yang, 2018). Additionally, substantial P diffusive fluxes in the warmer season may occur under oxygenated bottom water conditions from the littoral/shallow areas of the lake (Markovic et al., 2019). The littoral sediments under aerobic conditions may contribute with more than 25% of the internal phosphorus load (Kim et al., 2003; Tammeorg et al., 2017; Kowalczewska-Madura et al., 2019). Furthermore, although there was not available P speciation data, ion (Fe_s) and aluminum (Al_s) sediment concentration were measured for R21 to R30. Though more

information on sediment chemical composition may be enlightening, it can be speculated the reservoirs' susceptibility to the release of metal-bound P, specially under alkali-anoxic conditions (Cavalcante et al., 2021).

Figure 4.4 - (a) Daily phosphorus gross fluxes and (b) seasonal average net, gross and external TP load

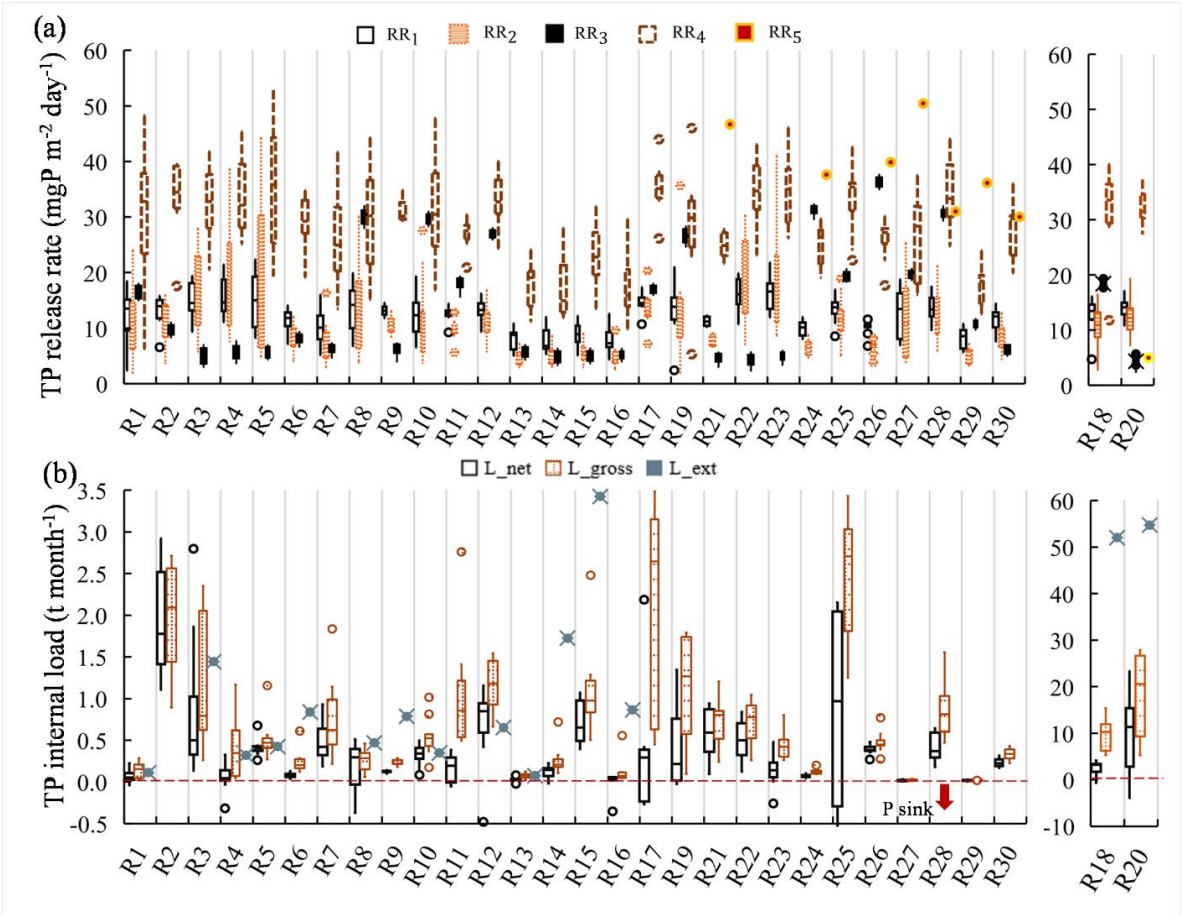

RR_1: Nürnberg and Shaw (1986); RR_2: Carter and Dzialowski (2012); RR_3: Moura et al., (2020); RR_4: Cheng et al., (2020); RR_5: Chapra and Canale (1991) and Lira et. al (2020) from measured sediment data from Ceará (2021).

According to an empirical model proposed by Moura et al., (2020) for semiarid reservoirs to estimate sediment concentration of P bound to iron and aluminium (P_{FeAl}), a reservoir 42 years old (average of the study sites) should have an amount of P_{FeAl} near to 714 mg kg^{-1}. For the study sites, these two compounds presented a positive correlation with TPs, but a more significant correlation was found between the ratios Fe_s:TP_s and Al_s:TP_s with an R^2 of 0.74. Ratios of metals and P are indicative of the underlying processes controlling P release and retention (Markovic et al., 2019) and may act as operational targets on the estimation of sediment P release potential. For the study sites, the ratios Fe_s:TP_s and Al_s:TP_s varied from 4.8 to 46.5 and 2.6 to 27, respectively. Jensen et al., (1992) observed the largest difference between TP_s and TP_w in lakes when Fe:P ratios were between 10 and 15, while Kopáček et al., (2005)

provided thresholds for the Al:P ratio beyond which P release may be negligible (Al:P>25 and Al:Fe>3). For the study sites the average ratios Al_s:TP_s and Al_s:Fe_s were 14.5 and 0.44, respectively, suggesting a high release potential.

4.3.2.2 Average seasonal net internal release rates

The estimates ranged from the most extreme values -4763.09 to 5930.63 mg m^{-2} dry $period^{-1}$ in R19 and R5 respectively, with average of 991 mg m^{-2} dry $period^{-1}$ (± 944). Negative estimates were calculated which means that P loss processes, such as removal throughout the lake volume or settling across the sediments, surpassed releasing mechanisms eventually. However, positive estimates prevailed in 92.8 % of the values. Although relatively high values were observed, they were punctual estimates influenced by sensible parameters and reflected particular situations. For R19, this estimation occurred in 2009 with a decrease in TP concentration from August to November from 0.473 to 0.204 mg L^{-1}. As 2009 was the rainiest year of the study period, it is believed that the high and abrupt input of external load in this period mixed, increased the concentration during the rainy season and then promoted a slow return to a lower level in the dry period. This process implied a settling process far superior than releasing events. For R5, the load estimate resulted from a TP concentration change from 0.278 to 0.574 mg L^{-1} in August to November. These concentrations were about 9 to 19-fold higher than the limiting concentration of 0.03 mg L^{-1} established by the National Environmental Agency (Brazil, 2005). Table A2 summarizes the statistics and parameters of the estimates encompassing all study sites.

The implications associated with high internal P loading in reservoirs regard mainly the aquatic ecological functioning and the risk of eutrophication, what is especially impactful in drinking water supply reservoirs. Due to the internal P release a high trophy level tends to persist in the long-term, even minimizing the external inputs, in addition to the risk of frequent algal blooms. A direct effect is the increase in the treatment costs of the water for human consumption. From a management perspective, mitigation strategies direct on the internal load, such as artificial aeration and/or sediment dredging, are very cost demanding. In the study area, where there are about two-hundred strategic reservoirs managed by the water management company of the state, these strategies are unpractical on a large scale. Take measures upon the aquaculture practice, however, is the one viable management approach in a short-term perspective.

Apart from the extreme values already discussed, reservoir R16 presented the lowest values, followed by R13, while R8 presented the highest ones. Accordingly, R16 remained oligotrophic 45% of the study period while R13 remained mesotrophic 68%, both with low TP_w over time (Figure 2). In addition, peak values sensitively influenced the variability on the estimates evaluated through the CV. However, disregarding these peak estimates, the obtained CV was within the ranges reported in the literature for internal load estimation (0.33 – 0.83) (Spears et al., 2012; Nürnberg et al., 2009, 2012, 2019; Horpilla et al., 2017).

Previous studies that attempted to estimate P release rates in the warmer season have shown a range from 94 to 2117 mg m^{-2} $summer^{-1}$ (Nürnberg et al., 2012, 2013, 2019; Tammeorg et al., 2020), while long-term annual averages reached even higher values (-1,694 to 10,640 mg m^{-2} yr^{-1}) (Köhler et al., 2005; Horpilla et al., 2017; Orihe et al., 2017). The higher estimates obtained in this study in comparison to other average rates reported mostly for temperate ecosystems are consistent as the amount of phosphorus released from the sediments is enhanced in warmer climate (Cheng et al., 2020). An increase in temperature by 10 °C might induce an increase in TP release by 2-7 times (Nürnberg et al., 2019). In fact, Brazilian semiarid reservoirs have water temperature (~30ºC) about 3-fold and 1.5-fold higher than temperate (~10ºC) and tropical (~20ºC) lakes, respectively. Additionally, there is the trophic status influence. As the reservoirs remained mostly eutrophic (Table 4.1) and with lower flows due to the drought condition, higher P release rates are more likely to occur under these conditions (North et al., 2015).

4.3.3 The influence of trophic status and water level fluctuation on internal P load trends

Figure 4.5 summarizes TSI, Chl-a and z_{secchi} for different ranges of P release in a grouped analysis of all study sites. It is also shown the percentage of time during the study period for each trophic state by reservoir. To improve visualization, the y-axis scale was reduced and the few values under -3,000 mg L^{-1} were not shown. About 77% of the reservoirs remained eutrophic/hypereutrophic more than 50% of the time. The release rates increased across the trophic gradient being, on average, 184.86, 618.94, 752.20, and 1844.85 mg m^{-2} dry $period^{-1}$ for oligotrophic, mesotrophic, eutrophic, and hypertrophic status, respectively. The TSI is one of the main drivers of internal P loading that is hypothesized to be much higher in hypereutrophic lakes compared to lakes of lower trophic state (Carter and Dzialowski, 2012; Qin et al., 2016). This assumption was confirmed for the study sites where the differences among estimates under a hypereutrophic status and other groups were significant at a 99% level.

The ratio between the release rate in a hypereutrophic and a mesotrophic environment may reach up to 6-fold (Kowalczewska-Madura et al., 2015). Additionally, P release rate increased as Chl-a increased. This may be explained as the blue-green algae bloom and eutrophication trigger a regime shift from the clear to the turbid water and leads to the loss of submerged macrophytes which are essential for direct P uptake and increase sediment P-binding capacity. Overall, this algae contributes to increasing P release (Zhang et al. 2012).

An important consequence of the elevated productivity in eutrophic systems is anoxia (Snortheim et al., 2017). Internal loading is sometimes sufficient to maintain an eutrophic status even after external P sources reduction or elimination (Qin et al., 2016). Then, a stable mesotrophic condition is only achieved after a substantial reduction of these loadings (Lepori and Roberts, 2017) or after several times the lake hydraulic retention time on recovery (Ostrofsky and Marbach, 2019). Prolonged water quality recovery after external load reduction was already verified in other semiarid ecosystems in the study region (Freire et al., 2009). Other aspects, such as the temperature gradient between water and sediment (Kowalczewska-Madura et al., 2015), catchment soil erosion and landuse (Carter and Dzialowski, 2012), high intensity of solar radiation (Santos et al., 2014), volume reduction under dry conditions (Rocha Junior et al., 2018) and aquaculture practice (Rocha Junior et al., 2018), also contribute to the worsening on the trophic state. Ultimately, the water level fluctuation (WLF) is an additional driver that can further intensify eutrophication symptoms (Cavalcante et al., 2021; Lima Neto et al., 2022).

Figure 4.5 - (a) Distribution of the type of trophic status attributed to the reservoir by the measurement campaigns over the study period*. Trends of the seasonal net release rates with (b) Chl-a, (c) z_{secchi} and (d) trophic state.

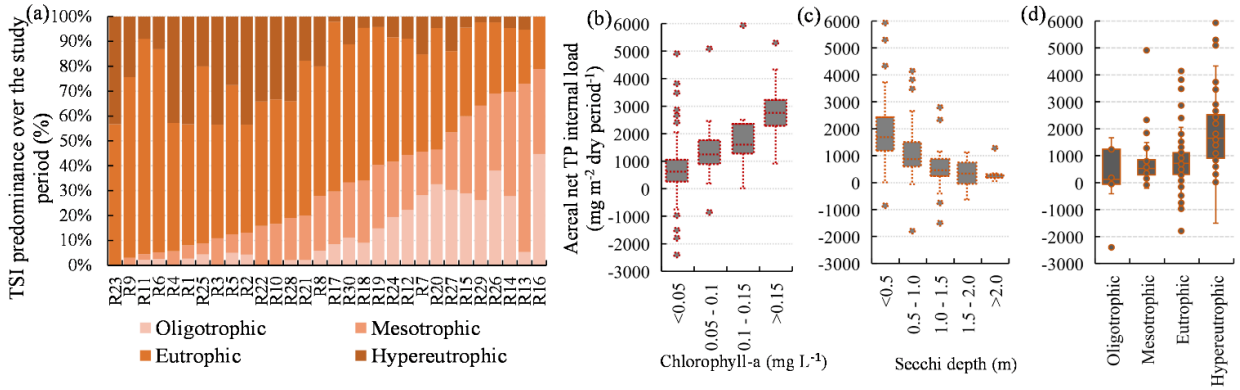

* Calculated from the sum of each trophic classification assigned to the reservoir by measurement campaign in relation to the total of campaigns carried out in the study period.

4.3.4 Water level fluctuation relationship with interannual internal P load trend

The relation between lake level fluctuation as consequence of the seasonal and interannual volume reduction and the interannual variability in P estimates is shown in Figure 4.6. From 2009 to 2016 the volume decreased continuously as a result of a drought event. The WLF (considering the water level difference between the two dates on which the TP measurements were performed) was on average -1.16 m, varying from -0.2 to -5.71 m annually. The sharpest WLF was observed in the largest reservoirs (R17, 20 and R25) in the driest years (2013-2016). The relative fluctuation varied from 2, mostly in 2009 when the reservoirs were full, to near 0.06 in 2015, during the lowest depths, with a steepest decrease observed from 2009 to 2013. On the opposite, a pronounced increase in the release rates was observed during the same period. From 2013-2016 the averages remained stable and then started a slow decrease. Analyzing the interannual variability in the release rates, significant statistical differences resulted from the paired analysis between the years 2009 and 2013-2020 ($p < 0.05$) and between the years 2012 and 2013-2016 ($p < 0.01$), when the reservoirs were gradually drying up. Similarly, significant differences ($p < 0.05$) were observed between 2015-2016 with the years 2019-2020, when the reservoirs were in a volume recover.

Large seasonal and annual WLF have a critical influence on the phosphorus dynamics of reservoirs in the semiarid climate zone, especially the shallower ones (Coppens et al., 2016). Unluckily, these regions are highly vulnerable to droughts which enhances WLF and volume decrease (Brasil et al., 2016). Under these conditions regime shifts or sudden transitions from one stable state to another are more likely (Huang et al., 2020) and the release capability increases with the strong disturbance intensity (Tong et al., 2017). Furthermore, in deeper lakes water level fluctuations also influence the internal nutrient mixing (Gownaris et al., 2018). Direct and inverse relationships between WLF and limnological variables such as dissolved oxygen, TP, TN, N:P ratio, total phytoplankton biomass and euphotic depth are widely known (Yang et al., 2016; Gownaris et al., 2018). It is also important to evaluate the temporal scale when considering WLF impacts, as interannual and seasonal fluctuations did not influence the same ecosystem attributes.

Some researchers suggest the water level management in small and medium-sized reservoirs to reduce WLF potential negative effects on the ecosystems (Yang et al., 2016; Huang et al., 2020). However, the study sites are exposed to high evaporation rates (~2 m yr^{-1}) (Brazil, 2021) and recurrent drought events. These conditions turn unpractical WLF control and so the waterbodies respond freely to the environmental drivers. Furthermore, aquatic

ecosystems globally are likely to become more vulnerable to extreme WLF due to the combined effects of climate change and human activity (Fu et al., 2021), and the severity of droughts may be intensified in arid environments.

Figure 4.6 - TP release rate trends and WLF relative to the mean maximum depth over the study period

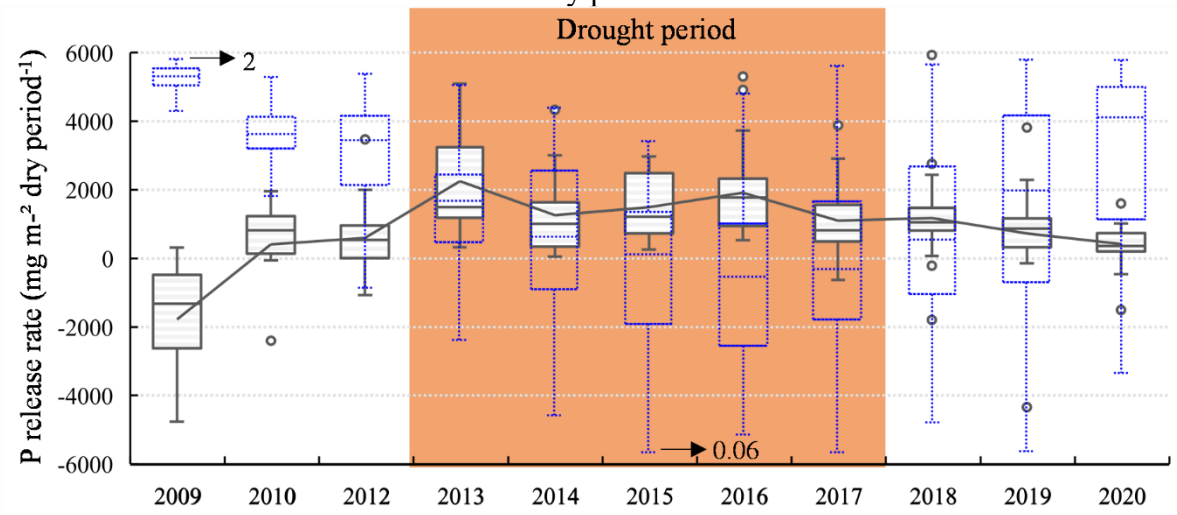

4.3.5 Physical and environmental drivers influencing P release

Figure 4.7 summarizes the grouped analysis of the climatic surrogates, their seasonality and the potential relations and impacts in the water quality parameters and in the estimated P release rate. As observed from Figure 4.7b and 4.7c, the climate in the study region is markedly hot with intense insolation in the dry period in comparison to the wet one. The insolation has the sharpest variation over the months. Although there is a seasonality in the temperature, there is only a narrow variation throughout the dry period (28.2 ±0.6 ºC). To evaluate the trends in Chl-a, TP_w and P release rate depending on the range of the climatic variables, some aspects should be noticed. Firstly, for temperature and insolation, as the measurement of the water quality parameters occurred mostly in August and November and the climatic stations presented similar values for these forcings during the dry period, the average over the measurement period favored one category and the threshold limits were very close. For the wind speed, however, it was possible to cover a wider range.

Firstly, the wind speed was classified into three groups: below 2.5 m s^{-1} (low speed), 2.5–3.5 m s^{-1} (mild speed) and over 3.5 m s^{-1} (high speed), similar with grouping propositions adopted in other studies (Zhang et al., 2017). Wind velocity ranged from 1.3 m s^{-1} in July to 5.2 m s^{-1} in November, with an average of 3.4 m s^{-1} (±0.8). The paired analysis resulted in significant *p*-value ($p < 0.05$) for the three parameters evaluated. Increasing Chl-a, TP_w and P

release was observed as wind speed increased. The differences were more significant ($p < 0.001$) for TP_w when comparing low speeds with high speeds. Similarly, for P release the most significant differences ($p < 0.005$) were observed between mild and high speeds.

TP_w increased from 0.05 to 0.09 mg L^{-1}, Chl-a from 0.01 to 0.03 mg L^{-1} and P release from 508.5 to 1006.1 mg m^{-2} dry $period^{-1}$ as wind changed from low to high speed. Increasing TP_w along with increasing wind speed was already found in other eutrophic reservoir in the study region (Mesquita et al., 2020). Similarly, Huang et. al (2016) studying a large Chinese shallow lake found that the TP release doubled as wind speed increased by roughly 2.2-fold. On the other hand, between mild and high speeds there was no significant differences for P release ($p = 0.32$), which suggested a stabilizing pattern of wind disturbance influencing P resuspension. Threshold wind speed that exceeds critical shear stress and trigger resuspension is still variable in literature (3-6 m s^{-1}) (Zheng et al., 2015; Jalil et al., 2019; Araújo et al., 2019; Wang et al., 2021). In this study, though, the value of 3.5 m s^{-1} was observed as already promoting significant disturbance in lake response.

For the temperature influence, significant differences ($p < 0.005$) were observed for TP_w and Chl-a between the groups (27–27.5 ºC) and (> 27.5 ºC) with a decrease in these parameters as temperature increased. Although there was an increase in these parameters when temperature changed from (< 27 ºC) to the other groups, as the number of observations is unequal and small for low temperature values, the statistical analysis resulted in no significant differences. Zhang et al., (2020) also found that the TP_w response to different intervals of air temperature could have a positive or negative correlation. As previously mentioned, the range of variation in the air temperature was very narrow (25 ºC – 29 ºC), with mostly high values (minimum of 25.5 ºC), in comparison with the water temperature (24 ºC – 32 ºC). When analyzing paired data between TP_w and water temperature, a positive correlation with increasing TP_w was observed. Statistically significant differences were obtained between groups (T < 25 ºC) and (T > 30 ºC) in accordance with what is commonly expected. Validate water quality degradation with temperature increase usually requires final temperature significantly higher than the initial one (Zhang et al., 2016).

As for the response in P release, a slightly increase in the median values was observed as temperature increased. Increasing air temperature followed by increasing water temperature partially explain the increasing trend in internal load (Nürnberg and LaZerte, 2016). Higher P release rates are expected under high temperatures (Cavalcante et al., 2021), which was actually observed in the study sites. Regarding the response of Chl-a for both temperature and insolation forcings, significant differences were observed with a decrease in concentration as these drivers

increased. Studies about the phytoplankton response to light reported a growth-irradiance curve based on the continuous light exposure and a sensitive response to light fluctuation (Litchman, 2000). Depending on the species, the curve has a maximum growth rate level regardless of radiance increase, while others have a decrease pattern after a certain irradiance level. Irradiance is tolerated until a limiting, saturating and inhibiting level beyond which the species decrease in number.

Figure 4.7 - Boxplot showing monthly and seasonal variation of the climatic variables wind speed, air temperature and insolation and trends of the water quality indicators and the internal P release with the categories of this climatic surrogates.

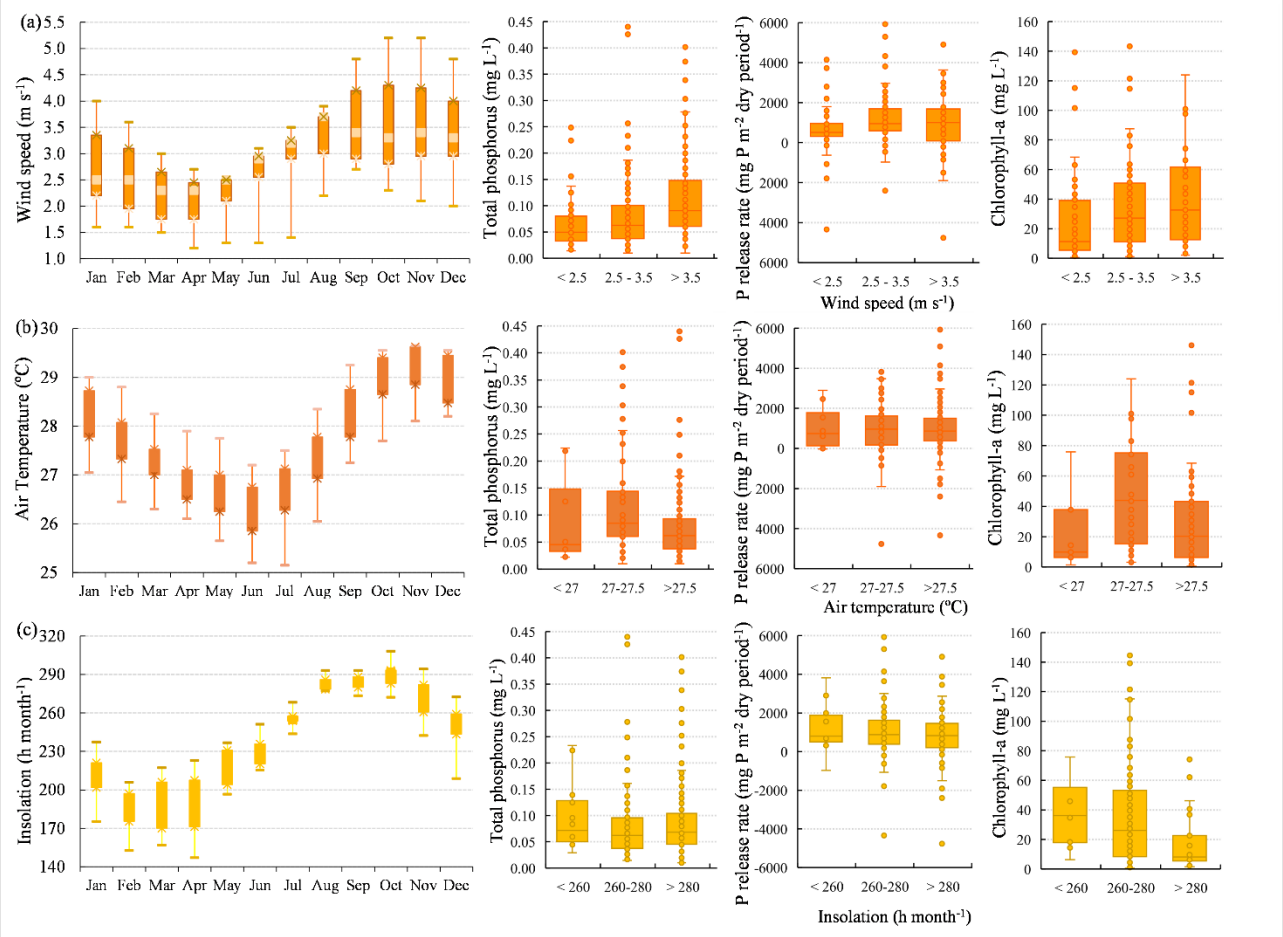

4.3.6 Ratio between wind speed and reservoir volume as an explanatory variable for sediment P release

Proposed as an explanatory variable to the internal loading production, the ratio of wind speed to reservoir volume was correlated with the net areal TP release rates, as presented in Figure 4.8. The applicability of surrogates involves a trade-off between its accuracy in the representation of the target and its transferability (Lindenmayer et al., 2015). Satisfactory r^2

(0.26-0.93 with median of 0.67) and r_a^2 (0.14-0.92 with median of 0.60) were obtained (Moriasi et al., 2015). The median MAPE was 36%. The few models with average performance, low r^2 and high MAPE were influenced by peak estimates from significant TP increase (R13 in 2016 and R15 in 2014) or a sharp decrease (R12 in 2017) over the dry period for specific years. R8 (Figure 4.8a) presented the best adjustment (R^2 = 0.93) and also the most complete dataset. Consistently, the shallowest reservoirs (R1, R4 and R27) presented the highest wind speed-reservoir volume ratios (Figure 4.8e), while the largest ones (R18 and R20) presented the lowest ratios (Figure 4.8c). The parameters of the equations and the metrics of each fitted model are available in the supplementary material.

The models also presented a stabilizing rising pattern for P release, which was considered a consistent behavior as the releasing process do not increase indefinitely. A stabilizing limit may be achieved since nutrient release eventually reach an equilibrium state in SWI (Cyr et al., 2009). One possible explanation is that stronger winds trigger higher water current volatility and the dispersion of the pollutants from the most to least polluted zones (Zhang et al., 2017). Then, and overall increasing TP concentration is likely to occur in the reservoir. Furthermore, threshold values control the geochemical behavior of P in sediment – water system and adsorption processes prevail when P concentration surpasses this value. This way, the intensity of the release might be associated with TP_w, where higher P concentration implies less P release (Zhang et al., 2016).

From the obtained models and summarizing all the topics discussed in previous sections, may be inferred that the studied reservoirs accumulate several influencing aspects to the pressing internal P regeneration during the dry season such as: the instability of the water column, high water temperatures, high wind speed, high WLF, high trophic status, low DO concentrations and low water depth over the study period. Additionally, to acknowledge how these variables help the understanding of internal P loading through a study carried in a broader scale, encompassing several and different reservoirs, turns the findings and evidence more trustful. This means that each reservoir is unique but still respond similarly to others regarding the behavior of the internal P loading to a specific explanatory variable.

Figure 4.8 - Regression models developed between the ratio wind speed to reservoir volume and average seasonal TP release rate.

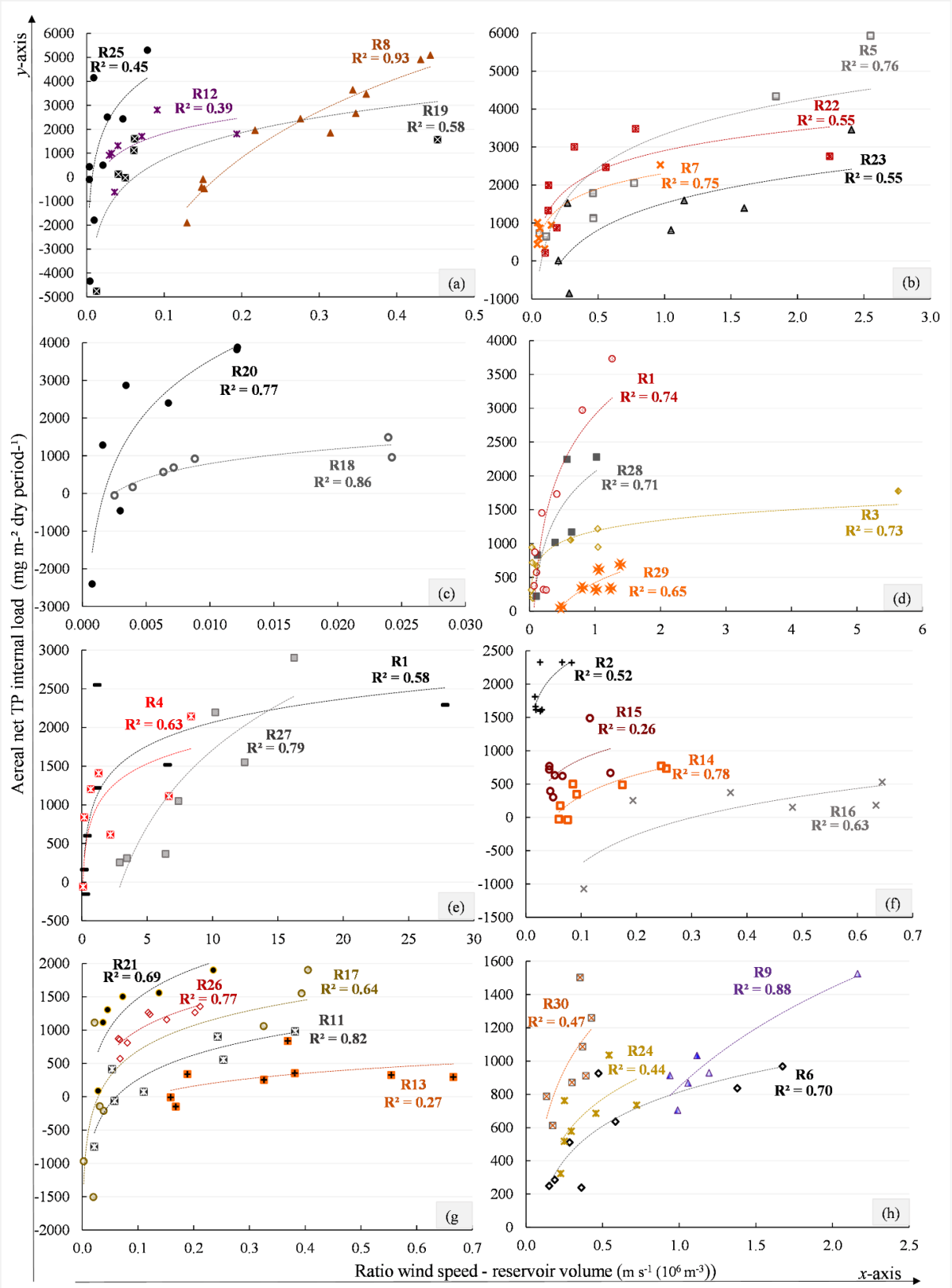

4.4 Modeling implications, uncertainty analysis and limitations

Accounting for a seasonal timescale and a long-term P budget, this work applied well stablished methods of estimating internal P loading under P speciation and sediment P limited data, but sufficient water quality information. To estimate gross loads, the product of the anoxic factor with the P release rate estimated from TP_w was originally proposed by Nürnberg and LaZerte (2001) and widely applied since then (Nürnberg et al., 2009, 2012, 2013; North et al., 2015; Horppila et al., 2017; Rocha and Lima Neto, 2021a). To obtain net loads, the classical whole-lake mass balance approach was applied (Orihe et al., 2017). This methodology is suitable to semiarid regions where strategic water supply reservoirs are threatened in the dry period by the impact of internal load to water quality deterioration. Additionally, the quantification of this important P source is favored by the intermittent regime of the rivers and a dry period of negligible inflow.

Low variability on the estimates, as already discussed through the coefficient of variation, reinforced the modeling predictive ability to estimate with acceptable accuracy seasonal loads under long term studies. As for model sensitiveness, the variability in the volume and the ratio $TP_w/TP_{w,0}$ were evaluated. This last indicator was more impactful since if considerable average TP increase or decrease is observed, especially if it occurs in a short time interval, it may imply the occurrence of extreme load events that triggered the change and induce modeling significant under/overestimation. The 75^{th} of the ratio $TP_w/TP_{w,0}$ was 1.48 with average of 1.25, which is slightly lower than the suggested threshold of 1.5 (Rocha and Lima Neto, 2021a). As for the volume impact, its large interannual variability is typical of semiarid regions and the response in the internal load estimates is supported by the associated physical and biogeochemical processes.

Limitations on modelling may occur due to potential underestimation or overestimation of the net release rates (Tammeorg et al., 2020) influenced by factors such as: (i) use of average concentrations (Nikolai and Dzialowski, 2014), (ii) spatial variability due to sediment heterogeneity, (iii) quantification of anoxia extent by the anoxic factor and (iv) under representation of extreme values as hypolimnion sampling were not always available. Moreover, the effect sediment derived P loss via re-sedimentation (Nürnberg et al., 2013) was not possible to consider. However, despite eventual inaccuracies intrinsic of the modeling process, the estimates seem reasonable since: (i) they are corroborated by several independent approaches, (ii) the mass balance approach is enhanced when calculating multiyear averages and (iii) they were significant when compared to external inputs. Furthermore, the reservoirs

accumulated several influencing aspects to the pressing internal P estimated, as already discussed in the previous section.

4.5. Conclusions

This study assessed the long-term internal P loading contribution in thirty strategic water supplies reservoirs located in the Brazilian semiarid. Net and gross release estimates were obtained by seasonal P budget and regression approaches accounting for the components water column and sediment TP concentration, anoxic duration, water temperature, fish contribution and reservoir age. Further analyses statistically connected the estimates with in-lake water quality indicators, physical surrogates, and environmental drivers. Finally, a new indicator was proposed along with predictive regression models to enable P release estimation from easily available data.

The average seasonal net estimates were 991 mg m^{-2} dry $period^{-1}$ (±944), while average gross estimates varied from 17.64 mg m^{-2} day^{-1} to 35.99 mg m^{-2} day^{-1}. The rates were slightly higher than reported for temperate ecosystems, which may be attributed to the enriched sediments allied with warmer water temperature and prolonged anoxic periods. Furthermore, the average P release rates significantly increased across the trophic gradient (p<0.05), about 10-fold higher under hypertrophic status than in oligotrophic one. The results also indicated that the highest releases occurred in the driest years with the reservoirs in their lowest volumes.

Regarding the predictive models for P release, the coupling of the wind speed with the mean reservoir volume proved to be a strong surrogate to estimate sediment P release (r^2: 0.26-0.93). The behavior of the adjusted models was physically consistent. A stabilizing pattern was achieved since there is a threshold P concentration in SWI that restricts unlimited P release. This surrogate also balanced accuracy and transferability, in order to be replicable to other regions. Despite modelling uncertainties, the obtained results are supported since the study sites accumulated several influencing aspects for the internal P production during the dry season. Additionally, independent methodologies supported each other. Especially in dryland regions where water supply reservoirs are under critical water quality and environmental conditions, the finding of this study may help to support phosphorus pollution management strategies

CHAPTER 5

General Conclusions

This study assessed the long-term phosphorus loading dynamics through an integrated catchment-reservoir approach for strategic water supply reservoirs of the Brazilian semiarid. Combined, the results presented in Chapters 2, 3 and 4 advanced the knowledge of phosphorus dynamics in tropical semiarid reservoirs and provided simple methodologies and new models to assist integrated water quality management actions in the study region. The findings of this work and the practical tools and indicators proposed to estimate the phosphorus load can potentially support the decision-making process related with phosphorus pollution and consequently, reservoirs enrichment and water quality degradation. Furthermore, the methods proposed herein may be replicable to other arid and semiarid regions.

References

Ahlgren, I. Frisk, T. Lars Kamp-Nielsen, L. 1988. Empirical and theoretical models of phosphorus loading, retention and concentration vs. lake trophic state. Hydrobiologia. 170. 285-303.

APHA. American Public Health association. 2005. Standard Methods for the Examination Water and Wastewater. 21st Ed. Washington: APHA. 1083p.

Andrade, E.M., Ferreira, K.C.D., Lopes, F.B., Araújo, I.C. da S., da Silva, A.G.R., 2020. Balance of nitrogen and phosphorus in a reservoir in the tropical semiarid region: Balanço de nitrogênio e fósforo em um reservatório na região semi-árida tropical. Rev. Cienc. Agron. 51, 1–10. https://doi.org/10.5935/1806-6690.20200020

Ansari, A.A., Gill, S.S., 2014. Eutrophication: Causes, consequences and control: Volume 2. Eutrophication Causes, Consequences Control Vol. 2 1–262. https://doi.org/10.1007/978-94-007-7814-6

Araújo, G.M., Lima Neto, I.E., Becker, H., 2019. Phosphorus dynamics in a highly polluted urban drainage channelshallow reservoir system in the Brazilian semiarid. An. Acad. Bras. Cienc. 91. https://doi.org/10.1590/0001-3765201920180441

Araújo, J.C., Medeiros, P.H.A., 2013. Impact of Dense Reservoir Networks on Water Resources in Semiarid Environments. Australas. J. Water Resour. 17, 87–100. https://doi.org/10.7158/13241583.2013.11465422

Arunbabu, E., Ravichandran, S., Sreeja, P., 2014. Sedimentation and internal phosphorus loads in Krishnagiri Reservoir, India. Lakes Reserv. Res. Manag. 19, 161–173. https://doi.org/10.1111/lre.12069

Bai, Y.; Gao, J.; Zhang, Y. (2020) Research on wind-induced nutrient release in Yangshapao Reservoir, China. Water Supply, 20, 469-477. http://dx.doi.org/10.2166/ws.2019.180.

Barbosa, J. do S.B., Bellotto, V.R., da Silva, D.B., Lima, T.B., 2019. Nitrogen and phosphorus budget for a deep tropical reservoir of the Brazilian Savannah. Water (Switzerland) 11. https://doi.org/10.3390/w11061205

Barbosa, J.E. de L., Medeiros, E.S.F., Brasil, J., Cordeiro, R. da S., Crispim, M.C.B., da Silva, G.H.G., 2012. Ecossistemas aquáticos do semi-árido brasileiro: Aspectos limnológicos e manejo. Acta Limnol. Bras. 24, 103–118. https://doi.org/10.1590/S2179-975X2012005000030

Bieroza, M.Z., Heathwaite, A.L., 2015. Seasonal variation in phosphorus concentration-discharge hysteresis inferred from high-frequency in situ monitoring. J. Hydrol. 524,

333–347. https://doi.org/10.1016/j.jhydrol.2015.02.036

Bowes, M.J., Jarvie, H.P., Naden, P.S., Old, G.H., Scarlett, P.M., Roberts, C., Armstrong, L.K., Harman, S.A., Wickham, H.D., Collins, A.L., 2014. Identifying priorities for nutrient mitigation using river concentration-flow relationships: The Thames basin, UK. J. Hydrol. 517, 1–12. https://doi.org/10.1016/j.jhydrol.2014.03.063

Bowes, M.J., Neal, C., Jarvie, H.P., Smith, J.T., Davies, H.N., 2010. Predicting phosphorus concentrations in British rivers resulting from the introduction of improved phosphorus removal from sewage effluent. Sci. Total Environ. 408, 4239–4250. https://doi.org/10.1016/j.scitotenv.2010.05.016

Bowes, M.J., Smith, J.T., Jarvie, H.P., Neal, C., 2008. Modelling of phosphorus inputs to rivers from diffuse and point sources. Sci. Total Environ. 395, 125–138. https://doi.org/10.1016/j.scitotenv.2008.01.054

Bowes, M.J., Smith, J.T., Neal, C., 2009. The value of high-resolution nutrient monitoring: A case study of the River Frome, Dorset, UK. J. Hydrol. 378, 82–96. https://doi.org/10.1016/j.jhydrol.2009.09.015

Braga, B.B., de Carvalho, T.R.A., Brosinsky, A., Foerster, S., Medeiros, P.H.A., 2019. From waste to resource: Cost-benefit analysis of reservoir sediment reuse for soil fertilization in a semiarid catchment. Sci. Total Environ. 670, 158–169. https://doi.org/10.1016/j.scitotenv.2019.03.083

Brasil, J., Attayde, J.L., Vasconcelos, F.R., Dantas, D.D.F., Huszar, V.L.M., 2016. Drought-induced water-level reduction favors cyanobacteria blooms in tropical shallow lakes. Hydrobiologia 770, 145–164. https://doi.org/10.1007/s10750-015-2578-5

Brazil. Ministério do Meio Ambiente: Conselho Nacional de Meio Ambiente, CONAMA. Resolução CONAMA nº 357, de 17 de março de 2005. 2005. Disponível em: http://www.mma.gov.br. Acesso em: 04 mar 2021.

Brazil. Instituto Nacional de Meteorologia. Normais climatológicas. 2021. Disponível em: < https://portal.inmet.gov.br/normais>. Acesso em: 17 jan. 2021.

Broad, K., Pfaff, A., Taddei, R., Sankarasubramanian, A., Lall, U., de Assis de Souza Filho, F., 2007. Climate, stream flow prediction and water management in northeast Brazil: Societal trends and forecast value. Clim. Change 84, 217–239. https://doi.org/10.1007/s10584-007-9257-0

Campos, J.N.B., Lima Neto, I.E., Studart, T.M.C., Nascimento, L.S.V., 2016. Trade-off between reservoir yield and evaporation losses as a function of lake morphology in semi-arid Brazil. An. Acad. Bras. Cienc. 88, 1113–1125. https://doi.org/10.1590/0001-

3765201620150124

Carneiro, F.M., Nabout, J.C., Vieira, L.C.G., Roland, F., Bini, L.M., 2014. Determinants of chlorophyll-a concentration in tropical reservoirs. Hydrobiologia 740, 89–99. https://doi.org/10.1007/s10750-014-1940-3

Carpenter, S.R., Booth, E.G., Kucharik, C.J., Lathrop, R.C., 2014. Extreme daily loads: role in annual phosphorus input to a north temperate lake. Aquat. Sci. 77, 71–79. https://doi.org/10.1007/s00027-014-0364-5

Carter, L.D., Dzialowski, A.R., 2012. Predicting sediment phosphorus release rates using landuse and water-quality data. Freshw. Sci. 31, 1214–1222. https://doi.org/10.1899/11-177.1

Castellano, L., Ambrosetti, W., Barbanti, L., Rolla, A., 2010. The residence time of the water in Lago Maggiore (N. Italy): First results from an Eulerian-Lagrangian approach. J. Limnol. 69, 2. https://doi.org/10.3274/JL10-69-1-02

Castagnino, W. A. Investigación de modelos simplificados de eutroficación en lagos tropicales. Organizacion Panamericana de la Salud, Centro Panamericano de Ingenieria Sanitaria y Ciencias del Ambiente, Versión Revisada. 1982.

Castro Medeiros, L., Mattos, A., Lürling, M., Becker, V., 2015. Is the future blue-green or brown? The effects of extreme events on phytoplankton dynamics in a semi-arid man-made lake. Aquat. Ecol. 49, 293–307. https://doi.org/10.1007/s10452-015-9524-5

Cavalcante, Herika, Araújo, F., Becker, V., 2018. Phosphorus dynamics in the water of tropical semiarid reservoirs in a prolonged drought period. Acta Limnol. Bras. 30. https://doi.org/10.1590/s2179-975x1617

Cavalcante, H., Araújo, F., Becker, V., de Lucena Barbosa, J.E., 2021. Internal phoshorus loading potential of a semiarid reservoir: An experimental study. Acta Limnol. Bras. 33, 1–13. https://doi.org/10.1590/s2179-975x10220

Cavalcante, H., Araújo, F., Noyma, N.P., Becker, V., 2018. Phosphorus fractionation in sediments of tropical semiarid reservoirs. Sci. Total Environ. 619–620, 1022–1029. https://doi.org/10.1016/j.scitotenv.2017.11.204

Ceará. Bureau of Water Resources of the Government of the State of Ceará. Plan of strategic actions in water resources of the State of Ceará, 2018. Available in: https://www.srh.ce.gov.br/wp-content/uploads/sites/90/2018/07/PLANO-DE-ACOES-ESTRATEGICAS-DE-RECURSOS-HIDRICOS-CE_2018.pdf

Ceará. Companhia de Gestão dos Recursos Hídricos: Inventários ambientais. 2020. Disponível em: <http://www.hidro.ce.gov.br/hidro-ce-zend/mi/midia/show/150>. Acesso

em: 01 jan. 2020.

Ceará. Governo do Estado do Ceará. Instituto de Pesquisas e Estratégia Econômica do Estado do Ceará. Os recursos hídricos do Ceará: Integração, gestão e potencialidades. 2011.

Ceará. Companhia de Gestão dos Recursos Hídricos: Monitoramento Quantitativo e Qualitativo dos Recursos Hídricos. 2021. Disponível em: <http://www.hidro.ce.gov.br>. Acesso em: 25 abr. 2021.

Ceará. Companhia de Água e Esgoto do Ceará: Saneamento Básico. 2018. Disponível em: < http://www.mpce.mp.br/wp-content/uploads/2018/02/Cagece_-_Saneamento_Basico_-_Ceara_-_2_edicao.pdf>. Acesso em: 05 mai. 2021.

Chapra, S.C., 2008, Surface Water-Quality Modeling, Waveland Press, Long Grove, IL, 835 p.

Chapra, S.C., Canale, R.P., 1991. Long-term phenomenological model of phosphorus and oxygen for stratified lakes. Water Res. 25, 707–715. https://doi.org/10.1016/0043-1354(91)90046-S

Chapra, S.C., Dolan, D.M., 2012. Great Lakes total phosphorus revisited: 2. Mass balance modeling. J. Great Lakes Res. 38, 741–754. https://doi.org/10.1016/j.jglr.2012.10.002

Chapra, S.C., Dolan, D.M., Dove, A., 2016. Mass-balance modeling framework for simulating and managing long-term water quality for the lower Great Lakes. J. Great Lakes Res. 42, 1166–1173. https://doi.org/10.1016/j.jglr.2016.04.008

Chaves, F.Í.B., Lima, P. de F., Leitão, R.C., Paulino, W.D., Santaella, S.T., 2013. Influência da chuva no estado trófico de um reservatório do semiárido Brasileiro. Acta Sci. - Biol. Sci. 35, 505–511. https://doi.org/10.4025/actascibiolsci.v35i4.18261

Chaves, L.C.G., Lopes, F.B., Maia, A.R.S., Meireles, A.C.M., Andrade, E.M. de, 2019. Water quality and anthropogenic impact in the watersheds of service reservoirs in the Brazilian semi-arid region. Rev. Ciência Agronômica 50, 223–233. https://doi.org/10.5935/1806-6690.20190026

Chen, D., Hu, M., Guo, Y., Dahlgren, R.A., 2015a. Influence of legacy phosphorus, land use, and climate change on anthropogenic phosphorus inputs and riverine export dynamics. Biogeochemistry 123, 99–116. https://doi.org/10.1007/s10533-014-0055-2

Chen, D., Hu, M., Guo, Y., Dahlgren, R.A., 2015b. Reconstructing historical changes in phosphorus inputs to rivers from point and nonpoint sources in a rapidly developing watershed in eastern China, 1980-2010. Sci. Total Environ. 533, 196–204. https://doi.org/10.1016/j.scitotenv.2015.06.079

Chen, M., Ding, S., Chen, X., Sun, Q., Fan, X., Lin, J., Ren, M., Yang, L., Zhang, C., 2018. Mechanisms driving phosphorus release during algal blooms based on hourly changes in

iron and phosphorus concentrations in sediments. Water Res. 133, 153–164. https://doi.org/10.1016/j.watres.2018.01.040

Cheng, X., Huang, Y., Li, R., Pu, X., Huang, W., Yuan, X., 2020. Impacts of water temperature on phosphorus release of sediments under flowing overlying water. J. Contam. Hydrol. 235, 103717. https://doi.org/10.1016/j.jconhyd.2020.103717

Cleophas T.J., Zwinderman A.H., 2016. Non-parametric Tests for Three or More Samples (Friedman and Kruskal-Wallis). In: Clinical Data Analysis on a Pocket Calculator. Springer, Cham. https://doi.org/10.1007/978-3-319-27104-0_34

Coppens, J., Özen, A., Tavşanoğlu, T.N., Erdoğan, Ş., Levi, E.E., Yozgatligil, C., Jeppesen, E., Beklioğlu, M., 2016. Impact of alternating wet and dry periods on long-term seasonal phosphorus and nitrogen budgets of two shallow Mediterranean lakes. Sci. Total Environ. 563–564, 456–467. https://doi.org/10.1016/j.scitotenv.2016.04.028

Costa, R.L., Macedo de Mello Baptista, G., Gomes, H.B., Daniel dos Santos Silva, F., Lins da Rocha Júnior, R., de Araújo Salvador, M., Herdies, D.L., 2020. Analysis of climate extremes indices over northeast Brazil from 1961 to 2014. Weather Clim. Extrem. 28. https://doi.org/10.1016/j.wace.2020.100254

Cyr, H., McCabe, S.K., Nürnberg, G.K., 2009. Phosphorus sorption experiments and the potential for internal phosphorus loading in littoral areas of a stratified lake. Water Res. 43, 1654–1666. https://doi.org/10.1016/j.watres.2008.12.050

Dantas E. W, Moura, A. N., and Bittencourt, M. C. O., 2011. Cyanobacterial blooms in stratified and destratified eutrophic reservoirs in semi-arid region of Brazil. An Acad Bras Cienc 83: 1327-1338.

Delkash, M., Al-faraj, F.A.M., 2014. Comparing the Export Coefficient Approach with the Soil and Water Assessment Tool to Predict Phosphorous Pollution : The Kan Watershed Case Study. https://doi.org/10.1007/s11270-014-2122-7

Ding, S., Chen, M., Gong, M., Fan, X., Qin, B., Xu, H., Gao, S.S., Jin, Z., Tsang, D.C.W., Zhang, C., 2018. Internal phosphorus loading from sediments causes seasonal nitrogen limitation for harmful algal blooms. Sci. Total Environ. 625, 872–884. https://doi.org/10.1016/j.scitotenv.2017.12.348

Ding, X., Shen, Z., Hong, Q., Yang, Z., Wu, X., Liu, R., 2010. Development and test of the Export Coefficient Model in the Upper Reach of the Yangtze River. J. Hydrol. 383, 233–244. https://doi.org/10.1016/j.jhydrol.2009.12.039

Doan, P.T.K., Watson, S.B., Markovic, S., Liang, A., Guo, J., Mugalingam, S., Stokes, J., Morley, A., Zhang, W., Arhonditsis, G.B., Dittrich, M., 2018. Phosphorus retention and

internal loading in the Bay of Quinte, Lake Ontario, using diagenetic modelling. Sci. Total Environ. 636, 39–51. https://doi.org/10.1016/j.scitotenv.2018.04.252

Dolan, D.M., Yui, A.K., Geist, R.D., 1981. Evaluation of River Load Estimation Methods for Total Phosphorus. J. Great Lakes Res. 7, 207–214. https://doi.org/10.1016/S0380-1330(81)72047-1

dos Santos, J.C.N., de Andrade, E.M., de Araújo Neto, J.R., Meireles, A.C.M., de Queiroz Palácio, H.A., 2014. Land use and trophic state dynamics in a tropical semi-arid reservoir. Rev. Cienc. Agron. 45, 35–44. https://doi.org/10.1590/s1806-66902014000100005

Freire, R. H. F. ; Calijuri, M. C. ; Santaella, S.T., 2009. Longitudinal patterns and variations in water quality in a reservoir in the semiarid region of NE Brazil: responses to hydrological and climatic changes. Acta Limnológica Bras. 21, 251–262.

Fu, C., Wu, Huawu, Zhu, Z., Song, C., Xue, B., Wu, Haohao, Ji, Z., Dong, L., 2021. Exploring the potential factors on the striking water level variation of the two largest semi-arid-region lakes in northeastern Asia. Catena 198, 105037. https://doi.org/10.1016/j.catena.2020.105037

Fukushima, T., Matsushita, B., Subehi, L., Setiawan, F., Wibowo, H., 2017. Will hypolimnetic waters become anoxic in all deep tropical lakes? Sci. Rep. 7, 1–8. https://doi.org/10.1038/srep45320

Gownaris, N.J., Rountos, K.J., Kaufman, L., Kolding, J., Lwiza, K.M.M., Pikitch, E.K., 2018. Water level fluctuations and the ecosystem functioning of lakes. J. Great Lakes Res. 44, 1154–1163. https://doi.org/10.1016/j.jglr.2018.08.005

Greene, S., Johnes, P.J., Bloomfield, J.P., Reaney, S.M., Lawley, R., Elkhatib, Y., Freer, J., Odoni, N., Macleod, C.J.A., Percy, B., 2015. A geospatial framework to support integrated biogeochemical modelling in the United Kingdom. Environ. Model. Softw. 68, 219–232. https://doi.org/10.1016/j.envsoft.2015.02.012

Greene, S., Taylor, D., McElarney, Y.R., Foy, R.H., Jordan, P., 2011. An evaluation of catchment-scale phosphorus mitigation using load apportionment modelling. Sci. Total Environ. 409, 2211–2221. https://doi.org/10.1016/j.scitotenv.2011.02.016

Gurgel-Lourenço, R.C., Rodrigues-Filho, C.A. de S., Angelini, R., Garcez, D.S., Sánchez-Botero, J.I., 2015. On the relation amongst limnological factors and fish abundance in reservoirs at semiarid region. Acta Limnol. Bras. 27, 24–38. https://doi.org/10.1590/s2179-975x2414

Håkanson, L., 2005. The importance of lake morphometry and catchment characteristics in

limnology - Ranking based on statistical analyses. Hydrobiologia 541, 117–137. https://doi.org/10.1007/s10750-004-5032-7

Han, C., Zheng, B., Qin, Y., Ma, Y., Yang, C., Liu, Z., Cao, W., Chi, M., 2018. Impact of upstream river inputs and reservoir operation on phosphorus fractions in water-particulate phases in the Three Gorges Reservoir. Sci. Total Environ. 610–611, 1546–1556. https://doi.org/10.1016/j.scitotenv.2017.06.109

Harmel, R.D., Cooper, R.J., Slade, R.M., Haney, R.L., Arnold, J.G., 2006. Cumulative uncertainty in measured streamflow and water quality data for small watersheds. Trans. ASABE 49, 689–701.

Harmel, R.D., Smith, D.R., King, K.W., Slade, R.M., 2009. Estimating storm discharge and water quality data uncertainty: A software tool for monitoring and modeling applications. Environ. Model. Softw. 24, 832–842. https://doi.org/10.1016/j.envsoft.2008.12.006

Hejzlar, J., Šámalová, K., Boers, P., Kronvang, B. 2006. Modelling Phosphorus Retention in Lakes and Reservoirs. Water, Air, and Soil Pollution: 6, 487–494.

Hollaway, M.J., Beven, K.J., Benskin, C.M.W.H., Collins, A.L., Evans, R., Falloon, P.D., Forber, K.J., Hiscock, K.M., Kahana, R., Macleod, C.J.A., Ockenden, M.C., Villamizar, M.L., Wearing, C., Withers, P.J.A., Zhou, J.G., Barber, N.J., Haygarth, P.M., 2018. A method for uncertainty constraint of catchment discharge and phosphorus load estimates. Hydrol. Process. 32, 2779–2787. https://doi.org/10.1002/hyp.13217

Hong, B., Swaney, D.P., Mörth, C.M., Smedberg, E., Eriksson Hägg, H., Humborg, C., Howarth, R.W., Bouraoui, F., 2012. Evaluating regional variation of net anthropogenic nitrogen and phosphorus inputs (NANI/NAPI), major drivers, nutrient retention pattern and management implications in the multinational areas of Baltic Sea basin. Ecol. Modell. 227, 117–135. https://doi.org/10.1016/j.ecolmodel.2011.12.002

Horppila, J., Holmroos, H., Niemistö, J., Massa, I., Nygrén, N., Schönach, P., Tapio, P., Tammeorg, O., 2017. Variations of internal phosphorus loading and water quality in a hypertrophic lake during 40 years of different management efforts. Ecol. Eng. 103, 264–274. https://doi.org/10.1016/j.ecoleng.2017.04.018

Hu, M., Liu, Y., Zhang, Y., Shen, H., Yao, M., Dahlgren, R.A., Chen, D., 2020. Long-term (1980–2015) changes in net anthropogenic phosphorus inputs and riverine phosphorus export in the Yangtze River basin. Water Res. 177, 115779. https://doi.org/10.1016/j.watres.2020.115779

Huang, J., Xu, Q., Wang, X., Ji, H., Quigley, E.J., Sharbatmaleki, M., Li, S., Xi, B., Sun, B., Li, C., 2021. Effects of hydrological and climatic variables on cyanobacterial blooms in

four large shallow lakes fed by the Yangtze River. Environ. Sci. Ecotechnology 5, 100069. https://doi.org/10.1016/j.ese.2020.100069

Hunter, M., Westgate, M., Barton, P., Calhoun, A., Pierson, J., Tulloch, A., Beger, M., Branquinho, C., Caro, T., Gross, J., Heino, J., Lane, P., Longo, C., Martin, K., McDowell, W.H., Mellin, C., Salo, H., Lindenmayer, D., 2016. Two roles for ecological surrogacy: Indicator surrogates and management surrogates. Ecol. Indic. 63, 121–125. https://doi.org/10.1016/j.ecolind.2015.11.049

Jacomine, P.K.T., Almeida, J.C., Medeiros, L.A.R. Levantamento exploratório - reconhecimento de solos do Estado do Ceará. Superintendência de Desenvolvimento do Nordeste – SUDENE, Recife, 1973.

Jalil, A., Li, Y., Zhang, K., Gao, X., Wang, W., Khan, H.O.S., Pan, B., Ali, S., Acharya, K., 2019. Wind-induced hydrodynamic changes impact on sediment resuspension for large, shallow Lake Taihu, China. Int. J. Sediment Res. 34, 205–215. https://doi.org/10.1016/j.ijsrc.2018.11.003

Jarvie, H.P., Sharpley, A.N., Withers, P.J.A., Scott, J.T., Haggard, B.E., Neal, C., 2013. Phosphorus Mitigation to Control River Eutrophication: Murky Waters, Inconvenient Truths, and "Postnormal" Science. J. Environ. Qual. 42, 295–304. https://doi.org/10.2134/jeq2012.0085

Jarvie, H.P., Withers, P.J.A., Bowes, M.J., Palmer-Felgate, E.J., Harper, D.M., Wasiak, K., Wasiak, P., Hodgkinson, R.A., Bates, A., Stoate, C., Neal, M., Wickham, H.D., Harman, S.A., Armstrong, L.K., 2010. Streamwater phosphorus and nitrogen across a gradient in rural-agricultural land use intensity. Agric. Ecosyst. Environ. 135, 238–252. https://doi.org/10.1016/j.agee.2009.10.002

Jensen, H.S., Kristensen, P., Jeppesen, E., Skytthe, A., 1992. Iron:phosphorus ratio in surface sediment as an indicator of phosphate release from aerobic sediments in shallow lakes. Hydrobiologia 235–236, 731–743. https://doi.org/10.1007/BF00026261

Jepson, W., Tomaz, P., Santos, J. O., Baek, J., (2021) A comparative analysis of urban and rural household water insecurity experiences during the 2011–17 drought in Ceará, Brazil. Water International. 46, 697-722. http://dx.doi.org/10.1080/02508060.2021.1944543.

Jeznach, L.C., Hagemann, M., Park, M.H., Tobiason, J.E., 2017. Proactive modeling of water quality impacts of extreme precipitation events in a drinking water reservoir. J. Environ. Manage. 201, 241–251. https://doi.org/10.1016/j.jenvman.2017.06.047

Johansson, T., Nordvarg, L., 2002. Empirical mass balance models calibrated for freshwater

fish farm emissions. Aquaculture 212, 191–211. https://doi.org/10.1016/S0044-8486(02)00013-3

Johnes, P.J., 2007. Uncertainties in annual riverine phosphorus load estimation: Impact of load estimation methodology, sampling frequency, baseflow index and catchment population density. J. Hydrol. 332, 241–258. https://doi.org/10.1016/j.jhydrol.2006.07.006

Johnes, P.J., 1996. Evaluation and management of the impact of land use change on the nitrogen and phosphorus load delivered to surface waters : the export coefficient modelling approach 183, 323–349.

Katsev, S., 2017a. When large lakes respond fast: A parsimonious model for phosphorus dynamics. J. Great Lakes Res. 43, 199–204. https://doi.org/10.1016/j.jglr.2016.10.012

Katsev, S., 2017b. When large lakes respond fast: A parsimonious model for phosphorus dynamics. J. Great Lakes Res. 43, 199–204. https://doi.org/10.1016/j.jglr.2016.10.012

Katsev, S., Tsandev, I., L'Heureux, I., Rancourt, D.G., 2006. Factors controlling long-term phosphorus efflux from lake sediments: Exploratory reactive-transport modeling. Chem. Geol. 234, 127–147. https://doi.org/10.1016/j.chemgeo.2006.05.001

Kelly, L.A., 1993. Release rates and biological availability of phosphorus released from sediments receiving aquaculture wastes. Hydrobiologia 253, 367–372. https://doi.org/10.1007/BF00050762

Kiani, M., Tammeorg, P., Niemistö, J., Simojoki, A., Tammeorg, O., 2020. Internal phosphorus loading in a small shallow Lake: Response after sediment removal. Sci. Total Environ. 725, 138279. https://doi.org/10.1016/j.scitotenv.2020.138279

Kim, L.H., Choi, E., Gil, K.I., Stenstrom, M.K., 2004. Phosphorus release rates from sediments and pollutant characteristics in Han River, Seoul, Korea. Sci. Total Environ. 321, 115–125. https://doi.org/10.1016/j.scitotenv.2003.08.018

Kim, L.H., Choi, E., Stenstrom, M.K., 2003. Sediment characteristics, phosphorus types and phosphorus release rates between river and lake sediments. Chemosphere 50, 53–61. https://doi.org/10.1016/S0045-6535(02)00310-7

Köhler, J., Hilt, S., Adrian, R., Nicklisch, A., Kozerski, H.P., Walz, N., 2005. Long-term response of a shallow, moderately flushed lake to reduced external phosphorus and nitrogen loading. Freshw. Biol. 50, 1639–1650. https://doi.org/10.1111/j.1365-2427.2005.01430.x

Kolding, J., van Zwieten, P.A.M., 2012. Relative lake level fluctuations and their influence on productivity and resilience in tropical lakes and reservoirs. Fish. Res. 115–116, 99–109.

https://doi.org/10.1016/j.fishres.2011.11.008

Kopáček, J., Borovec, J., Hejzlar, J., Ulrich, K.U., Norton, S.A., Amirbahman, A., 2005. Aluminum control of phosphorus sorption by lake sediments. Environ. Sci. Technol. 39, 8784–8789. https://doi.org/10.1021/es050916b

Kowalczewska-Madura, K., Dondajewska, R., Gołdyn, R., Rosińska, J., Podsiadłowski, S., 2019a. Internal phosphorus loading as the response to complete and then limited sustainable restoration of a shallow lake. Ann. Limnol. 55. https://doi.org/10.1051/limn/2019003

Kowalczewska-Madura, K., Gołdyn, R., Bogucka, J., Strzelczyk, K., 2019b. Impact of environmental variables on spatial and seasonal internal phosphorus loading in a mesoeutrophic lake. Int. J. Sediment Res. 34, 14–26. https://doi.org/10.1016/j.ijsrc.2018.08.008

Kowalczewska-Madura, K., Gołdyn, R., Dera, M., 2015. Spatial and seasonal changes of phosphorus internal loading in two lakes with different trophy. Ecol. Eng. 74, 187–195. https://doi.org/10.1016/j.ecoleng.2014.10.033

Krasa, J., Dostal, T., Jachymova, B., Bauer, M., Devaty, J., 2019. Soil erosion as a source of sediment and phosphorus in rivers and reservoirs – Watershed analyses using WaTEM/SEDEM. Environ. Res. 171, 470–483. https://doi.org/10.1016/j.envres.2019.01.044

Kulasova, A., Smith, P.J., Beven, K.J., Blazkova, S.D., Hlavacek, J., 2012. A method of computing uncertain nitrogen and phosphorus loads in a small stream from an agricultural catchment using continuous monitoring data. J. Hydrol. 458–459, 1–8. https://doi.org/10.1016/j.jhydrol.2012.05.060

Lacerda, L.D., Santos, J.A., Marins, R. V., Da Silva, F.A.T.F., 2018. Limnology of the largest multi-use artificial reservoir in NE Brazil: The Castanhão Reservoir, Ceará State. An. Acad. Bras. Cienc. 90, 2073–2096. https://doi.org/10.1590/0001-3765201820180085

Le Moal, M., Gascuel-Odoux, C., Ménesguen, A., Souchon, Y., Étrillard, C., Levain, A., Moatar, F., Pannard, A., Souchu, P., Lefebvre, A., Pinay, G., 2019. Eutrophication: A new wine in an old bottle? Sci. Total Environ. 651, 1–11. https://doi.org/10.1016/j.scitotenv.2018.09.139

Lemos, W. E. D., 2015. Seasonal climate forecast of the reservoir thermal and hydrodynamic regime. Thesis (Doctorate) - Civil Engineering Course, Universidade Federal do Ceará, Fortaleza, 2015. 166 f. (in Portuguese)

Lepori, F., Roberts, J.J., 2017. Effects of internal phosphorus loadings and food-web structure

on the recovery of a deep lake from eutrophication. J. Great Lakes Res. 43, 255–264. https://doi.org/10.1016/j.jglr.2017.01.008

Li, B., Li, P., Zeng, X.C., Yu, W., Huang, Y.F., Wang, G.Q., Young, B.R., 2020. Assessing the sustainability of phosphorus use in China: Flow patterns from 1980 to 2015. Sci. Total Environ. 704. https://doi.org/10.1016/j.scitotenv.2019.135305

Li, H., Shi, A., Li, M., Zhang, X., 2013. Effect of pH, temperature, dissolved oxygen, and flow rate of overlying water on heavy metals release from storm sewer sediments. J. Chem. 2013. https://doi.org/10.1155/2013/434012

Li, N.X., Xu, J.F., Yin, W., Chen, Q.Z., Wang, J., Shi, Z.H., 2020. Effect of local watershed landscapes on the nitrogen and phosphorus concentrations in the waterbodies of reservoir bays. Sci. Total Environ. 716. https://doi.org/10.1016/j.scitotenv.2020.137132

Lima, B. P. Framing of waterbodies in the Brazilian Northeast as an instrument for environmental management and sustainability: The case of the Acarape do Meio watershed in Ceará. 271 f. Thesis (Doctorate). Agricultural Engineering Course, Department of Agricultural Engineering, Federal University of Ceará, Fortaleza, 2016.

Lima Neto, I.E., Wiegand, M.C., Carlos de Araújo, J., 2011. Redistribution des sédiments due à un réseau dense de réservoirs dans un grand bassin versant semi-aride du Brésil. Hydrol. Sci. J. 56, 319–333. https://doi.org/10.1080/02626667.2011.553616

Lima Neto, Iran E., 2019. Impact of artificial destratification on water availability of reservoirs in the Brazilian semiarid. Anais da Academia Brasileira de Ciências. 91. http://dx.doi.org/10.1590/0001-3765201920171022.

Lima Neto, I. E., Medeiros, P. H. A., Costa, A. C., Wiegand, M. C., Barros, A. R. M.; Barros, M. U. G. (2022) Assessment of phosphorus loading dynamics in a tropical reservoir with high seasonal water level changes. Sci. Total Environ. 815, 152-162. http://dx.doi.org/10.1016/j.scitotenv.2021.152875.

Lindenmayer, D., Pierson, J., Barton, P., Beger, M., Branquinho, C., Calhoun, A., Caro, T., Greig, H., Gross, J., Heino, J., Hunter, M., Lane, P., Longo, C., Martin, K., McDowell, W.H., Mellin, C., Salo, H., Tulloch, A., Westgate, M., 2015. A new framework for selecting environmental surrogates. Sci. Total Environ. 538, 1029–1038. https://doi.org/10.1016/j.scitotenv.2015.08.056

Lira, C.C.S., Medeiros, P.H.A., Neto, I.E.L., 2020. Modelling the impact of sediment management on the trophic state of a tropical reservoir with high water storage variations. An. Acad. Bras. Cienc. 92, 1–18. https://doi.org/10.1590/0001-3765202020181169

Litchman, E., 2000. Growth rates of phytoplankton under fluctuating light. Freshw. Biol. 44, 223–235. https://doi.org/10.1046/j.1365-2427.2000.00559.x

Liu, Q., Ding, S., Chen, X., Sun, Q., Chen, M., Zhang, C., 2018. Effects of temperature on phosphorus mobilization in sediments in microcosm experiment and in the field. Appl. Geochemistry 88, 158–166. https://doi.org/10.1016/j.apgeochem.2017.07.018

Loh, P.S., Molot, L.A., Nürnberg, G.K., Watson, S.B., Ginn, B., 2013. Evaluating relationships between sediment chemistry and anoxic phosphorus and iron release across three different water bodies. Inl. Waters 3, 105–118. https://doi.org/10.5268/IW-3.1.533

Lopes, F.B., de Andrade, E.M., Meireles, A.C.M., Becker, H., Batista, A.A., 2014. Assessment of the water quality in a large reservoir in semiarid region of Brazil. Rev. Bras. Eng. Agric. e Ambient. 18, 437–445. https://doi.org/10.1590/S1415-43662014000400012

Lun, F., Liu, J., Ciais, P., Nesme, T., Chang, J., Wang, R., Goll, D., Sardans, J., Peñuelas, J., Obersteiner, M., 2018. Global and regional phosphorus budgets in agricultural systems and their implications for phosphorus-use efficiency. Earth Syst. Sci. Data 10, 1–18. https://doi.org/10.5194/essd-10-1-2018

Mackey, R. M. K., Van Mooy, B., Cade-Menun, B. J., Paytan, A. (2019). Reference Module in Life Sciences || Phosphorus Dynamics in the Environment. Encyclopedia of Microbiology. doi:10.1016/B978-0-12-809633-8.20911-4

Mamede, G.L., Araújo, N.A.M., Schneider, C.M., De Araújo, J.C., Herrmann, H.J., 2012. Overspill avalanching in a dense reservoir network. Proc. Natl. Acad. Sci. U. S. A. 109, 7191–7195. https://doi.org/10.1073/pnas.1200398109

Mamede, G.L., Guentner, A., Medeiros, P.H.A., Araújo, J.C. De, Bronstert, A., 2018. Modeling the Effect of Multiple Reservoirs on Water and Sediment Dynamics in a Semiarid Catchment in Brazil 23, 1–13. https://doi.org/10.1061/(ASCE)HE.1943-5584.0001701.

Markovic, S., Liang, A., Watson, S.B., Guo, J., Mugalingam, S., Arhonditsis, G., Morley, A., Dittrich, M., 2019. Biogeochemical mechanisms controlling phosphorus diagenesis and internal loading in a remediated hard water eutrophic embayment. Chem. Geol. 514, 122–137. https://doi.org/10.1016/j.chemgeo.2019.03.031

Marques, L.O.D.A., Taffarello, D., Calijuri, M.D.C., Mendiondo, E.M., Ferreira, M. de S., Cunha, D.G.F., 2019. Phosphorus and thermotolerant coliforms' loads in brazilian watersheds with limited data: Considerations on the integrated analysis of water quality and quantity. Rev. Bras. Recur. Hidricos 24, 1–13. https://doi.org/10.1590/2318-0331.241920170137

Marsden, M.W., Mackay, D.W., 2001. Water quality in Scotland: The view of the regulator. Sci. Total Environ. 265, 369–386. https://doi.org/10.1016/S0048-9697(00)00677-X

Martins, E., Filho, F., Porto, M., 2006. O Processo de Mistura em Reservatórios do Semi-Árido e sua Implicação na Qualidade da Água. Rev. Bras. Recur. Hídricos 11, 109–119. https://doi.org/10.21168/rbrh.v11n4.p109-119

Matias, N., Johnes, P.J., 2012. Catchment Phosphorous Losses : An Export Coefficient Modelling Approach with Scenario Analysis for Water Management 1041–1064. https://doi.org/10.1007/s11269-011-9946-3

Matisoff, G., Kaltenberg, E.M., Steely, R.L., Hummel, S.K., Seo, J., Gibbons, K.J., Bridgeman, T.B., Seo, Y., Behbahani, M., James, W.F., Johnson, L.T., Doan, P., Dittrich, M., Evans, M.A., Chaffin, J.D., 2016. Internal loading of phosphorus in western Lake Erie. J. Great Lakes Res. 42, 775–788. https://doi.org/10.1016/j.jglr.2016.04.004

Meireles A. C. M., Frischkorn H., and Andrade E. M., 2007. Seasonality of water quality in the Edson Queiroz reservoir, Acaraú basin, in the semi-arid region of Ceará. Rev Ciênc Agron, 38(1): 25-31 (in Portuguese).

Mesquita, J.B. de F., Lima Neto, I.E., Raabe, A., de Araújo, J.C., 2020. The influence of hydroclimatic conditions and water quality on evaporation rates of a tropical lake. J. Hydrol. 590, 125456. https://doi.org/10.1016/j.jhydrol.2020.125456

Mockler, E.M., Deakin, J., Archbold, M., Gill, L., Daly, D., Bruen, M., 2017. Sources of nitrogen and phosphorus emissions to Irish rivers and coastal waters: Estimates from a nutrient load apportionment framework. Sci. Total Environ. 601–602, 326–339. https://doi.org/10.1016/j.scitotenv.2017.05.186

Moss, B., 2011. Allied attack: climate change and eutrophication. Inl. Waters 1, 101–105. https://doi.org/10.5268/iw-1.2.359

Moura, Diana Souza, De Almeida, A.S.O., Pestana, C.J., Girão, L.G., Capelo-Neto, J., 2020a. Internal loading potential of phosphorus in reservoirs along a semiarid watershed. Rev. Bras. Recur. Hidricos 25, 1–11. https://doi.org/10.1590/2318-0331.252020180023

Moura, Diana S., Lima Neto, I.E., Clemente, A., Oliveira, S., Pestana, C.J., Aparecida de Melo, M., Capelo-Neto, J., 2020b. Modeling phosphorus exchange between bottom sediment and water in tropical semiarid reservoirs. Chemosphere 246. https://doi.org/10.1016/j.chemosphere.2019.125686

Mouri, G., Takizawa, S., Oki, T., 2011. Spatial and temporal variation in nutrient parameters in stream water in a rural-urban catchment, Shikoku, Japan: Effects of land cover and human impact. J. Environ. Manage. 92, 1837–1848.

https://doi.org/10.1016/j.jenvman.2011.03.005

Nicholls, K.H., 1999. Effects of temperature and other factors on summer phosphorus in the inner Bay of Quinte, Lake Ontario: Implications for climate warming. J. Great Lakes Res. 25, 250–262. https://doi.org/10.1016/S0380-1330(99)70734-3

Nikolai, S.J., Dzialowski, A.R., 2014. Effects of internal phosphorus loading on nutrient limitation in a eutrophic reservoir. Limnologica 49, 33–41. https://doi.org/10.1016/j.limno.2014.08.005

Noori. R., Ansari, E., Jeong, Y., Aradpour, S., Maghrebi, M., Hosseinzadeh, M., Bateni, Sayed M. 2021a. Hyper-Nutrient Enrichment Status in the Sabalan Lake, Iran. Water. 13, 2874, 1. http://dx.doi.org/10.3390/w13202874.

Noori, R., Berndtsson, R., Adamowski, J. F., Abyaneh, M. R., 2018. Temporal and depth variation of water quality due to thermal stratification in Karkheh Reservoir, Iran. Journal of Hydrology: Regional Studies. 19, 279-286. http://dx.doi.org/10.1016/j.ejrh.2018.10.003.

Noori, R., Ansari, E., Bhattarai, R., Tang, Q., Aradpour, S., Maghrebi, M., Haghighi, A. T., Bengtsson, L., Kløve, B. 2021b. Complex dynamics of water quality mixing in a warm mono-mictic reservoir. Sci. Total Environ. 777, http://dx.doi.org/10.1016/j.scitotenv.2021.146097

North, R.L., Johansson, J., Vandergucht, D.M., Doig, L.E., Liber, K., Lindenschmidt, K.E., Baulch, H., Hudson, J.J., 2015. Evidence for internal phosphorus loading in a large prairie reservoir (Lake Diefenbaker, Saskatchewan). J. Great Lakes Res. 41, 91–99. https://doi.org/10.1016/j.jglr.2015.07.003

Nurnberg, G.K., 2009. Assessing internal phosphorus load - Problems to be solved. Lake Reserv. Manag. 25, 419–432. https://doi.org/10.1080/00357520903458848

Nurnberg, G.K., 1988. Prediction ease Rates from in Anoxic Lake. Can.J.Fish.Aquat.Sci 45, 453–462.

Nürnberg, G.K., 2019. Quantification of Anoxia and Hypoxia in Water Bodies. Encycl. Water 1–9. https://doi.org/10.1002/9781119300762.wsts0081

Nürnberg, G.K., 2005. Quantification of internal phosphorus loading in polymictic lakes. SIL Proceedings, 1922-2010 29, 623–626. https://doi.org/10.1080/03680770.2005.11902753

Nürnberg, G.K., 1995. Quantifying anoxia in lakes. Limnol. Oceanogr. 40, 1100–1111. https://doi.org/10.4319/lo.1995.40.6.1100

Nürnberg, G.K., Howell, T., Palmer, M., 2019. Long-term impact of Central Basin hypoxia and internal phosphorus loading on north shore water quality in Lake Erie. Inl. Waters 9,

362–373. https://doi.org/10.1080/20442041.2019.1568072

Nürnberg, G.K., LaZerte, B.D., 2016. More than 20 years of estimated internal phosphorus loading in polymictic, eutrophic Lake Winnipeg, Manitoba. J. Great Lakes Res. 42, 18–27. https://doi.org/10.1016/j.jglr.2015.11.003

Nürnberg, G.K., LaZerte, B.D., Loh, P.S., Molot, L.A., 2013. Quantification of internal phosphorus load in large, partially polymictic and mesotrophic Lake Simcoe, Ontario. J. Great Lakes Res. 39, 271–279. https://doi.org/10.1016/j.jglr.2013.03.017

Nurnberg, G.K., Shaw, M., Dillon, P.J., McQueen, D.J., 1986. Internal phosphorus load in an oligotrophic Precambrian Shield Lake with an anoxic hypolimnion. Can. J. Fish. Aquat. Sci. 43, 574–580. https://doi.org/10.1139/f86-068

Nürnberg, G.K., Tarvainen, M., Ventelä, A.M., Sarvala, J., 2012. Internal phosphorus load estimation during biomanipulation in a large polymictic and mesotrophic lake. Inl. Waters 2, 147–162. https://doi.org/10.5268/IW-2.3.469

Oliveira, K.F., Lacerda, L.D., Peres, T.F., Bezerra, M.F., da Silva Dias, F.J., 2015. Emission factor and balance of mercury in fish farms in an artificial reservoir in NE Brazil. Environ. Sci. Pollut. Res. 22, 18278–18287. https://doi.org/10.1007/s11356-015-5102-6

Orihe, D.M., Baulch, H.M., Casson, N.J., North, R.L., Parsons, C.T., Seckar, D.C.M., Venkiteswaran, J.J., 2017. Internal phosphorus loading in canadian fresh waters: A critical review and data analysis. Can. J. Fish. Aquat. Sci. 74, 2005–2029. https://doi.org/10.1139/cjfas-2016-0500

Orihel, D.M., Schindler, D.W., Ballard, N.C., Graham, M.D., O'Connell, D.W., Wilson, L.R., Vinebrooke, R.D., 2015. The "nutrient pump:" Iron-poor sediments fuel low nitrogen-to-phosphorus ratios and cyanobacterial blooms in polymictic lakes. Limnol. Oceanogr. 60, 856–871. https://doi.org/10.1002/lno.10076

Ostrofsky, M.L., Marbach, R.M., 2019. Predicting internal phosphorus loading in stratified lakes. Aquat. Sci. 81, 1–9. https://doi.org/10.1007/s00027-018-0618-8

Pacheco, C.H.A., Lima Neto, I.E., 2017. Effect of artificial circulation on the removal kinetics of cyanobacteria in a hypereutrophic shallow lake. J. Environ. Eng. (United States) 143, 1–8. https://doi.org/10.1061/(ASCE)EE.1943-7870.0001289

Paula Filho, F.J., Sampaio, A.D. de S., Menezes, J.M.C., Costa, C.T.F. da, Santiago, M.O., 2019. Land uses, Nitrogen and Phosphorus estimated fluxes in a Brazilian semi-arid watershed. J. Arid Environ. 163, 41–49. https://doi.org/10.1016/j.jaridenv.2019.01.001

Perrin, J.L., Salles, C., Bancon-Montigny, C., Raïs, N., Chahinian, N., Dowse, L., Rodier, C., Tournoud, M.G., 2018. Comparison of index systems for rating water quality in

intermittent rivers. Environ. Monit. Assess. https://doi.org/10.1007/s10661-017-6396-2

Qin, L., Zeng, Q., Zhang, W., Li, X., Steinman, A.D., Du, X., 2016. Estimating internal P loading in a deep water reservoir of northern China using three different methods. Environ. Sci. Pollut. Res. 23, 18512–18523. https://doi.org/10.1007/s11356-016-7035-0

Rattan, K.J., Corriveau, J.C., Brua, R.B., Culp, J.M., Yates, A.G., Chambers, P.A., 2017. Quantifying seasonal variation in total phosphorus and nitrogen from prairie streams in the Red River Basin, Manitoba Canada. Sci. Total Environ. 575, 649–659. https://doi.org/10.1016/j.scitotenv.2016.09.073

Rocha Junior, C.A.N. da, Costa, M.R.A. da, Menezes, R.F., Attayde, J.L., Becker, V., 2018. Water volume reduction increases eutrophication risk in tropical semi-arid reservoirs. Acta Limnol. Bras. 30. https://doi.org/10.1590/s2179-975x2117

Rocha, M. J.D., Lima Neto, I.E., 2021a. Phosphorus mass balance and input load estimation from the wet and dry periods in tropical semiarid reservoirs. Environ. Sci. Pollut. Res. https://doi.org/10.1007/s11356-021-16251-w

Rocha, M. J.D., Lima Neto, I.E., 2021b. Modeling flow-related phosphorus inputs to tropical semiarid reservoirs. J. Environ. Manage. 295, 113123. https://doi.org/10.1016/j.jenvman.2021.113123

Rocha, S. M. G., Mesquita, J. B. F., Lima Neto, I. E., 2019. Análise e modelagem das relações entre nutrientes e fitoplâncton em reservatórios do Ceará. Revista Brasileira de Ciências Ambientais, 54, 134-147.

Salas, H., Martino, P. A., 1991. Simplified phosphorus trophic state model for warm-water tropical lakes. Water Research, 25, 341-350. https://doi.org/10.1016/0043-1354(91)90015-I

Santos, J.A. dos, de Oliveira, K.F., da Silva Araújo, I.C., Avelino, I.I.F., de Sousa Cajuí, K.N., de Lacerda, L.D., Marins, R.V., 2016. Phosphorus partitioning in sediments from a tropical reservoir during a strong period of drought. Environ. Sci. Pollut. Res. 23, 24237–24247. https://doi.org/10.1007/s11356-016-7629-6

Santos, J.A., Marins, R. V., Aguiar, J.E., Chalar, G., Silva, F.A.T.F., Lacerda, L.D., 2017. Hydrochemistry and trophic state change in a large reservoir in the Brazilian northeast region under intense drought conditions. J. Limnol. 76, 41–51. https://doi.org/10.4081/jlimnol.2016.1433

SAS. SAS User Guide. Cary, North Carolina, USA: SAS Institute Inc.; 2018. Taylor MP.

Schauser, I., Chorus, I., 2009. Water and phosphorus mass balance of Lake Tegel and Schlachtensee - A modelling approach. Water Res. 43, 1788–1800.

https://doi.org/10.1016/j.watres.2009.01.007

Seitz, C., Scordo, F., Vitale, A.J., Vélez, M.I., Perillo, G.M.E., 2020. The effects of extreme drought events on the morphometry of shallow lakes: Implications for sediment resuspension and littoral and pelagic zone distribution. J. South Am. Earth Sci. 103, 102743. https://doi.org/10.1016/j.jsames.2020.102743

Sharpley, A., Jarvie, H.P., Buda, A., May, L., Spears, B., Kleinman, P., 2013. Phosphorus Legacy: Overcoming the Effects of Past Management Practices to Mitigate Future Water Quality Impairment. J. Environ. Qual. 42, 1308–1326. https://doi.org/10.2134/jeq2013.03.0098

Shimoda, Y., Arhonditsis, G.B., 2015. Integrating hierarchical Bayes with phosphorus loading modelling. Ecol. Inform. 29, 77–91. https://doi.org/10.1016/j.ecoinf.2015.07.005

Shinohara, R., Hiroki, M., Kohzu, A., Imai, A., Inoue, T., Furusato, E., Komatsu, K., Satou, T., Tomioka, N., Shimotori, K., Miura, S., 2017. Role of organic phosphorus in sediment in a shallow eutrophic lake. Water Resour. Res. 53, 7175–7189. https://doi.org/10.1002/2017WR020486

Snortheim, C.A., Hanson, P.C., McMahon, K.D., Read, J.S., Carey, C.C., Dugan, H.A., 2017. Meteorological drivers of hypolimnetic anoxia in a eutrophic, north temperate lake. Ecol. Modell. 343, 39–53. https://doi.org/10.1016/j.ecolmodel.2016.10.014

Song, K., Adams, C.J., Burgin, A.J., 2017. Relative importance of external and internal phosphorus loadings on affecting lake water quality in agricultural landscapes. Ecol. Eng. 108, 482–488. https://doi.org/10.1016/j.ecoleng.2017.06.008

Souza Filho, F. A, Martins, E. S. P. R., Porto, M. F. A., 2006. The Mixing Process in Semi-Arid Reservoirs and its Implication in Water Quality. Rev Bras Recur Hídricos 11, 109-119.

Spears, B.M., Carvalho, L., Perkins, R., Kirika, A., Paterson, D.M., 2012. Long-term variation and regulation of internal phosphorus loading in Loch Leven. Hydrobiologia 681, 23–33. https://doi.org/10.1007/s10750-011-0921-z

Sperling, M. V. (2007). Wastewater Cahracteristcs, Treatment and Disposal, Iwa Publishing, New York, 292 pp.

Stefanidis, K., Varlas, G., Vourka, A., Papadopoulos, A., Dimitriou, E., 2021. Delineating the relative contribution of climate related variables to chlorophyll-a and phytoplankton biomass in lakes using the ERA5-Land climate reanalysis data. Water Res. 196, 117053. https://doi.org/10.1016/j.watres.2021.117053

Tammeorg, O., Möls, T., Niemistö, J., Holmroos, H., Horppila, J., 2017. The actual role of

oxygen deficit in the linkage of the water quality and benthic phosphorus release: Potential implications for lake restoration. Sci. Total Environ. 599–600, 732–738. https://doi.org/10.1016/j.scitotenv.2017.04.244

Tammeorg, O., Nürnberg, G., Niemistö, J., Haldna, M., Horppila, J., 2020. Internal phosphorus loading due to sediment anoxia in shallow areas: implications for lake aeration treatments. Aquat. Sci. 82, 1–10. https://doi.org/10.1007/s00027-020-00724-0

Toledo, A.P.J., Talarico, M., Chinez, S.J., Agudo, E.G., 1983. The application of simplified models for the evaluation of the eutrophication process in tropical lakes and reservoirs. In: Brazilian Congress of Sanitary and Environmental Engineering, Santa Catarina. Brazilian Association of Sanitary and Environmental Engineering. p.1-34 (in portuguese).

Toné, A., Lima Neto, I., 2019. Modelagem simplificada do fósforo total em lagos e reservatórios brasileiros. Rev. DAE 221, 142–156. https://doi.org/10.36659/dae.2020.012

Tong, Y., Liang, T., Wang, L., Li, K., 2017. Simulation on phosphorus release characteristics of Poyang Lake sediments under variable water levels and velocities. J. Geogr. Sci. 27, 697–710. https://doi.org/10.1007/s11442-017-1401-9

Torres, I.C., Resck, R.P., Pinto-Coelho, R.M. 2007. Mass balance estimation of nitrogen, carbon, phosphorus and total suspended solids in the urban eutrophic, Pampulha reservoir, Brazil. Acta Limnol. Bras. 19,1, 79-91.

Townsend, S.A., 1999. The seasonal pattern of dissolved oxygen, and hypolimnetic deoxygenation, in two tropical Australian reservoirs. Lakes Reserv. Res. Manag. 4, 41–53. https://doi.org/10.1046/j.1440-1770.1999.00077.x

Tsakiris, G., Alexakis, D., 2015. Water quality models : An overview 33–46.

Vollenweider, R. A., 1968. Water management research. Scientific fundamentals of the eutrophication of lakes and flowing waters with particular reference to nitrogen and phosphorus as factors in eutrophication. Organization for Economic Co-operation and De. Limnology and Oceanography, 15, 169–170. https://doi.org/10.4319/lo.1970.15.1.0169

Vollenweider, R. A., 1976. Advances in defining critical loading levels for phosphorus in lake eutrophication. Memorie Dell'istituto Italiano di Idrobiologia, 33, 53-83.

Von Schiller, D., Bernal, S., Dahm, C.N., Martí, E., 2017. Nutrient and Organic Matter Dynamics in Intermittent Rivers and Ephemeral Streams, in: Intermittent Rivers and Ephemeral Streams: Ecology and Management. Elsevier Inc., pp. 135–160. https://doi.org/10.1016/B978-0-12-803835-2.00006-1

Wang, J., Chen, J., Ding, S., Luo, J., Xu, Y., 2015. Effects of temperature on phosphorus release in sediments of Hongfeng Lake, southwest China: an experimental study using diffusive gradients in thin-films (DGT) technique. Environ. Earth Sci. 74, 5885–5894. https://doi.org/10.1007/s12665-015-4612-3

Wang, M., Zhang, H., Du, C., Zhang, W., Shen, J., Yang, S., Yang, L., 2021. Spatiotemporal differences in phosphorus release potential of bloom-forming cyanobacteria in Lake Taihu. Environ. Pollut. 271, 116294. https://doi.org/10.1016/j.envpol.2020.116294

Westgate, M.J., Barton, P.S., Lane, P.W., Lindenmayer, D.B., 2014. Global meta-analysis reveals low consistency of biodiversity congruence relationships. Nat. Commun. 5, 1–8. https://doi.org/10.1038/ncomms4899

Wiegand, M.C., do Nascimento, A.T.P., Costa, A.C., Lima Neto, I.E., 2021. Trophic state changes of semi-arid reservoirs as a function of the hydro-climatic variability. J. Arid Environ. 184. https://doi.org/10.1016/j.jaridenv.2020.104321

Willmott, C. J. 1981. On the validation of models, Phys. Geogr., 2, 184-194.

Wu, P., Qin, B., Yu, G., 2016. Estimates of long-term water total phosphorus (TP) concentrations in three large shallow lakes in the Yangtze River basin, China. Environ. Sci. Pollut. Res. 23, 4938–4948. https://doi.org/10.1007/s11356-015-5736-4

Xu, Z., Yu, C., Sun, H., Yang, Z., 2020. The response of sediment phosphorus retention and release to reservoir operations: Numerical simulation and surrogate model development. J. Clean. Prod. 271, 122688. https://doi.org/10.1016/j.jclepro.2020.122688

Yang, J., Lv, H., Yang, J., Liu, L., Yu, X., Chen, H., 2016. Decline in water level boosts cyanobacteria dominance in subtropical reservoirs. Sci. Total Environ. 557–558, 445–452. https://doi.org/10.1016/j.scitotenv.2016.03.094

Yokom, S., Axler, R., McDonald, M., Wilcox, D., 1997. Recovery of a mine pit lake from aquacultural phosphorus enrichment: Model predictions and mechanisms. Ecol. Eng. 8, 195–218. https://doi.org/10.1016/S0925-8574(97)00010-4

Zhang, B., Ding, W., Xu, B., Wang, L., Li, Y., Zhang, C., 2020. Spatial characteristics of total phosphorus loads from different sources in the Lancang River Basin. Sci. Total Environ. 722. https://doi.org/10.1016/j.scitotenv.2020.137863

Zhang, C., Yan, Q., Kuczyńska-Kippen, N., Gao, X., 2020. An Ensemble Kalman Filter approach to assess the effects of hydrological variability, water diversion, and meteorological forcing on the total phosphorus concentration in a shallow reservoir. Sci. Total Environ. 724. https://doi.org/10.1016/j.scitotenv.2020.138215

Zhang, H., Boegman, L., Scavia, D., Culver, D.A., 2016. Spatial distributions of external and

internal phosphorus loads in Lake Erie and their impacts on phytoplankton and water quality. J. Great Lakes Res. 42, 1212–1227. https://doi.org/10.1016/j.jglr.2016.09.005

Zhang, W., Xu, Q., Wang, X., Hu, X., Wang, C., Pang, Y., Hu, Y., Zhao, Y., Zhao, X., 2017. Spatiotemporal distribution of eutrophication in Lake Tai as affected by wind. Water (Switzerland) 9. https://doi.org/10.3390/w9030200

Zhang, Y., He, F., Liu, Z., Liu, B., Zhou, Q., Wu, Z., 2016. Release characteristics of sediment phosphorus in all fractions of West Lake, Hang Zhou, China. Ecol. Eng. 95, 645–651. https://doi.org/10.1016/j.ecoleng.2016.06.014

Zhang, Z., Chen, X., Xu, C.Y., Hong, Y., Hardy, J., Sun, Z., 2015. Examining the influence of river-lake interaction on the drought and water resources in the Poyang Lake basin. J. Hydrol. 522, 510–521. https://doi.org/10.1016/j.jhydrol.2015.01.008

Zheng, S. sha, Wang, P. fang, Wang, C., Hou, J., 2015. Sediment resuspension under action of wind in Taihu Lake, China. Int. J. Sediment Res. 30, 48–62. https://doi.org/10.1016/S1001-6279(15)60005-1

Zhu, G., Yang, Y., 2018. Variation laws and release characteristics of phosphorus on surface sediment of Dongting Lake. Environ. Sci. Pollut. Res. 25, 12342–12351. https://doi.org/10.1007/s11356-018-1777-9

Zou, R., Wu, Z., Zhao, L., Elser, J.J., Yu, Y., Chen, Y., Liu, Y., 2020. Seasonal algal blooms support sediment release of phosphorus via positive feedback in a eutrophic lake: Insights from a nutrient flux tracking modeling. Ecol. Modell. 416, 108881. https://doi.org/10.1016/j.ecolmodel.2019.108881

Appendix

Figure A1 - Average precipitation over the catchments of the twenty studied reservoirs described in Chapter 3. The data was provided by the Foundation of Meteorology and Water Resources of the State of Ceará (FUNCEME).

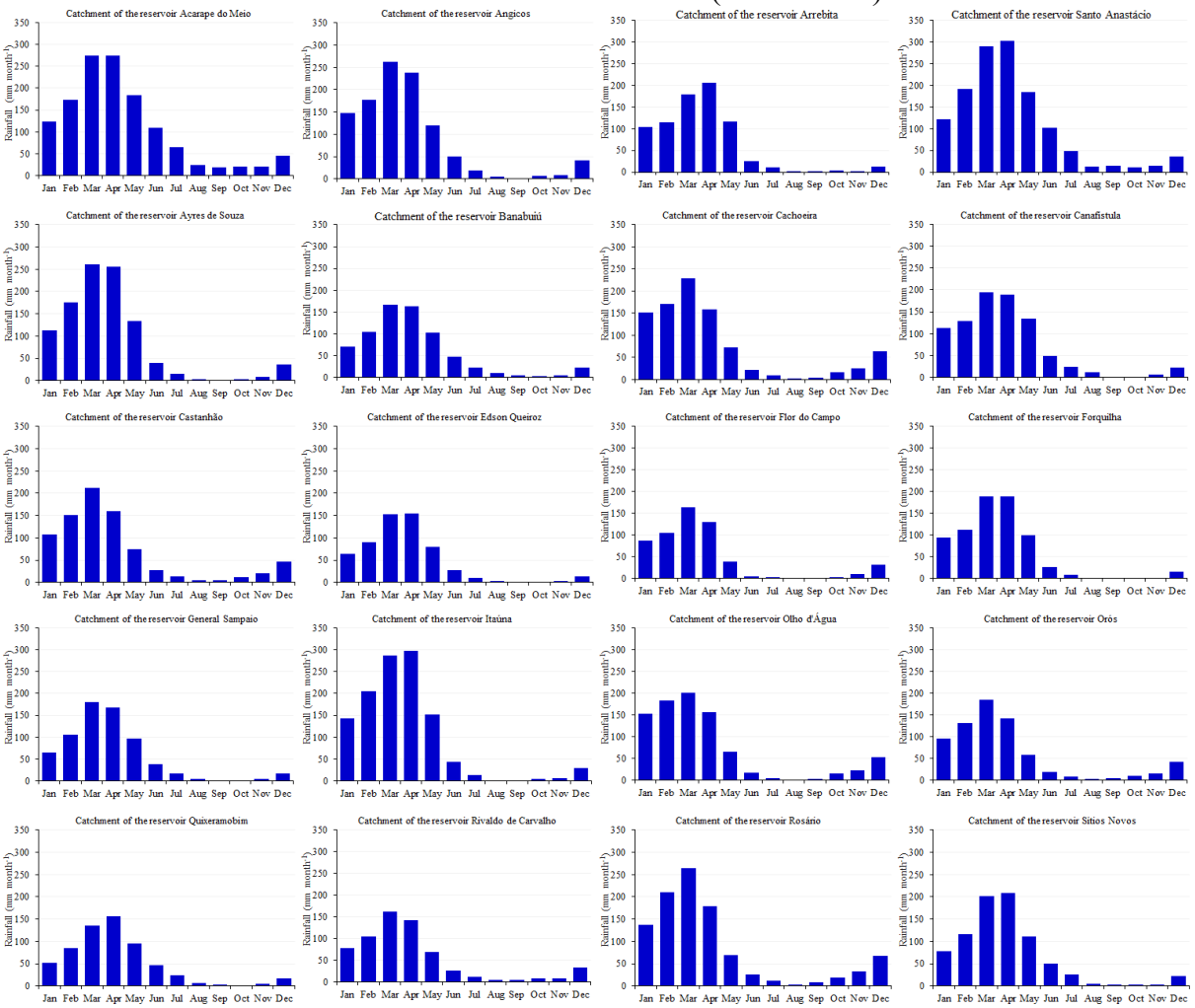

Figure A2 - Contour plots for the vertical profile of TP concentration (mg L^{-1}) in the sampling point of the reservoirs described in Chapter 4.

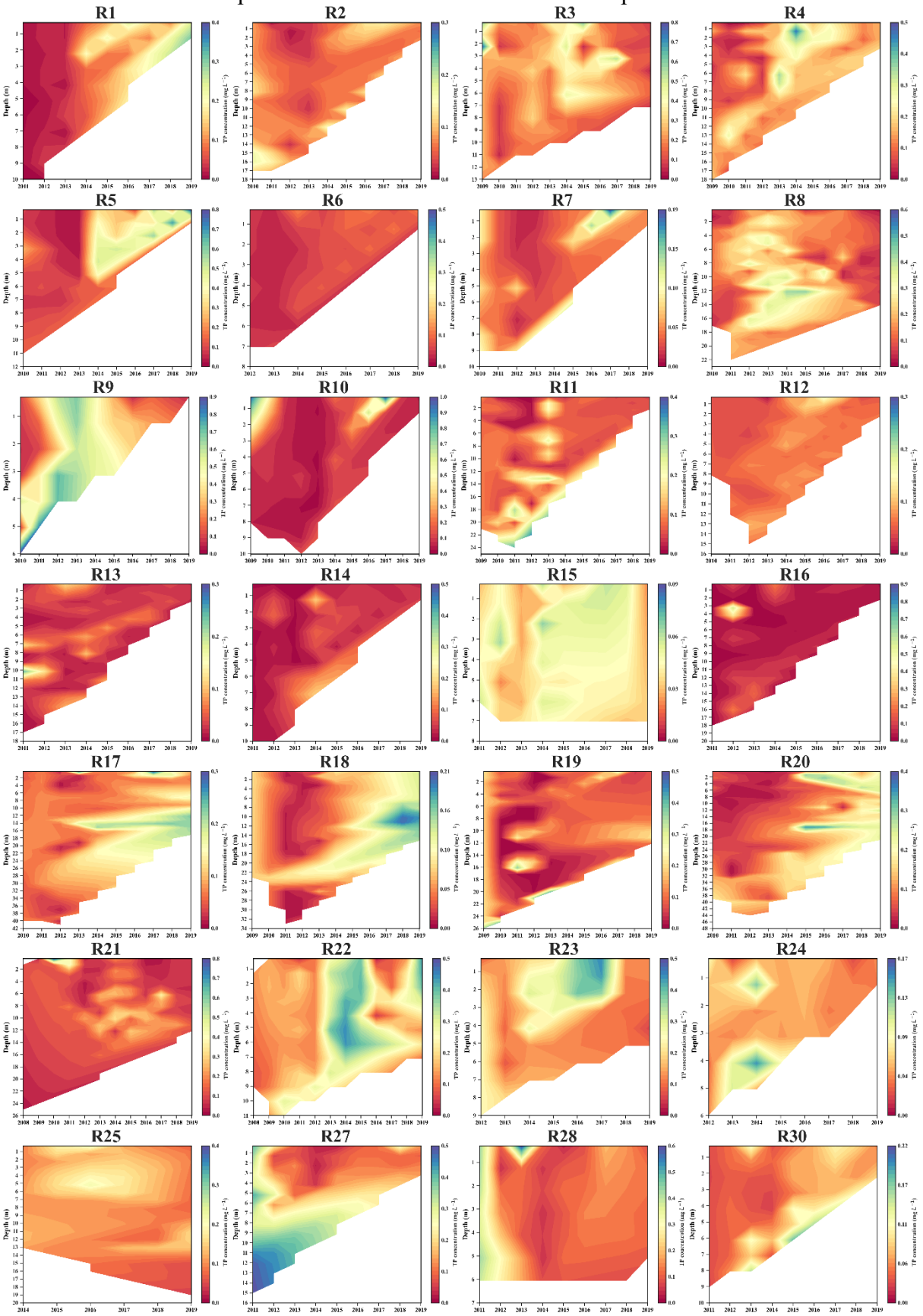

Figure A3 - Contour plots for the vertical profile of DO concentration (mg L^{-1}) in the sampling point of the reservoirs described in Chapter 4.

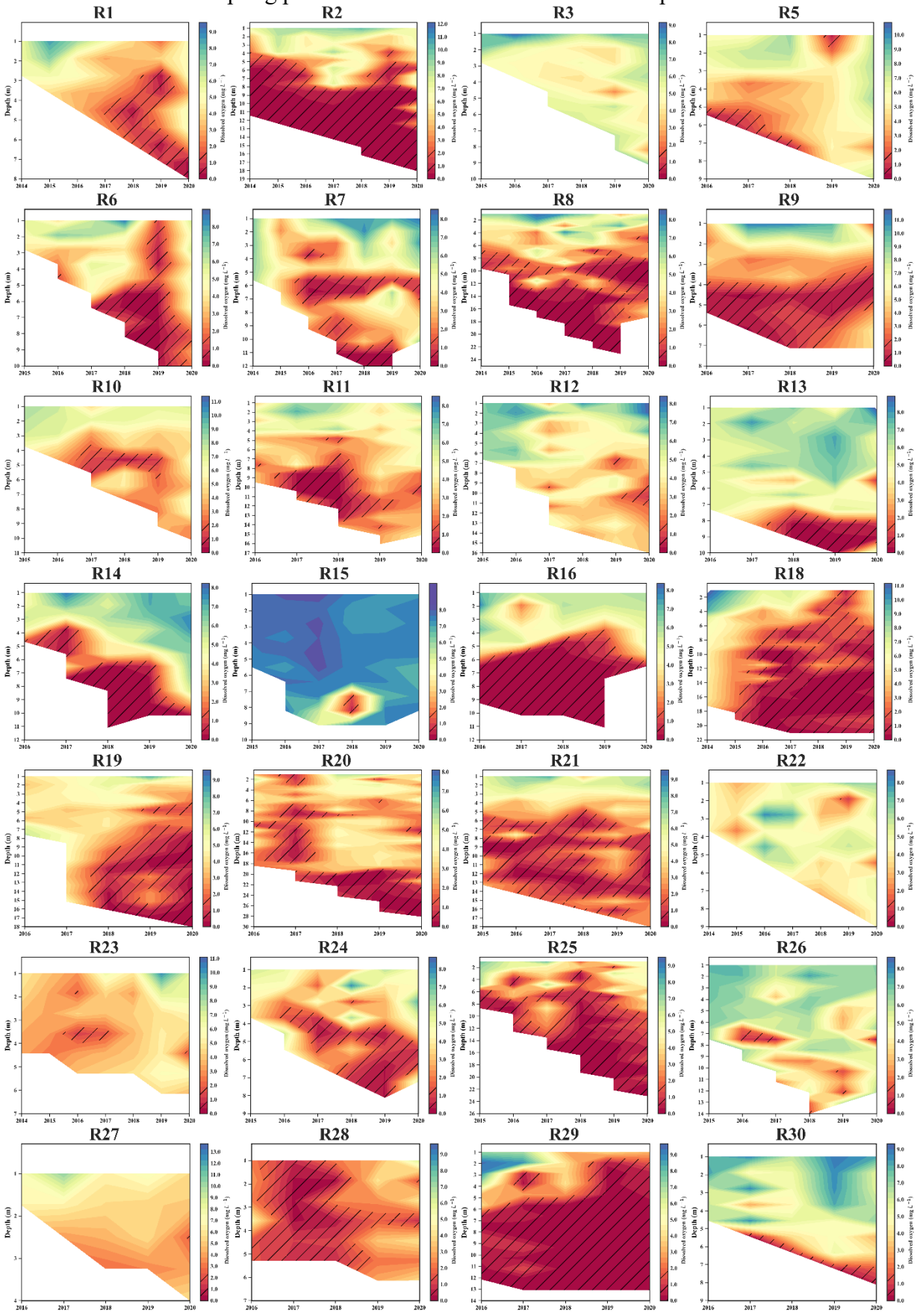

Figure A4 - Contour plots for the vertical profile of pH in the sampling point of the reservoirs described in Chapter 4.

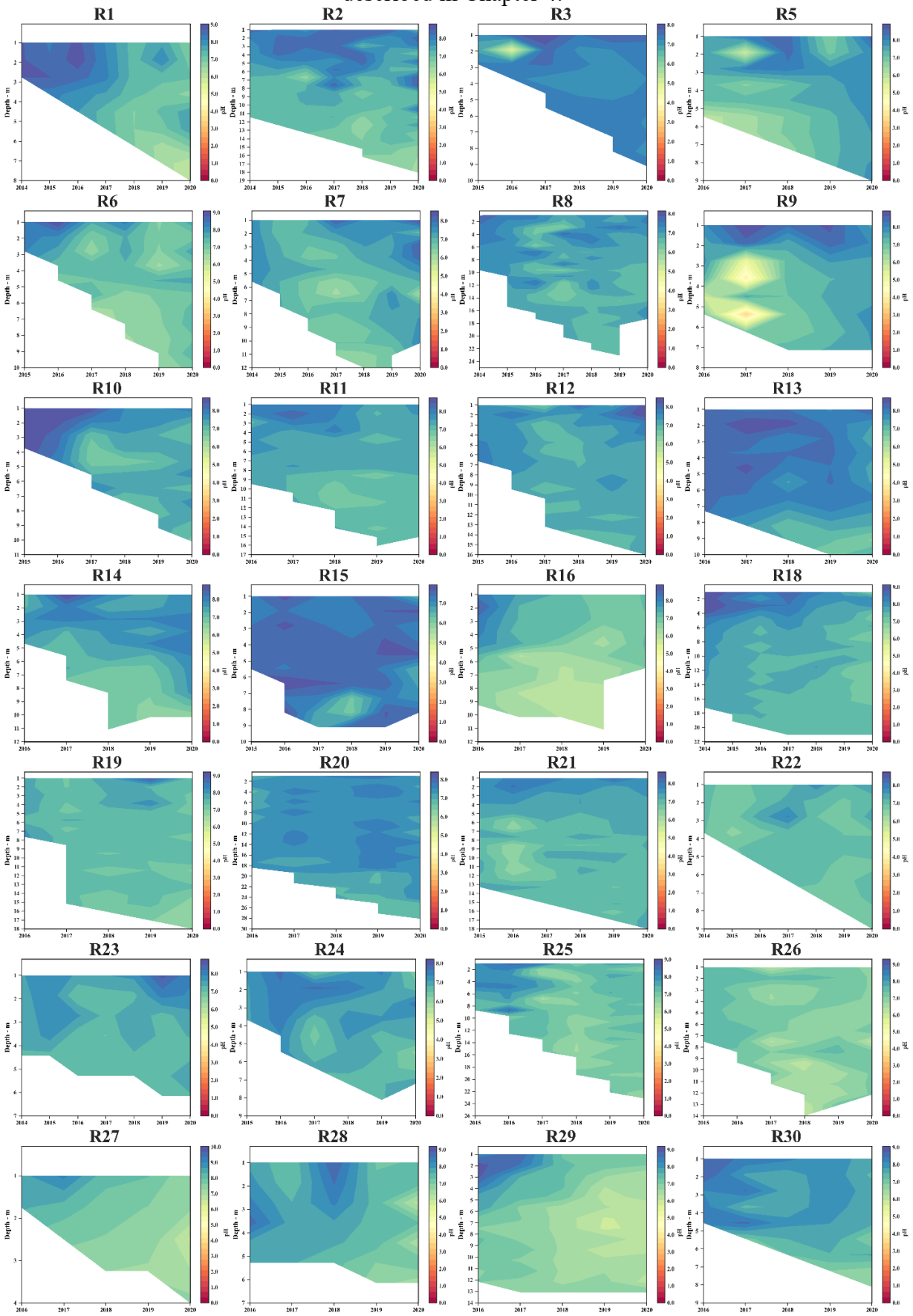

Figure A5 - Contour plots for the vertical profile of temperature the sampling point of the reservoirs described in Chapter 4.

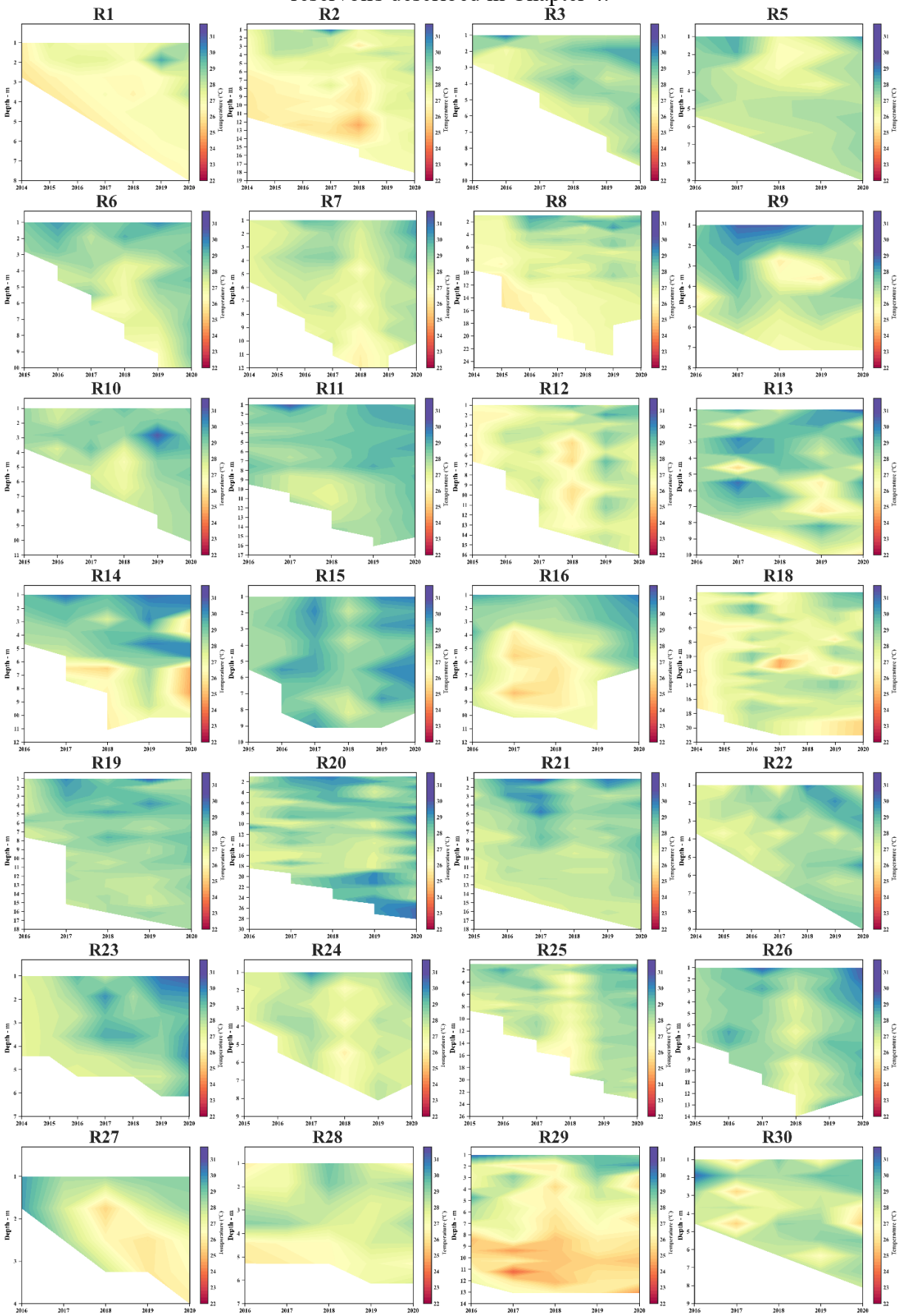

Figure A6 – Average monthly inflow over the study period for the catchment of the study sites of Chapter 4. Data from the water balance provided by the Water Management Company of the State of Ceará.

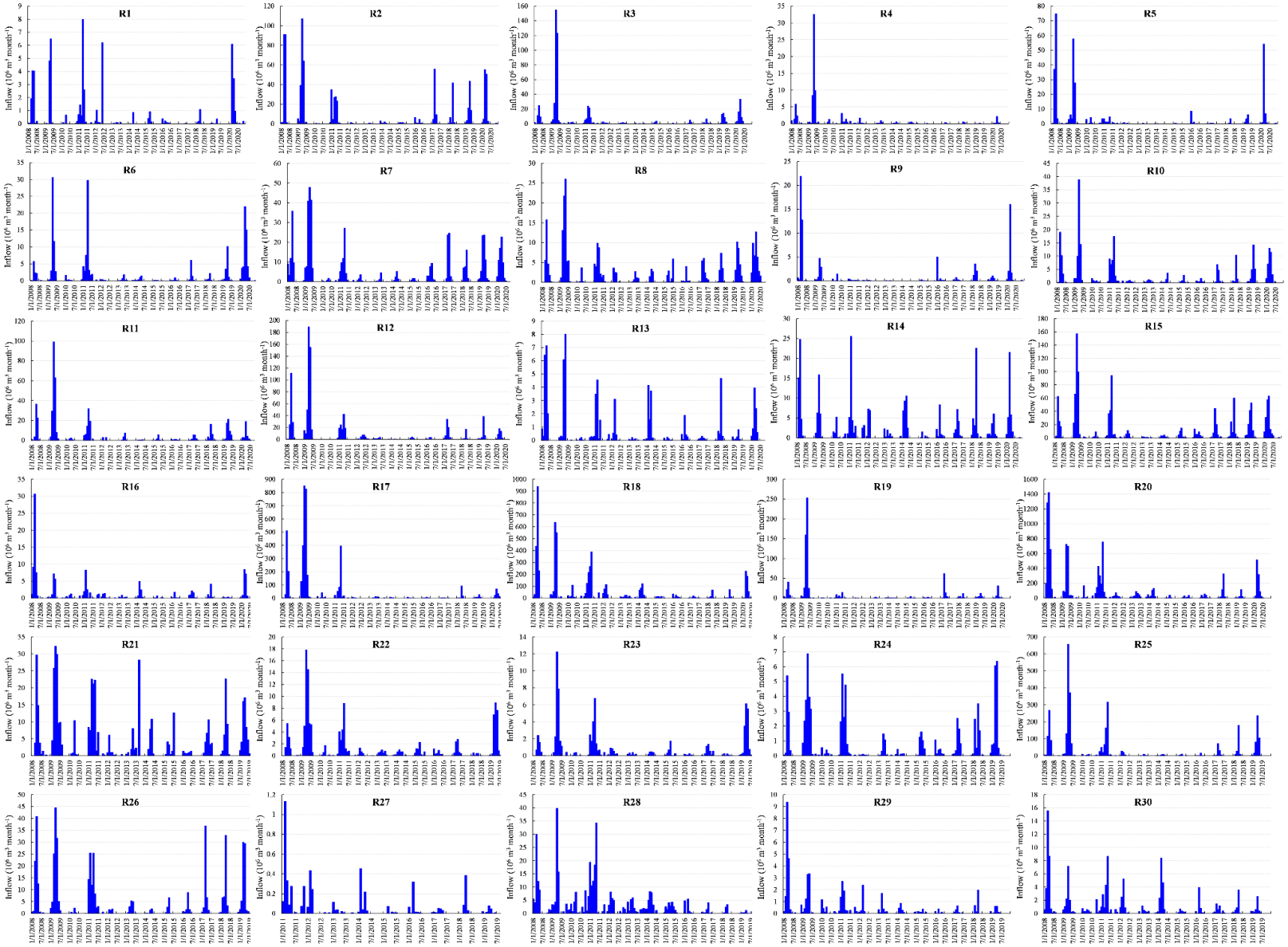

Figure A7 – Historical average monthly rainfall for study sites of Chapter 4. Data provided by the Foundation of Meteorology and Water Resources of the State of Ceará.

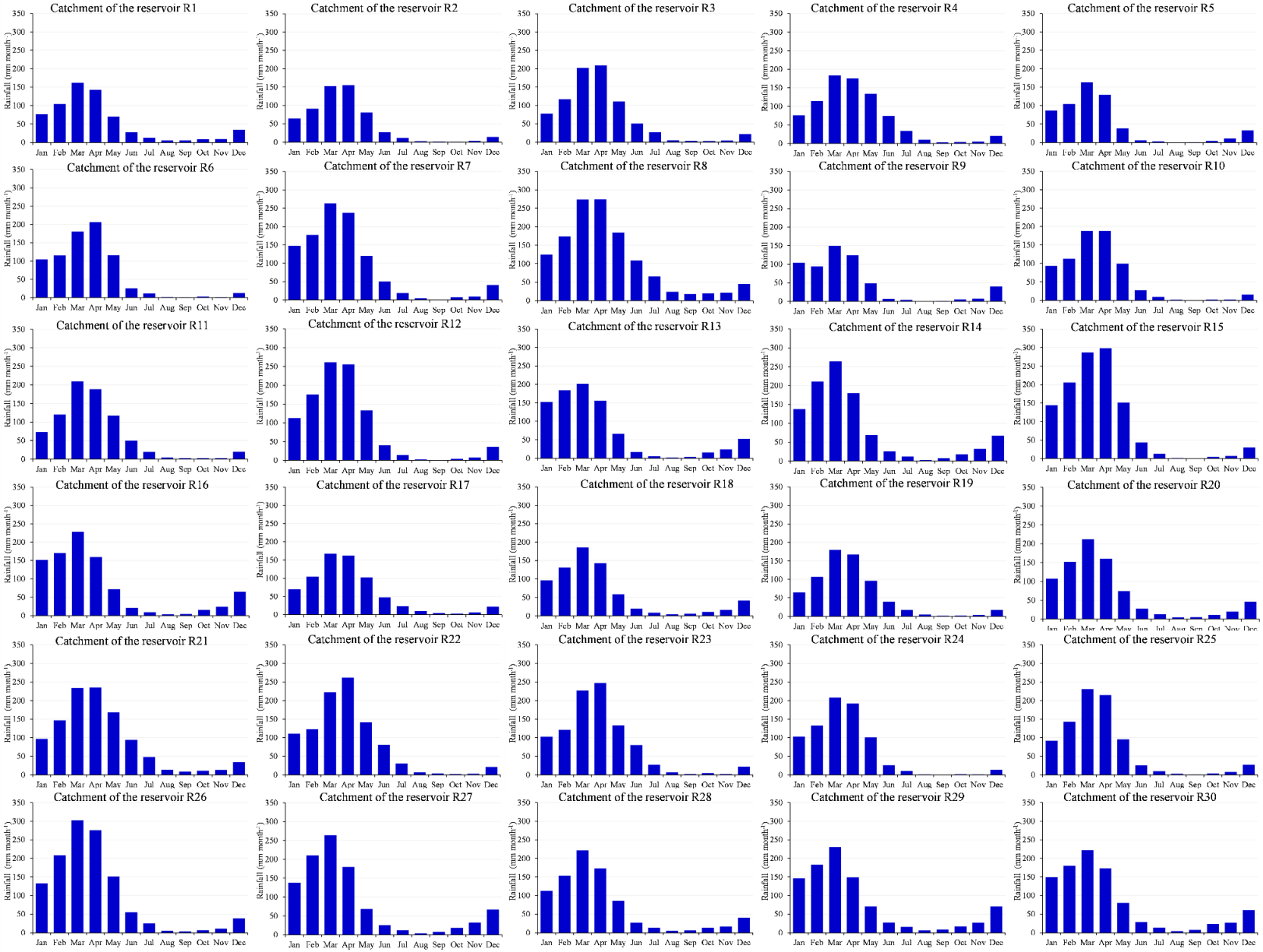

Figure A8 – Total phosphorus point source and non-point source load characterization for the catchments of the study sites of Chapter 4.

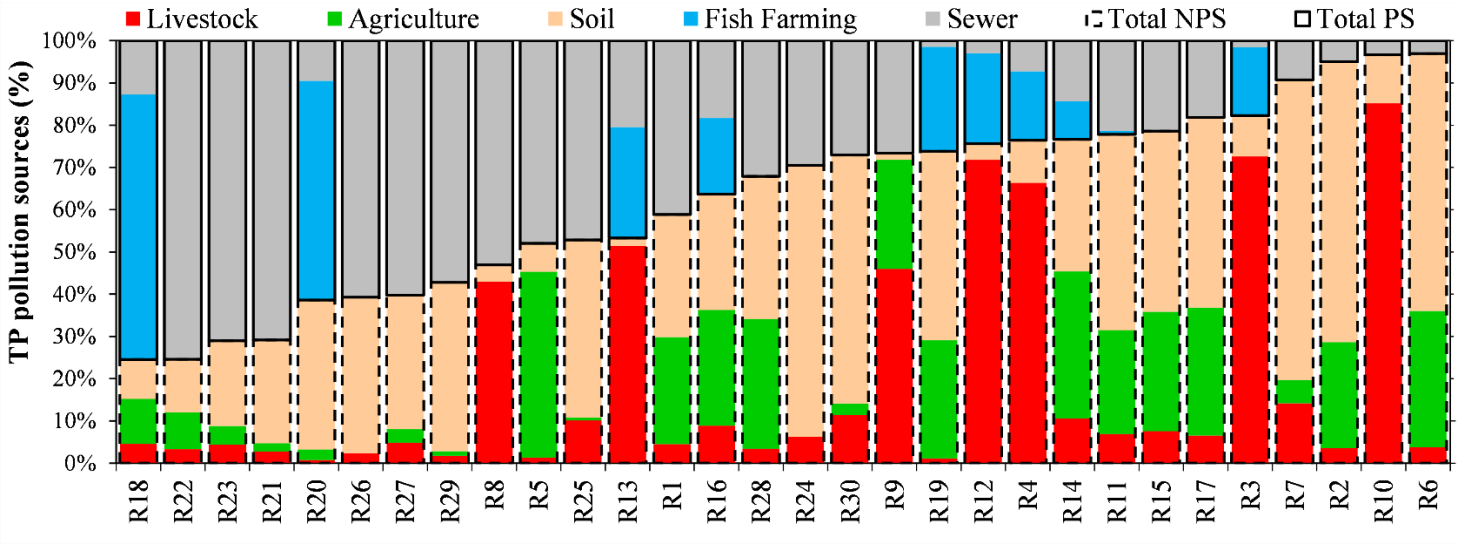

Figure A9 – Daily reservoir volume and monthly inflow of the study sites of Chapter 2.

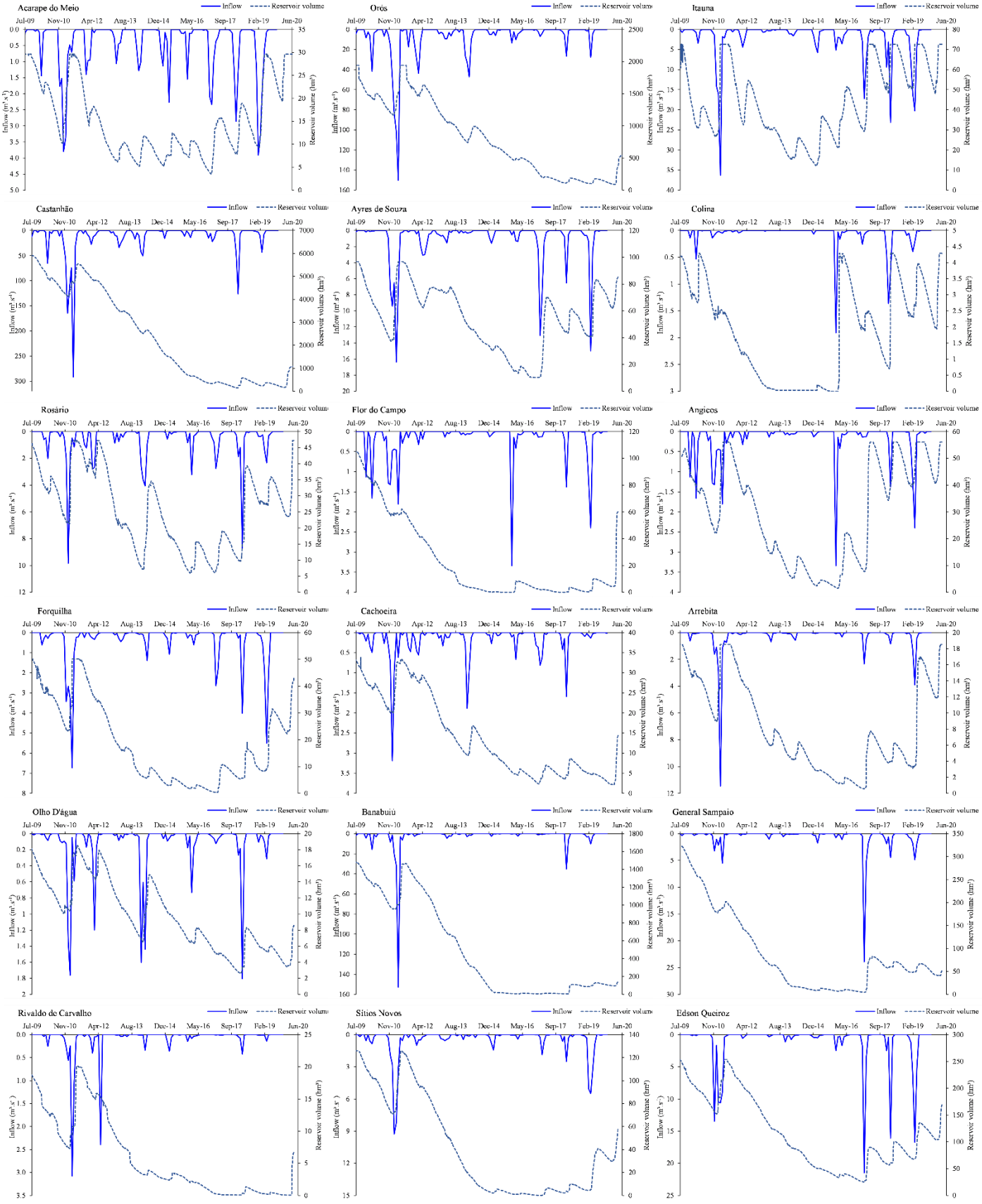

Table A1 - Descriptive statistics of the estimated net P release rates (mg m^{-2} dry $period^{-1}$)

ID	Min.	25th	50th	Med.	75th	Max.	CV
Min.	-4763.09	-399.80	219.37	-63.15	344.20	532.13	0.18
25th	-720.16	210.65	584.75	601.41	878.22	1388.89	0.51
50th	73.50	406.77	890.77	1007.40	1360.06	1903.71	0.70
Med.	-418.14	485.22	1011.67	988.68	1506.75	2306.31	0.68
75th	310.74	826.28	1290.35	1243.59	1843.76	2877.04	0.86
Max.	1595.17	1617.17	2400.55	2373.56	3514.83	5930.63	1.20

Table A2 - Parameters of the adjusted logarithmic regression models along with the metrics of the model performance presented in Figure 4.8

	Parameters of the logarithmic regression model		Metrics of performance		
ID	a	b	r^2	r_a^2	MAPE
R1	439.05	1053.86	0.58	0.50	36%
R2	418.03	3384.54	0.52	0.44	9%
R3	226.68	1184.94	0.73	0.70	44%
R4	380.66	917.35	0.64	0.58	65%
R5	1273.09	3335.4	0.76	0.71	53%
R6	295.32	813.41	0.7	0.65	24%
R7	582.84	2307.11	0.75	0.70	20%
R8	4765.25	8484.55	0.93	0.92	23%
R9	862.41	845.95	0.88	0.85	9%
R10	1073.38	2901.36	0.74	0.70	34%
R11	527.8	1475.46	0.82	0.78	43%
R12	947.7	4004.86	0.39	0.27	28%
R13	277.85	606.98	0.27	0.15	59%
R14	465.19	1388.54	0.78	0.74	23%
R15	372.32	1730.57	0.26	0.14	38%
R16	631.86	757.08	0.63	0.54	73%
R17	550.47	1956.13	0.64	0.58	61%
R18	565.28	3395.54	0.86	0.83	39%
R19	1586.35	4411.22	0.58	0.48	88%
R20	1992.98	12707.98	0.77	0.72	36%
R21	636.95	2944.75	0.69	0.61	16%
R22	771.18	2905.99	0.55	0.48	29%
R23	1018.69	1520.22	0.55	0.46	64%
R24	325.74	997.9	0.44	0.33	21%
R25	1724.61	8534.77	0.45	0.37	61%
R26	505.37	2162.31	0.77	0.74	12%
R27	1431.18	-1586.35	0.79	0.75	43%
R28	733.23	2060.03	0.71	0.64	40%
R29	486.32	421.04	0.65	0.56	26%
R30	463.24	1586.72	0.47	0.36	18%

Table A10 – Specific characterization of the study sites of chapter 4 and detailing of the load characterization and main TP sources from the catchment.

ID	Name	Management catchment	Lat.	Lon.	Maximum storage capacity (106 m³)	Depth (2013 – 2016) (m)a	Total annual external load (t yr-1)b	Point source (PS) contribution to the annual budget (%)b	Non-point source (NPS) contribution to the annual budget (%)b	Contribution from source type to the total annual external load (%)b				
										Livestock (NPS)	Agriculture (NPS)	Soil and vegetation (NPS)	Pisciculture (PS)	Sewer (PS)
R1	Rivaldo de Carvalho	Alto Jaguaribe	-39.93	-6.28	20	8.5	1.34	40%	60%	4%	25%	29%	0%	41%
R2	Edson Queiroz	Acaraú	-40.04	-4.24	254	13.1	99.22	5%	95%	4%	25%	66%	0%	5%
R3	Sítios Novos	Metropolitanas	-38.94	-3.80	126	6.7	17.33	18%	82%	73%	0%	10%	16%	2%
R4	Castro	Metropolitanas	-38.91	-4.58	62	7.1	3.86	24%	76%	66%	0%	10%	16%	7%
R5	Flor do Campo	Sertões de Crateús	-40.67	-5.58	105	3.5	5.09	48%	52%	1%	44%	7%	0%	48%
R6	Arrebita	Acaraú	-40.26	-3.89	19	6.8	10.08	3%	97%	4%	32%	61%	0%	3%
R7	Angicos	Coreaú	-40.82	-3.67	56	9.0	144.03	9%	91%	14%	5%	71%	0%	9%
R8	Acarape do Meio	Metropolitanas	-38.29	-4.22	30	14.7	5.63	47%	53%	43%	0%	4%	0%	53%
R9	Colina	Sertões de Crateús	-40.71	-5.75	4	4.2	9.44	27%	39%	46%	26%	2%	0%	27%
R10	Forquilha	Acaraú	-40.24	-3.21	50	6.2	4.17	3%	97%	85%	0%	12%	0%	3%
R11	Caxitoré	Curu	-39.34	-3.77	202	7.5	83.32	22%	78%	7%	25%	46%	1%	21%
R12	Ayres de Sousa	Acaraú	-40.48	-3.82	97	17.4	7.83	24%	76%	72%	0%	4%	21%	3%
R13	Olho D'água	Salgado	-39.37	-6.79	19	12.6	0.91	47%	53%	51%	0%	2%	26%	21%
R14	Rosário	Salgado	-39.08	-6.89	47	12.8	20.71	23%	77%	11%	35%	31%	9%	14%
R15	Itauna	Coreaú	-41.14	-3.16	73	6.6	41.11	21%	79%	8%	28%	43%	0%	21%
R16	Cachoeira	Salgado	-39.02	-6.99	34	13.3	10.37	36%	64%	9%	27%	27%	18%	18%
R17	Banabuiú	Banabuiú	-38.92	-5.33	1601	22.3	94.42	18%	82%	7%	30%	45%	0%	18%
R18	Orós	Alto Jaguaribe	-38.93	-6.27	1940	29.3	624.19	75%	25%	5%	11%	9%	63%	13%
R19	General Sampaio	Curu	-39.45	-4.09	322	11.5	287.30	36%	64%	1%	28%	45%	25%	1%
R20	Castanhão	Médio Jaguaribe	-38.45	-5.49	6700	45.3	656.91	62%	38%	1%	2%	35%	52%	10%
R21	Aracoiaba	Metropolitanas	-38.69	-4.40	162	11.8	20.95	38%	62%	3%	2%	24%	0%	71%
R22	Malcozinhado	Metropolitanas	-38.28	-4.12	38	9.7	25.04	41%	59%	3%	9%	13%	0%	75%
R23	Catucinzenta	Metropolitanas	-38.42	-4.04	25	5.4	0.89	60%	40%	4%	4%	20%	0%	71%
R24	São Vicente	Acaraú	-40.26	-3.81	10	9.5	0.07	47%	53%	6%	0%	64%	0%	30%
R25	Araras	Acaraú	-40.44	-4.21	860	16.0	363.88	74%	26%	10%	1%	42%	0%	47%
R26	Acaraú Mirim	Acaraú	-40.28	-3.51	37	8.1	7.02	75%	25%	2%	0%	37%	0%	61%
R27	Junco	Salgado	-39.22	-6.89	2	4.8	0.02	90%	10%	5%	3%	32%	0%	60%
R28	Lima Campos	Salgado	-38.96	-6.40	66	8.5	6.67	36%	64%	3%	31%	34%	0%	32%
R29	Manoel Balbino	Salgado	-39.33	-7.11	37	20.0	0.08	46%	54%	2%	1%	40%	0%	57%
R30	Ubaldinho	Salgado	-39.24	-6.58	32	9.6	0.89	63%	37%	11%	3%	59%	0%	27%

[a] Maximum mean depth over the dry period (01/jul – 31/dez) during the drought period (2013-2016)

[b] Ceará (2021